MPR-SAT-64-13
February 26, 1964
(Supersedes MPR-SAT-63-1)

233

SATURN

MARSHALL SPACE FLIGHT CENTER

HUNTSVILLE, ALABAMA

RESULTS OF THE THIRD SATURN I LAUNCH VEHICLE TEST FLIGHT

SA-3

NATIONAL AERONAUTICS AND SPACE ADMINISTRATION

NASA

Orig. 26 Feb. 1964 82 p rejr

SECURITY NOTE

This document contains information affecting the national defense of the United States within the meaning of the Espionage Law, Title 18, U.S.C., Sections 793 and 794 as amended. The revelation of its contents in any manner to an unauthorized person is prohibited by law.

GEORGE C. MARSHALL SPACE FLIGHT CENTER

MPR-SAT-64-13

RESULTS OF THE THIRD SATURN I LAUNCH VEHICLE TEST FLIGHT

By Saturn Flight Evaluation Working Group

ABSTRACT

This report presents the results of the Early Engineering Evaluation of the Saturn SA-3 test flight. The performance of each major vehicle system is discussed with special emphasis on malfunctions and deviations.

The SA-3 flight test was a complete success, with all missions of the flight being accomplished. No major malfunction or deviation which would be considered a serious system failure or design deficiency occurred.

Any questions or comments pertaining to the information contained in this report are invited and should be directed to:

Director, George C. Marshall Space Flight Center
Huntsville, Alabama
Attention: Chairman, Flight Evaluation Working Group, R-AERO-F (Phone 876-2701)

[redacted]

GEORGE C. MARSHALL SPACE FLIGHT CENTER

MPR-SAT-64-13

RESULTS OF THE THIRD SATURN I LAUNCH VEHICLE TEST FLIGHT

SATURN FLIGHT EVALUATION
WORKING GROUP

[redacted]

ACKNOWLEDGEMENT

Acknowledgement is made to the various laboratories and elements of MSFC and Launch Operations Center for their contributions to this report. Without the joint efforts and assistance of these elements, this integrated report would not have been possible. The Saturn Flight Evaluation Working Group is especially indebted to the following MSFC elements for their major contributions:

Aero-Astrodynamics Laboratory

- Aerodynamics Division
- Flight Mechanics and Dynamics Division
- Flight Evaluation and Operations Studies Division

Astrionics Laboratory

- Electrical Networks Division
- Guidance and Control Division
- Inertial Sensors and Stabilizers Division
- Instrumentation Division

Computation Laboratory

- Research and Development Applications Division

Launch Vehicle Operations

- Electronic Engineering and Instrumentation Systems
- Electrical Engineering Guidance and Control Systems
- Mechanical and Propulsion Systems

Propulsion and Vehicle Engineering Laboratory

- Propulsion Division
- Structures Division
- Systems and Design Integration Division

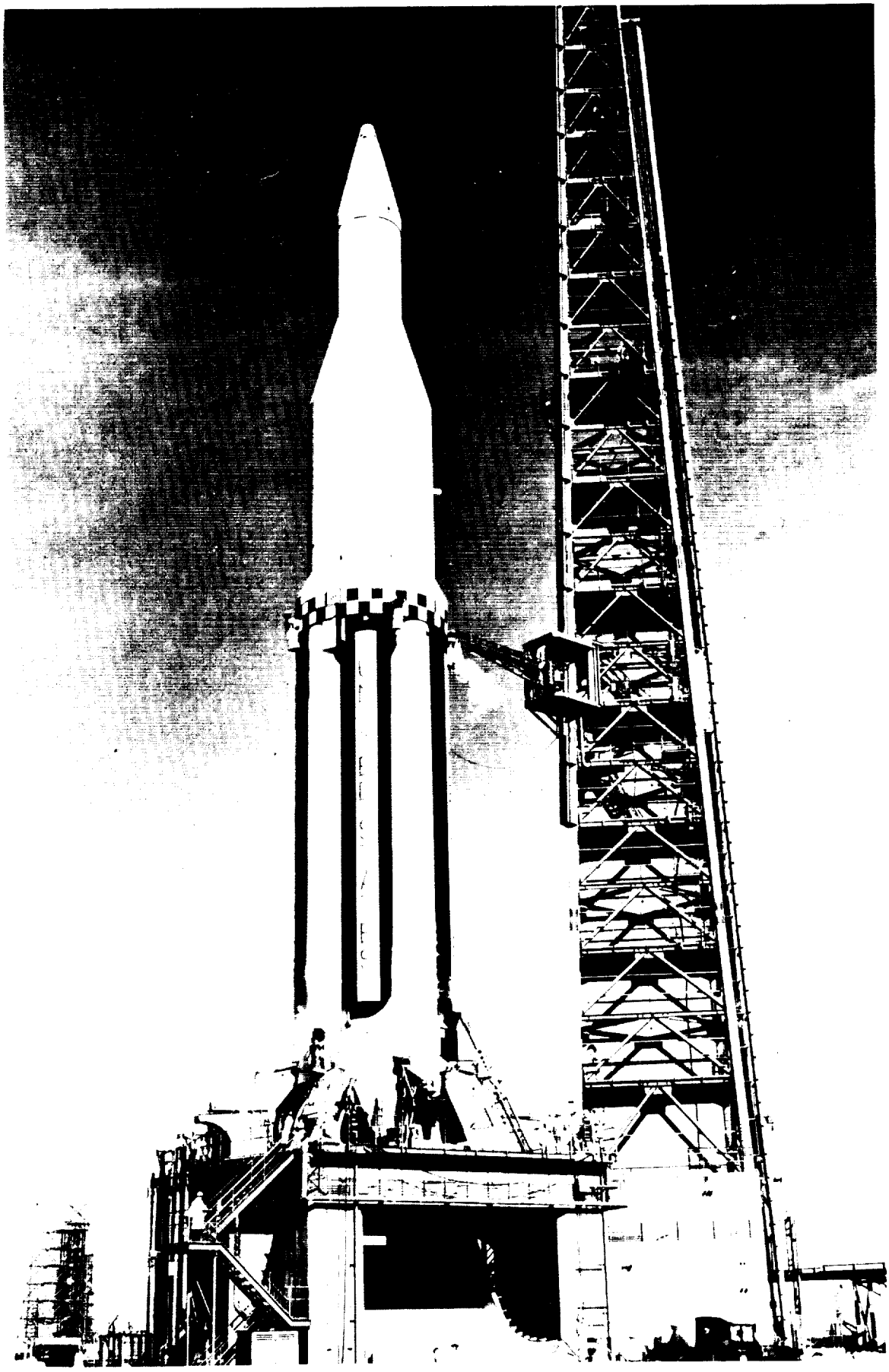

TABLE OF CONTENTS

TABLE OF CONTENTS (CONT'D)

TABLE OF CONTENTS (CONT'D)

LIST OF ILLUSTRATIONS

LIST OF ILLUSTRATIONS (CONT'D)

LIST OF ILLUSTRATIONS (CONT'D)

LIST OF TABLES

ABBREVIATIONS AND SYMBOLS

Abbreviation	Definition
AFC	automatic frequency control
AGC	automatic gain control
AM	amplitude modulation
ARDC	Air Research and Development Center
FM	frequency modulation
GBI	Grand Bahama Island
G&C	Guidance and Control
GG	gas generator
IECO	inboard engine cutoff
LPGG	liquid propellant gas generator
MFV	main fuel valve
MLV	main LOX valve
OECO	outboard engine cutoff
PAM	pulse amplitude modulation
PCM	pulse code modulation
PU	propellant utilization
q	dynamic pressure
RF	radio frequency
RMS	root mean square
S-I	first (booster) stage of the Saturn I vehicle
S-IVD	second (dummy) stage of the Saturn I vehicle
S-VD	third (dummy) stage of the Saturn I vehicle
SPGG	solid propellant gas generator
SS	single sideband
TM	telemeter
UDOP	Ultra High Frequency Doppler
UHF	ultra high frequency
VHF	very high frequency

CONVERSION FACTORS FOR PREFERRED MSFC
MEASURING UNITS

Quantity	Multiply	By	To Obtain
1. Acceleration	ft/s^2	3.04800×10^{-1}	m/s^2
2. Area	in^2	6.4516×10^{-4}	m^2
3. Density	$\frac{lb\text{-}s^2}{ft^4}$	5.25539×10^{1}	$\frac{kg\text{-}s^2}{m^4}$
	$slug/ft^3$	5.25539×10^{1}	$\frac{kg\text{-}s^2}{m^4}$
4. Energy	BTU	2.51996×10^{-1}	kcal
5. Force	lb	4.53592×10^{-1}	kg
6. Length	in	2.54000×10^{-2}	m
7. Mass	$\frac{lb\text{-}s^2}{ft}$	1.48816	$\frac{kg\text{-}s^2}{m}$ = TMU
8. Mass Flow Rate	$\frac{lb\text{-}s}{ft}$	1.48816	$\frac{kg\text{-}s}{m}$
9. Pressure	lb/in^2	7.03067×10^{-2}	kg/cm^2
10. Temperature	°F-32°	5.55556×10^{-1}	°C
11. Velocity	ft/s	3.04800×10^{-1}	m/s
12. Volume	gal (U.S.)	3.78543×10^{-3}	m^3
	ft^3	2.83168×10^{-2}	m^3
13. Volume Flow	ft^3/s	2.83168×10^{-2}	m^3/s
	gal/s	3.78543×10^{-3}	m^3/s

[redacted]

GEORGE C. MARSHALL SPACE FLIGHT CENTER

MPR-SAT-64-13

RESULTS OF THE THIRD SATURN I LAUNCH VEHICLE TEST FLIGHT

By Saturn Flight Evaluation Working Group

SECTION I. FLIGHT TEST SUMMARY

1.1 FLIGHT TEST RESULTS

Saturn space vehicle SA-3 was launched at 1245:02 hours EST on November 16, 1962. The flight test was a complete success, as were the first two Saturn flight tests. The flight test did not reveal any malfunctions or deviations which could be considered a serious system failure or design deficiency.

SA-3 was launched approximately eight weeks after arrival of the S-I stage at Cape Canaveral. The scheduled ten-hour countdown began at 0200 EST November 16, 1962. The count was continuous except for one 45-minute hold at 10:45 hours EST due to a ground generator power failure. All automatic propellant loading sequencing processes were within expected tolerances. Launch preparations, execution of the countdown, and launch were as expected and successfully demonstrated the compatibility between the ground support equipment and the space vehicle. The launch complex and support equipment suffered less damage than was expected from the low liftoff acceleration of SA-3.

The actual flight path of SA-3 was close to nominal. Slightly lower acceleration caused the altitude and range to be less than nominal at any time during powered flight, but a longer powered flight caused both to be greater than expected at times after burnout. Destruct of the SA-3 dummy stages for Project Highwater occurred at 292 seconds range time at an altitude of 167.2 km.

The performance of the propulsion system was very satisfactory for this flight test. The total cluster performance averaged within approximately one percent of predicted. Individual engine performance was satisfactory with no major deviations from predicted values being noted. The propellant tank pressurization systems functioned properly, with good results from the increased propellant load to simulate Block II gas ullage. All hydraulic systems operated well within expected limits.

The control system for the Saturn vehicle SA-3 was essentially the same as that used in SA-1 and SA-2. However, the control gains (a_o and b_o) were different. These were changed because of the increased propellant loading to maintain the same correlation with the vehicle mass as on SA-1 and SA-2.

Engine deflections, attitude angles, and angles-of-attack were less than those observed on SA-1 and SA-2 flights primarily due to the trajectory shape. The wind magnitude was almost the same in the pitch plane as experienced on SA-2.

Operations of the hydraulic actuators and the control computers was satisfactory.

The Saturn SA-3 vehicle was flown without active path guidance. However, passenger hardware for both ST-90 and ST-124P (Prototype) guidance systems was onboard to establish the operational capabilities of the guidance equipment in the Saturn flight environment. The telemetered data as well as a trajectory comparison indicated satisfactory performance of the ST-90 guidance system throughout powered flight. The operation of the ST-124P guidance system, as an engineering test, was quite satisfactory.

Erroneous outputs from the cross range accelerometer system mounted on the ST-124P platform were noted before ignition. No correction was made and the cross range measurement contained extraneous signals throughout flight. These extraneous signals were eliminated from the telemetered accelerometer output

[redacted]

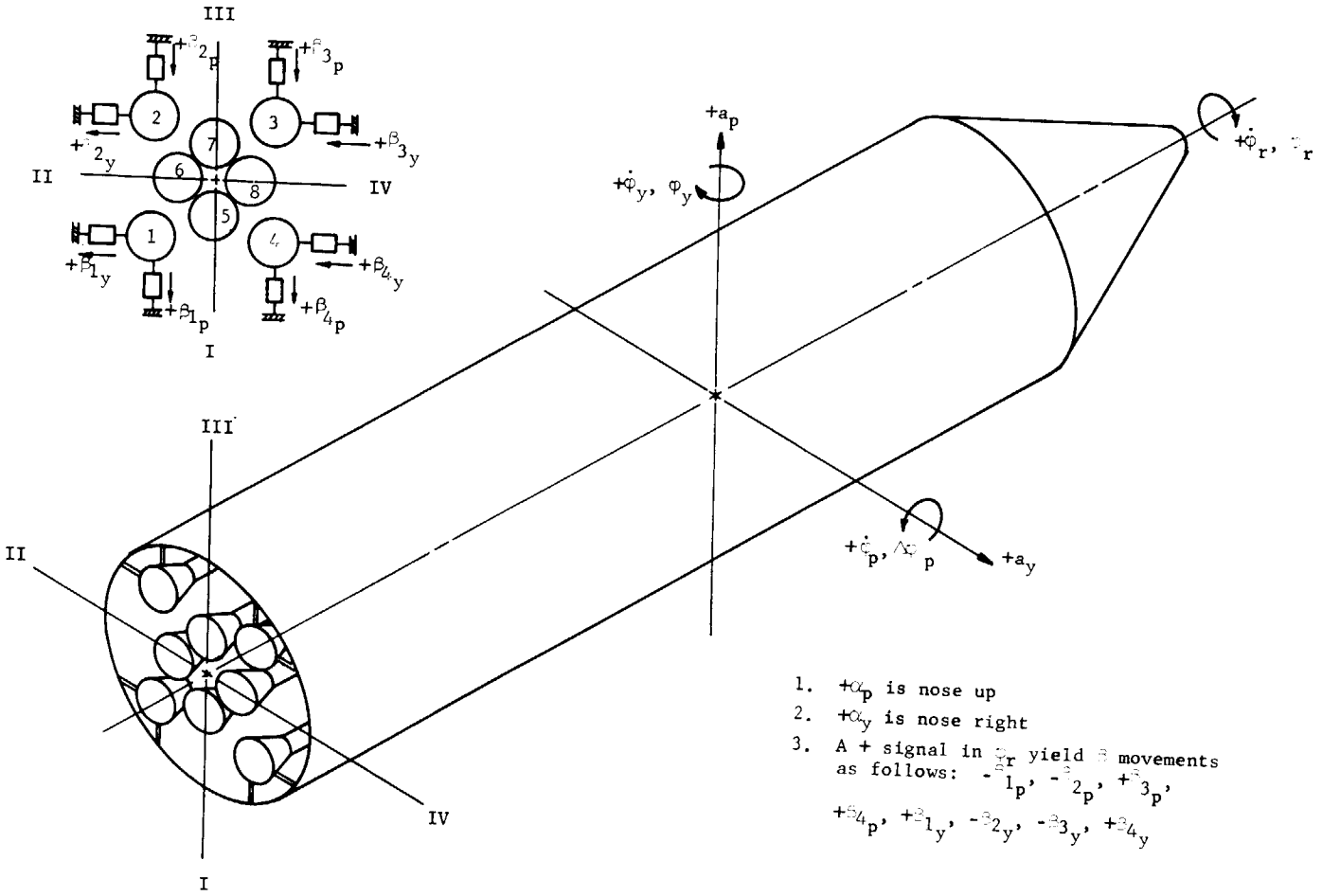

FIGURE 1-1. SATURN BOOSTER POLARITY CHART

and valid cross range information was deducted from the measurement.

The flight data indicated that the SA-3 vibration levels were generally similar to those recorded during the previous two Saturn flights.

The 10 bending accelerometers flown on SA-3 showed response at frequencies in the range of first and second vehicle bending. These frequencies were present in both pitch and yaw direction with a maximum amplitude at liftoff on the nose cone of 0.016 g's single amplitude for first mode of 2.0 cps. At OECO a forced response of 0.095 g's single amplitude occurred at a coupled frequency of 2.7 cps. The response is lower than on SA-2 before OECO.

The base region environment during the SA-3 flight was similar to that encountered on the two previous flights. Radiation heating rates on SA-3 are in good agreement with values obtained on the previous Saturn flights and are considered representative for the Saturn I, Block I vehicle.

A total of 607 flight measurements were flown on SA-3. Of these measurements, fourteen were completely unusable, six were partially usable and one was questionable. The signal strength of all RF systems, except C-Band radar, was very close to the expected values.

1.2 TEST OBJECTIVES

The objectives of the Saturn SA-3 flight test were as follows:

First Objective - Booster

Prove the propulsion system, structural design, and control system of the high thrust booster. Achieved.

Second Objective - Ground Support Equipment

Prove the operational concept of the associated supporting launch facilities for Saturn class vehicles; which include propellant systems, automatic checkout equipment, special instrumentation, launch pedestal with holddown arms, and other necessary handling and launching equipment. Achieved.

Third Objective - Vehicle in Flight

(a) Aeroballistics

Confirm values of aerodynamic characteristics, correlating predicted stability and performance with that encountered in flight. Achieved.

(b) Propulsion

Prove that the booster stage is capable of providing the proper thrust to propel the Block I vehicle through the desired trajectory at the required velocity. Determine the inflight performance of all eight engines, the controlling movements of the four outboard gimballed engines, engines' cutoff, propellant utilization, and other desired propulsion data. Achieved.

(c) Structural and Mechanical

Verify the structural integrity of the Block I airframe, by correlating theoretical calculations and specification requirements with conditions encountered during flight. Specifically, to determine the inflight stress, vibration levels, and associated frequency content at various locations throughout the vehicle structure, so that the dynamic increments to the shear and bending moments may be calculated and component vibration environment may be determined. Measure the overall structural response to define critical dynamic occurrences. Evaluate the presence of any excessive strain, body bending effects, and accumulate data which may be used to determine the mode shape of the bending curve during flight. Achieved.

(d) Guidance and Control

To demonstrate the capability of the G & C system (a modified ST-90 stabilized platform) to perform the required control, guidance, and operational sequence for the Block I flight tests. Specifically, to prove that the system will establish an accurate space-fixed coordinate reference for determining vehicle attitude and providing an accurate coordinate velocity signal. Achieved.

Fourth Objective - Project "Highwater"

A water cloud experiment (similar to the experiment conducted on SA-2) will be accomplished by injecting the upper stages' 87,329 kg (192,528 lb) of water ballast into the upper atmosphere, at an altitude of approximately 167 km, by rupturing the upper stages with primacord. Achieved.

TABLE 1-I. TIMES OF FLIGHT EVENTS

Event	Actual Range Time (sec)	Predicted (sec)	Act - Pred
Ignition Command	-3.79	-3.57	-0.22
Thrust Commit	-0.49	--	--
Launch Commit	-0.08	--	--
First Motion*	0.10	0.10	0
Liftoff Signal (Start Program Device)	0.33	--	--
Begin Tilt	10.33	--	--
Mach 1 Reached	68.10	68.03	0.07
Maximum Dynamic Pressure	78.60	78.28	0.32
Inboard Engine Cutoff	141.66	140.34	1.32
End of First Thrust Decay	144.25	--	--
Outboard Engine Cutoff	149.09	147.95	1.14
End of Second Thrust Decay	152.78	150.48	2.30
Retro Rockets Ignite	153.66	152.34	1.32
Project "Highwater"	292.00	292.00	0
Loss of Telemetry Signal	292.00	292.00	0

* Reference point for comparison

SECTION II. INTRODUCTION

Saturn space vehicle SA-3 was launched at 1245:02 EST on November 16, 1962, from Saturn Launch Complex 34, Atlantic Missile Range, Cape Canaveral, Florida. SA-3 was the third vehicle to be flight tested in the Saturn I R&D program. The major objective of this test was to evaluate the designs of the propulsion system, control system, and structure of the 590,000 kg (1.3 million lb) thrust booster.

This report presents the results of the early engineering evaluation of the SA-3 test flight. The performance of each major vehicle system is discussed with special emphasis on malfunctions and deviations.

This report is published by the Saturn Flight Evaluation Working Group, whose members are representatives from all Marshall Space Flight Center Divisions. Therefore, the report represents the official MSFC position at this time. This report will not be followed by a similarly integrated report unless continued analysis and/or new evidence should prove the conclusions presented here partly or wholly wrong. Final evaluation reports will, however, be published by the MSFC Divisions covering some of the major systems and/or special subjects as required.

SECTION III. LAUNCH OPERATIONS

3.1 SUMMARY

Saturn Vehicle SA-3, scheduled for launching at 1200 hours EST on November 16, 1962, was launched at 1245:02 hours EST, on that date. The vehicle was launched on an azimuth of 100 degrees East of North from complex 34, Geodetic Latitude 28.52153 degrees North and Longitude 80.56136 degrees West.

The scheduled 10-hour countdown began at 0200 EST, November 16, 1962. The count was continuous except for one hold at 1045 hours EST. There was a ground generator power failure at this time. The hold continued for 45 minutes and the count was resumed at 1130 hours EST. All automatic propellant loading sequencing processes were within expected tolerances. Launch preparations, execution of the countdown, and launch were as expected and successfully demonstrated the compatibility between the ground support equipment and the flight configuration. The complex and support equipment suffered less damage than was expected from the low liftoff acceleration of SA-3.

3.2 PRELAUNCH MILESTONES

Date	
September 19, 1962	S-I stage arrived at Cape Canaveral on Saturn barge "Promise"
September 21, 1962	S-I booster erected on launch pedestal at pad 34.
September 24, 1962	Dummy stages S-IV, S-V, and payload assembled to the S-I booster.
October 19, 1962	Service Structure removed for RF check.
October 31, 1962	Fuel test completed; S-IVD S-VD water loading completed.
November 2, 1962	LOX loading test completed
November 6, 1962	Overall test 4 completed
November 9, 1962	Retro Rocket installation completed
November 13, 1962	Simulated flight test performed
November 14, 1962	RP-1 fuel loaded
November 16, 1962	Launch

3.3 PRELAUNCH ATMOSPHERIC SURFACE CONDITIONS

General weather conditions around Cape Canaveral at the time of launch were exceptionally good. There were no clouds along the flight path. The visibility was 16 km (10 miles) or better. Barometric pressure was 764 mm of mercury (1018.5 mbs), relative humidity 36 percent, and temperature 24.7 degrees centigrade. Surface winds were from 215 degrees (SW) at 3 m/s.

3.4 COUNTDOWN

Launch countdown began at T minus 600 minutes at 0200 EST on November 16, 1962 and was continuous except for one 45-minute hold caused by a ground generator power failure at T minus 75 minutes (Figure 3-1). The events of the hold were as follows:

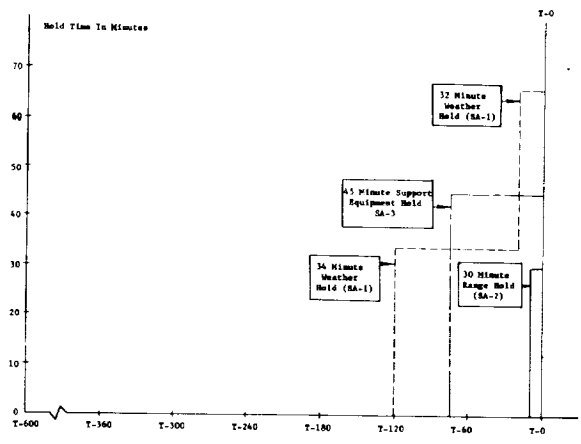

FIGURE 3-1. COUNTDOWN TIME IN MINUTES

Holds

Network generator number 2 dropped out, apparently due to the over-voltage sensing circuit, causing the hold. The nominal value for activation of the over-voltage device is 37 volts; however, it was found that the over-voltage sensing device for this generator had shifted to 35 volts (approximately the terminal voltage of the generator at the moment of dropout). The sensing device was replaced. The over-voltage bypass circuit for all generators (normally energized at "LOX bubbling complete") were then jumpered for the remainder of the countdown to avoid further difficulties in this area. The count was resumed at 1130 hours EST and continued until launch.

Automatic Countdown

The automatic countdown sequence was initiated by the firing command 363.45 seconds prior to ignition command (T minus 0). This is 10.55 seconds later than the firing command on SA-2, due primarily to the time difference in LOX tank pressurization. The LOX tank pressurization time was shorter on SA-3 due to the smaller gas ullage associated with the full propellant loading for this vehicle as compared to the partial loading on SA-1 and SA-2. The times shown were read from sequence records. No digital output for events was available due to a computer malfunction.

3.5 HOLDDOWN

Engine start and transition were smooth with all engines receiving a positive ignition from a LOX lead in the gas generator ignition system. All critical blockhouse measurements were within the established redline values.

Two events from the sequence records show irregular signals. The "Support Retract Pressure OK" switch cycled several times about 500 ms after all engines were running. This could be due to vibration on one or more of the four switches. The function of these four switches (one on each support arm assembly at the pressure source) is to show that pressure is available to move the support retract arm. The switches were wired in series and vibration on any one switch would cause the cycling noted. This possible problem was noted early in the Saturn program and these switches were taken out of the cutoff circuit. The other irregular signal showed that the LOX bubbling valve stayed open for 137 seconds instead of the expected 60 seconds. This is considered a measuring error since other parameters (such as LOX temerpature in the tanks and at the pump inlet) did not reflect this long bubbling time.

3.6 LAUNCH COMPLEX AND GROUND SUPPORT EQUIPMENT

All items of ground support equipment functioned normally with the exception of the LOX fill mast, which failed to retract on command. This failure to retract did not interfere with the subsequent liftoff of the space vehicle. However, the failure to retract on command resulted in the ultimate failure of the LOX fill mast because of the vehicle blast breaking the mast cylinder mount, with the subsequent forward motion of the upper mast assembly. Post launch investigations of the cause of the mast failure to retract have been inconclusive. Sequence and event records show that the command for the mast to retract was received and responded to by the solenoid valve in the LOX fill mast assembly valve box. The actuation of this solenoid valve should have resulted in the application of pneumatic pressures to the retract cylinder, which would result in the ultimate retraction of the mast. The response of the solenoid valve to command was demonstrated during components test on T minus 1 day. The correct mechanical connections to the retract cylinder were verified prior to launch and reverified during the post launch investigation. The post launch analysis, so far, points most strongly to a theory which indicates that the retract cylinder failed to stroke, subsequent to the application of pressure. This failure could be due to two possibilities. The first would be a mechanical "freezing" of the retract cylinder piston within its cylinder. The second possibility would be that of a failure of the "cushion" regulator, or that one of the two-way "button" valves, used for remote coupling, could have leaked. Either of these possibilities would result in a net force toward the forward position rather than the retract position. The circumstances of the LOX fill mast failure to retract are being investigated to determine the most likely cause of failure and what steps can be taken to prevent its recurrence.

The complex and support equipment suffered less damage than was expected from the low liftoff acceleration of SA-3. Film coverage shows that SA-3 took approximately 3.2 seconds longer to reach 93 m altitude than either of the two previous Saturn vehicles. At this altitude, the exhaust flame and jets cease to "flare out." Therefore, since SA-3 remained in close contact with the pad, approximately 30 percent longer than either SA-1 or SA-2, more pad damage would be expected from SA-3.

Examination of the launcher and ground support equipment, after the launch of Saturn vehicle SA-3, revealed that the damage was of a level comparable to the damage observed after the launch of SA-1 and SA-2

The only observed damage readily attributable to the low liftoff acceleration was increased damage to the torus ring retaining bands and a noticeable larger increment of flame deflector warping. A damaged area of interest was the tubing on the exposed wall of the umbilical tower base room. This tubing was ripped loose from the wall and severely distorted. Although this tubing damage did not occur on the launches of SA-1 or SA-2, it would be difficult to associate the damage with any launch characteristic peculiar to SA-3. It is believed that this damage resulted from the mounting system being weakened during previous launches. Saturn vehicle SA-3 was the first to use an umbilical swing arm instead of the long cable mast assembly. The long cable mast assembly was essentially destroyed during the SA-1 and SA-2 launches. The umbilical swing arm installation used to service SA-3 sustained very minor damage during the launch and can be reused with minor refurbishment.

The following is a detailed assessment of damage to individual GSE items.

Short Cable Mast and Tail Cable Mast Assemblies. This equipment should be subject to refurbishment with a majority of the mechanical components being salvageable. The umbilical swing arm should be subject to refurbishment with minimum effort. The umbilical disconnect plate sustained damage to one ejection pin. The bungee cord redundant retract system, used on the umbilical disconnect plate, was burned away. The umbilical arm service platform sustained minor damage. Electrical cabling, in general, evidenced heat input but possibly will be reused, subject to qualification testing.

Fuel Loading Mast. This mast should be subject to refurbishment with a majority of the mechanical components being reusable. Flexible hose assemblies, electrical harnesses, and the retractable coupling are subject to replacement.

LOX Fill Mast. This sustained major damage, with very few components, other than the steel base and the valve box assembly, subject to salvage.

Retractable Support Arms. These support arms sustained minor damage consisting of random failure of tubing which is exposed nearly directly to the blast.

Holddown Arms and Associate Valve Panel. This equipment sustained minor damage consisting primarily of tubing and flex hose assemblies being burned away.

Flame Deflector. This can be reused. It suffered a pronounced increment of warpage; however, this warpage is not considered so severe as to compromise its usefulness.

The launch again proved the compatability of the vehicle and the ground support equipment. In addition, it also proved that a vehicle with low liftoff acceleration (11.4 m/s^2 compared to 13.6 m/s^2 for normal flights) would not damage the launch complex an excessive amount.

SECTION IV. TRAJECTORY

4.1 SUMMARY

The actual flight path of SA-3 was close to nominal. Slightly lower acceleration caused the altitude and range to be less than nominal at any time during powered flight, but a longer powered flight caused both to be greater than expected at times after burnout. Water release (Project Highwater) occurred at 292 seconds at an altitude of 167.2 km.

At IECO, the actual altitude was 1.4 km higher, the range was 1.8 km longer, and the velocity was 18.4 m/s greater than nominal.

4.2 TRAJECTORY ANALYSIS

The electronic tracking data obtained for establishing a post flight trajectory were somewhat poorer than that obtained on the first two vehicles. The acceleration components from UDOP were not usable prior to 35 seconds or after about 120 seconds. Acceleration components from Azusa were not usable prior to 75 or 80 seconds, and were intermittently available during the remaining flight. FPS-16 Radar data was intermittent during the entire flight from all stations. Acceleration components were not usable from any of the radar sites prior to 40 or 50 seconds.

The postflight trajectory is a combination of "Close-in" and "regular" Fixed Camera, Theodolite, and Mark II Azusa tracking data; with telemetered data using transients, and a ballistic trajectory computed from 160 seconds through water release at 292 seconds. The maximum difference between the position components from this synthesized trajectory and the tracking data during powered flight was about 20 m.

4.3 ACTUAL AND PREDICTED TRAJECTORY

4.3.1 POWERED FLIGHT

The initial longitudinal acceleration on SA-3 was 11.36 m/s^2 which was very close to nominal (11.27 m/s^2). The initial acceleration on this flight was lower than that on previous flights due to maximum propellant loading. This initial acceleration is equivalent to 1.16 g's as compared to approximately 1.38 g's on previous flights.

Actual and nominal altitude, range, and cross range (Z_e) are shown in Figure 4-1. The actual altitude and range were essentially the same until after the second cutoff (Figure 4-1). The actual cross range displacement (Z_e) was 0.41 km left of nominal at IECO. About 0.255 km of this deviation was due to the difference in alignment of the platform and vehicle (Section VIII), and approximately 0.110 km was caused by lateral winds. The remaining difference (0.045 km) is due to other small effects. The nominal trajectory is presented in Reference 1.

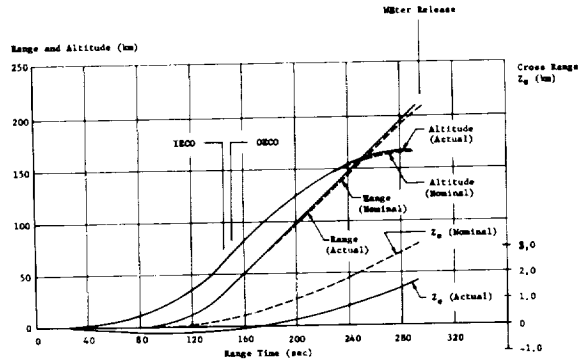

FIGURE 4-1. TRAJECTORY

The longitudinal acceleration was about 1.2 m/s^2 less than expected during the power flight; however, the maximum longitudinal acceleration was only 0.5 m/s^2 lower than nominal. The velocity at first cutoff was 18.4 m/s more than expected, since actual cutoff occurred 1.3 seconds later. The earth-fixed velocity is shown in Figure 4-2.

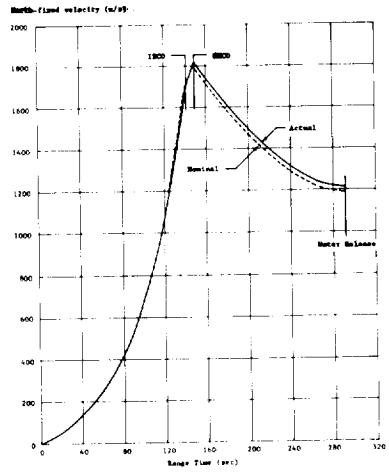

FIGURE 4-2. EARTH-FIXED VELOCITY

Actual and nominal Mach number and dynamic pressures are shown in Figure 4-3. These two parameters were calculated using measured meteorological data to an altitude of approximately 33.4 km. Between 33.4 and 47.0 km altitude, the measured data were gradually adjusted to the 1959 ARDC atmosphere, above which the 1959 ARDC was used. The actual peak dynamic pressure was slightly less (0.006 kg/cm^2) than nominal due to a lower velocity.

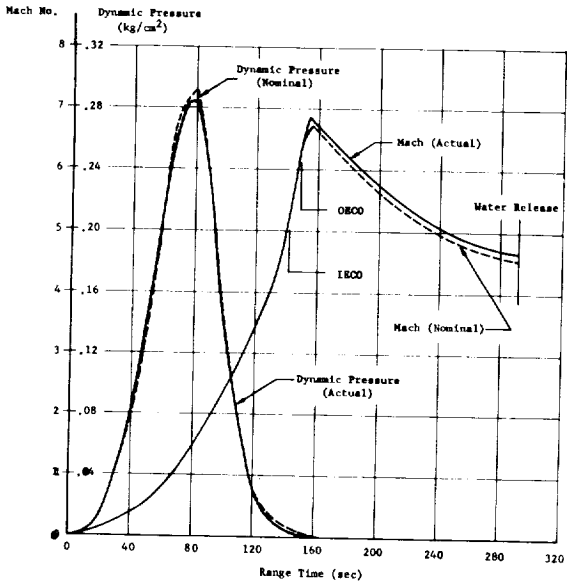

FIGURE 4-3. DYNAMIC PRESSURE AND MACH NUMBER

4.3.2 CUTOFF

A comparison of actual and nominal parameters at both inboard and outboard engine cutoff is shown in Table 4-I. At OECO, the actual altitude was 1.1 km higher, range was 1.8 km longer, and velocity was 11.9 m/s greater than predicted. The time interval between the two cutoff times was 7.43 seconds for the actual, and 7.61 seconds for the nominal. The acceleration level of both actual and nominal was about 21 m/s^2. Since the actual burning time between IECO and OECO was 0.2 second less than nominal, the velocity comparison would be expected to change by about 4 m/s between IECO and OECO. This would mean that the expected difference between actual and nominal velocity at OECO would be 14.4 m/s, instead of the 11.9 m/s observed. Figure 4-4 indicates that the acceleration level during outboard engine operation is less than nominal, resulting in an increasing velocity deficit from predicited.

Comparisons of actual and nominal parameters at significant event times are given in Table 4-II.

TABLE 4-I. CUTOFF CONDITIONS

Parameter	IECO			OECO		
	Actual	Nominal	Act-Nom	Actual	Nominal	Act-Nom
Range Time (sec)	141.66	140.34	1.32	149.09	147.95	1.14
Range (km)	32.42	30.64	1.78	41.13	39.36	1.77
Altitude (km)	61.46	60.10	1.36	71.11	70.00	1.11
Cross Range (Ze) (km)	-0.13	0.28	-0.41	-0.10	0.36	-0.46
Earth-fixed Velocity (m/s)	1700.6	1682.2	18.4	1808.8	1796.9	11.9
Longitudinal Acceleration (m/s^2)	41.05	41.53	-0.48	20.99	21.74	-0.75
Velocity Vector Elevation (deg)	48.37	49.16	-0.79	46.84	47.55	-0.71
Velocity Vector Azimuth (deg)	100.09	100.48	-0.39	100.18	100.56	-0.38

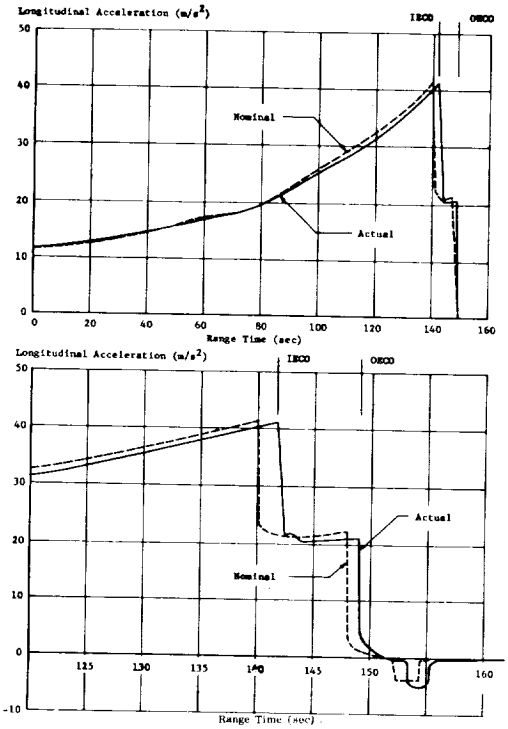

FIGURE 4-4. LONGITUDINAL ACCELERATION

TABLE 4-II. SIGNIFICANT EVENTS

Event	Parameter	Actual	Nominal	Act-Nom
First Motion	Range Time (sec)	0.10	0.10	
	Longitudinal Acceleration (m/s^2)	11.36	11.27	0.09
Mach 1	Range Time (sec)	68.10	68.03	0.07
	Altitude (km)	8.77	8.04	0.23
Maximum Dynamic Pressure	Range Time (sec)	78.60	78.28	0.32
	Dynamic Pressure (kg/cm^2)	0.2863	0.2926	-0.0063
	Altitude (km)	12.00	11.65	0.35
Maximum Longitudinal Acceleration	Range Time (sec)	141.80	140.44	1.36
	Longitudinal Acceleration (m/s^2)	41.12	41.60	-0.48
Maximum Earth-fixed Velocity	Range Time (sec)	149.50	148.25	1.25
	Earth-fixed Velocity (m/s^2)	1811.8	1800.0	11.8
Water Release	Range Time (sec)	292.0	292.0	
	Time from True Apex (sec)*	+3.5	+2.9	+0.6
	Altitude (km)	167.22	166.77	0.45
	Range (km)	211.41	207.65	3.76
	Elevation Angle from Pad (deg)	37.03	37.46	-0.43

* Water Release Time Minus Apex Time

[redacted]

4.3.3 THRUST DECAY

The actual velocity gain during outboard engine thrust decay was 7.9 m/s and the nominal velocity gain was 7.6 m/s. A comparison of the two has no significance, since LOX depletion occurred. In addition, the time of actual OECO was obtained from a commutated telemetry trace, which may be in error by as much as ± 83 ms. This time error is equivalent to a ± 1.7 m/s uncertainity in the velocity gain.

4.4 RETRO ROCKETS

SA-3 was the first Saturn vehicle to use retro rockets. The measured longitudinal acceleration (F7-13) during retro rocket operation is shown in the lower part of Figure 4-4. The velocity loss due to retro rocket operation was about 9 m/s or approximately the velocity loss predicted. Deviating from the Block II separation sequence, this velocity loss applies to the entire (unseparated) SA-3 vehicle.

4.5 WATER RELEASE (DESTRUCT)

Water release occurred at 292.0 seconds range time. The vehicle was 0.45 km higher and 3.76 km further in range than was expected.

[redacted]

5.1 SUMMARY

Vehicle propulsion system performance throughout the flight test of Saturn SA-3 was well within satisfactory limits. Performance of individual engines, hydraulic systems, and propellant tank pressurization systems did not deviate significantly from the predicted values. The vehicle longitudinal thrust was 0.15 percent lower and specific impulse 1.10 percent higher than corresponding predicted values.

All missions, including primary, secondary, and special missions, were accomplished. Results of the special missions of particular significance to the vehicle propulsion system are described below:

1. The full propellant load simulating Block II ullage volumes presented no problem to the propellant loading system, the pressurization system, or the engine operation.

2. The thrust OK cutoff of outboard engines due to LOX depletion, achieved a significant increase in propellant utilization with no problems in engine shutdown and vehicle control.

3. The retro rockets ignited and operated satisfactorily at the end of S-I stage powered flight.

5.2 INDIVIDUAL ENGINE PERFORMANCE

The performance of the individual engines on the SA-3 flight was satisfactory. The maximum deviation in engine thrust, between that calculated from flight data and predicted values, was approximately 1.8 percent, occurring on engine positions 6 and 8. The deviations for the other engines varied from minus 1.6 to plus 1.2 percent as compared to the predicted thrust (Figure 5-1). The engine-to-engine deviation from the actual mean thrust was from plus 1.5 to minus 0.8 percent

The maximum deviation in engine specific impulse, between that reconstructed from flight data and the predicted values, was approximately plus 2.6 percent, occurring on engine position 2. The deviations for the other engines varied from plus 0.35 to plus 2.26 percent as compared to the predicted impulse (Figure 5-2). The engine-to-engine deviation from the actual mean specific impulse was from plus 1.8 to minus 1.0 percent.

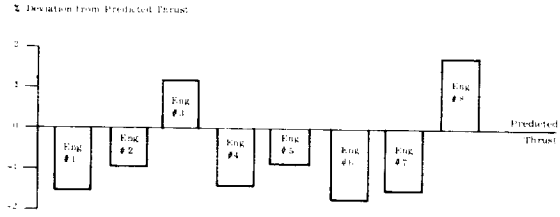

NOTE: Throughout this report, psia indicates an absolute pressure.

FIGURE 5-1. INDIVIDUAL ENGINE DEVIATION FROM PREDICTED THRUST

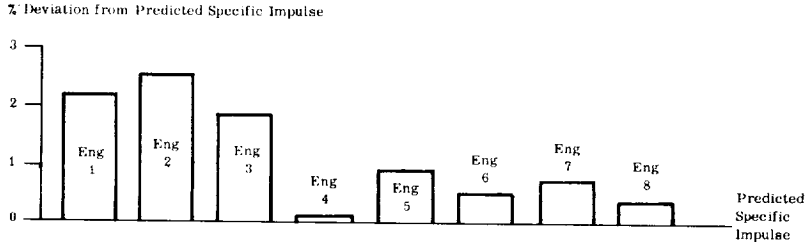

FIGURE 5-2. INDIVIDUAL ENGINE DEVIATION FROM PREDICTED SPECIFIC IMPULSE

Engine main propellant valve opening and closing times are shown in Table 5-I, and the cutoff impulse is shown in Table 5-II. All values shown in Table 5-II are based on chamber pressure decay. The cutoff signals for the outboard engines were measured on commutated channels and could, therefore, be in error by as much as 83 ms, which represents a possible error in impulse of 6760 kg-sec (14,900 lb-sec). When the possible 83 ms error in cutoff time is taken into consideration, the cutoff impulse values from chamber pressure decay are in good agreement with the impulse from trajectory information (Section IV Paragraph 4.3)

All engine subsystems and components were evaluated, and the data indicated acceptable levels of operation except for the gear case pressure on engine position 2, which exceeded the limit of 0.7 kg/cm^2 (10 psi gauge). The most plausible explanation of this occurrence appears to be an obstructed pressure sensing line (Section XIII Paragraph 13.2 for a detailed explanation). Detailed analysis of engine position 5 subsystems could not be made due to a failure in the measuring power supply feeding this area.

TABLE 5-I. ENGINE IGNITION AND CUTOFF INFORMATION

Engine No.	Ign. Signal Time After Ign. Command (ms)	GG LOX Lead (ms)	MLV Opening Time (ms)	MFV Opening Time (ms)	MLV Closing Time (ms)	MFV Closing Time (ms)
1	320	10	260	750	250	1300
2	220	10	200	670	300	1370
3	320	20	220	630	330	1250
4	220	20	280	600	300	1300
5	10	10	—	620	—	—
6	120	10	250	600	290	1250
7	10	20	200	680	220	1300
8	120	10	200	700	300	1350

NOTE: Engines started in pairs with a predicted 100 ms difference in starting time as follows:

No. 5 and No. 7
No. 6 and No. 8
No. 2 and No. 4
No. 1 and No. 3

LEGEND

GG - Gas Generator
MLV - Main LOX Valve
MFV - Main Fuel Valve

TABLE 5-II. ENGINE CUTOFF IMPULSE

Engine Position	Engine Cutoff Impulse (kg-sec)	(lb-sec)	Comparison with Nominal (kg-sec)	(lb-sec)
1	32,997 see Note 3	72,746	See Note 5	
2	28,817 see Note 3	63,530	See Note 5	
3	24,725 see Note 3	54,510	See Note 5	
4	-	-	-	-
5	25,348	55,883	-7038	-15,517
6	25,437	56,079	-6949	-15,321
7	24,281	53,530	-8106	-17,870
8	24,547	54,118	-7839	-17,282

NOTES:

1. The nominal cutoff impulse is 32,400 ± 2400 kg-sec (71,400 ± 5200 lb-sec) for a one sigma confidence level.
2. All values are based on chamber pressure decay data.
3. The cutoff signal for engines 1, 2, and 3 was commutated and could be in error by 83 ms, which represents an error in cutoff impulse of 6760 kg-sec (14,900 lb-sec) or 21 percent.
4. The cutoff impulse for engine 4 could not be calculated due to measurement failure; however, cutoff of engine 4 appears to have been normal.
5. The LOX depletion cutoff on the outboard engines prevents a comparison with nominal.

5.3 VEHICLE PROPULSION SYSTEM PERFORMANCE

Overall propulsion system performance, as reflected in vehicle performance, was very satisfactory. IECO occurred at 141.66 seconds range time and OECO occurred 7.43 seconds later at 149.09 seconds. IECO signal was initiated by the LOX tank 04 liquid level sensor. OECO signal came from the "thrust OK" switch on engine position 3, due to LOX depletion. Engine position 3 feeds from LOX tank 04. Engine positions 1, 2, and 3 had already entered the thrust decay period when the cutoff signal was given by engine position 3.

The engine starting sequence was within expected values of predicted. Figure 5-3 shows the chamber pressure buildup of all engines. The starting pairs by position number were 5, 7; 6, 8; 2, 4; and 1, 3 with a programed 100 ms delay between pairs. The maximum deviation in chamber pressure buildup of approximately 40 ms occurred between engines 1 and 3. This deviation is within expected engine-to-engine repeatability limits.

Inboard engine shutdown was normal on all four engines. The outboard engine cutoff characteristic was modified slightly by the LOX depletion cutoff (Figure 5-4).

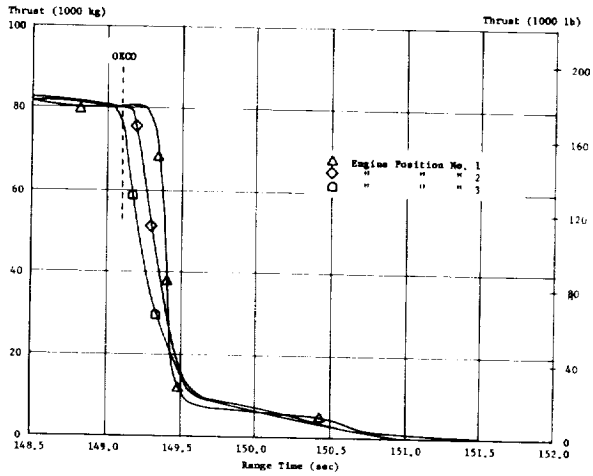

FIGURE 5-4. OUTBOARD ENGINE THRUST DECAY

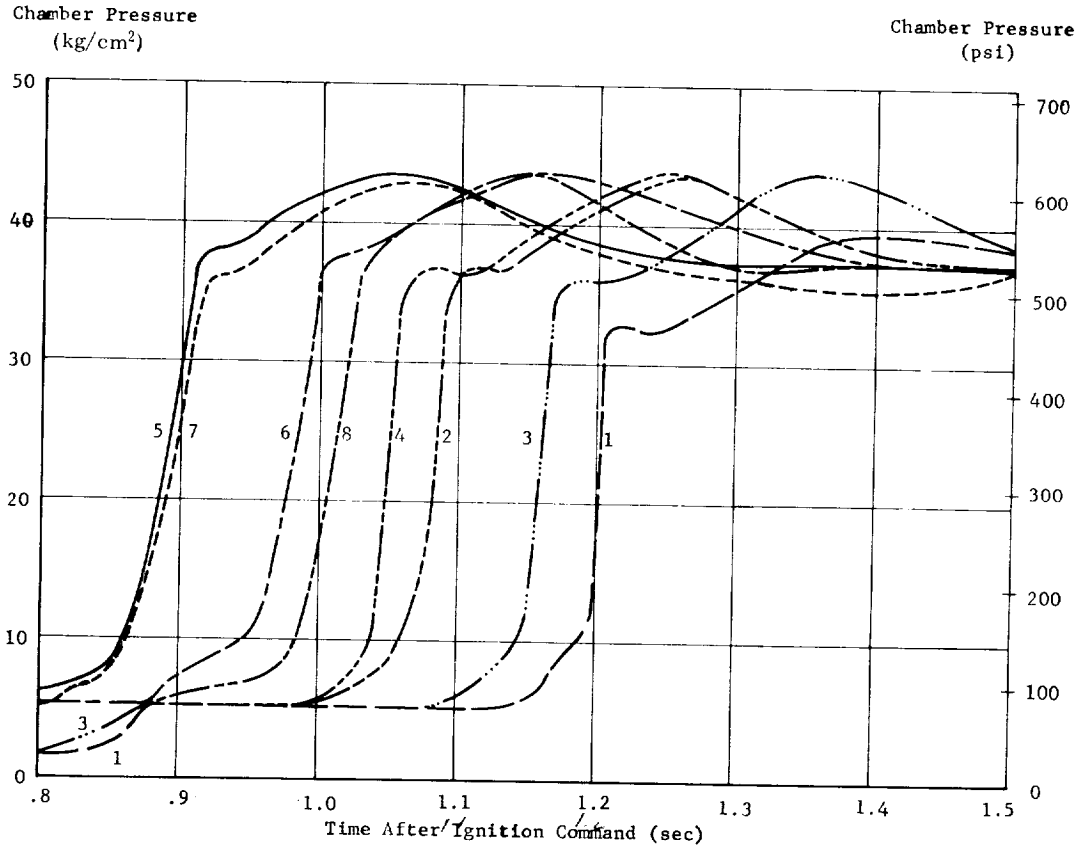

FIGURE 5-3. CHAMBER PRESSURE BUILDUP

Actual and predicted vehicle longitudinal thrust, total flow rate, mixture ratio, and specific impulse are shown in Figures 5-5 and 5-6.

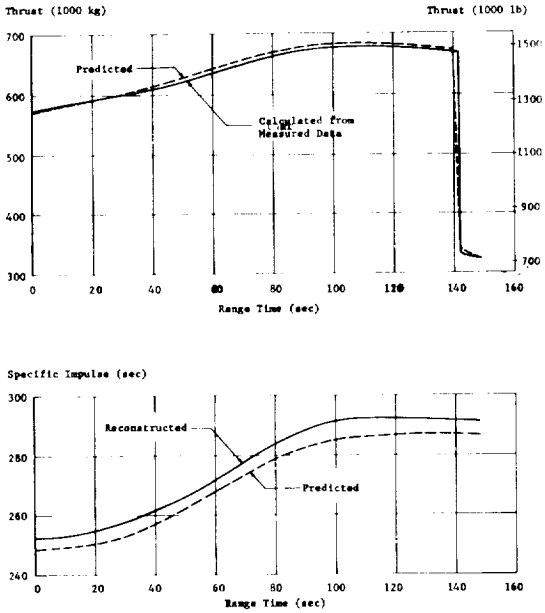

FIGURE 5-5. VEHICLE THRUST AND SPECIFIC IMPULSE

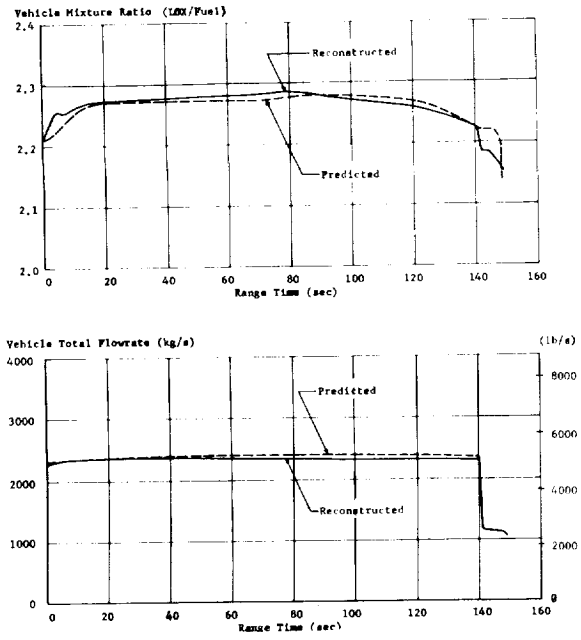

FIGURE 5-6. VEHICLE MIXTURE RATIO AND TOTAL FLOW RATE

There were two approaches used to evaluate the vehicle propulsion system performance. The first method compared propulsion system inflight measurements to corresponding predicted information. The vehicle thrust curve was calculated from measured combustion chamber pressures. The vehicle total propellant flow is defined as,total propellant expended by the vehicle to include engine flows, lube fuel flows, and vented GOX. The engine flows are reconstructed from flight parameters and discrete liquid level data and are considered more accurate than the flows determined from flow meters. However, the latter flows are important for the recognition of the flow transients. The vehicle specific impulse was determined from vehicle thrust and total propellant flow described above. The second approach is through the flight simulation method, which is a computer program with a differential correction precedure used to obtain adjustments to the propulsion parameter inputs which will produce a trajectory that matches the actual trajectory.

The percent deviation from predicted, along with the estimated accuracy limitations of each parameter from both approaches is shown in Table 5-III.

TABLE 5-III. PROPULSION PERFORMANCE DEVIATIONS

	Flight Propulsion Percent	Flight Simulation Percent
Thrust	-0.15 ± 1	-0.15 ± 0.25
Total Flow Rate	-1.63 ± 1	-1.24 ± 0.25
Specific Impulse	+1.50 ± 1	+1.10 ± 0.25

The deviations shown in Table 5-III are computed by subtracting predicted from actual and dividing by predicted. The largest deviation between the two approaches is only 0.4 percent, which is well within expected results from the two methods.

5.4 PRESSURIZATION SYSTEMS

5.4.1 FUEL TANK PRESSURIZATION

The fuel tank pressurization system operated satisfactorily during flight. Gaseous nitrogen, supplied by 48 high pressure spheres, showed a pressure of 205 kg/cm^2 (2920 psi gauge) at liftoff and decayed as expected to approximately 77.3 kg/cm^2 (1100 psi gauge) at OECO. During two time intervals the sphere pressure showed slight increases. The first increase occurred between 60 and 80 seconds. At 106 to 115 seconds, pressure again increased slightly. These small increases in pressure resulted from heat transferred through the sphere walls to the nitrogen at a time in flight when little or no gas is being used from

the spheres. The spheres showed a rest pressure of 70 kg/cm^2 (1000 psi gauge) at 160 seconds.

5.4.2 LOX TANK PRESSURIZATION

Initial pressurization of the LOX tanks, which was the final function in the automatic sequence prior to ignition start timer, was provided by helium from a ground source. Pressurization was begun at approximately T minus 115 seconds and was stopped by the LOX tank pressure switch at T minus 39 seconds at a pressure of 4.25 kg/cm^2 (60.4 psi). The pressurizing time of 76 seconds was 11 seconds shorter than the pressurizing time for Saturn SA-2, due primarily to smaller initial volumes on SA-3 caused by the increased propellant loading.

LOX tank pressurization throughout flight was as expected. The small ullage volumes associated with this flight caused some problem in accurately predicting the characteristics of the LOX tank pressure curves. The prediction technique will be refined for Block II vehicles, based on results of this flight.

The pressurization system is designed to maintain a differential pressure between the center and outboard LOX tanks. The differential pressure is necessary to cause depletion of the center tank prior to depletion of the outboard tanks to prevent trapping of usable LOX in the center tank. The required differential pressure is maintained by orifices located in the pressurizing interconnect lines. The pressure drop across these orifices was approximately 0.09 kg/cm^2 (1.3 psi) lower than predicted at IECO.

5.4.3 CONTROL PRESSURE SYSTEM

The control pressure system operated as expected throughout the SA-3 flight.

Blockhouse records showed the high-pressure-supply-sphere pressure to be 195 kg/cm^2 (2700 psi gauge) at liftoff. This pressure gradually decayed over flight to 144 kg/cm^2 (2050 psi gauge) at 150 seconds. Regulated pressure was 54.5 kg/cm^2 (775 psi) at liftoff and gradually decayed to 53.6 kg/cm^2 (762 psi) at 150 seconds. This absolute pressure decay is expected with a gauge type regulator.

5.4.4 AIR BEARING SUPPLY

The purpose of the air bearing supply was to provide clean gaseous nitrogen at a predetermined flow, temperature, and pressure to the air bearings of the ST-90 and ST-124P stabilized platforms.

Blockhouse records show that the air bearing high pressure supply was maintained prior to launch at approximately 210 kg/cm^2 (2990 psi gauge) for the ST-90 and 209 kg/cm^2 (2970 psi gauge) for the ST-124P, which was within the redline limits of 220 kg/cm^2 (3200 psi gauge) maximum and 183 kg/cm^2 (2600 psi gauge) minimum. The low pressure air to the air bearings of the ST-90 decayed slightly from 2.41 kg/cm^2 (34.3 psi) at 32 seconds range time to 2.37 kg/cm^2 (33.7 psi) at 150 seconds. The low pressure supply to the ST-124P remained constant at 2.24 kg/cm^2 (31.8 psi).

Specifications for the air bearing inlet air temperature stated that the temperature must be maintained at 25 ± 1 degree centigrade. Blockhouse records show that this temperature was maintained within specified limits. Blockhouse records show a cycling in the air bearing inlet air temperature of approximately 8.9 cycles per minute, which was the effect of the thermostatically controlled inlet air heater.

5.5 VEHICLE PROPELLANT UTILIZATION

Overall vehicle propellant utilization (PU) for the flight of SA-3 was one of the most significant results of the test. An evaluation of the PU, utilizing various types of flight data, indicates that 99.4 percent of predicted total usable propellant was consumed during the flight. The high percentage of propellant utilization resulted from the outboard engines being allowed to deplete the LOX tanks before cutoff by the "thrust OK" pressure switch. Center LOX tank depletion (gas break-through), which should have occurred near IECO, occurred approximately 0.7 seconds after IECO, due to a 0.09 kg/cm^2 (1.3 psi) lower-than-predicted differential pressure between center and outboard LOX tanks.

An evaluation of vehicle propellant utilization indicates that 2145 kg (4,728 lb) of LOX and 3892 kg (8,581 lb) of fuel remained onboard the vehicle at the end of outboard engine thrust decay. This compares well with the predicted residuals which were 1454 kg (3197 lb) of LOX and 2248 kg (4957 lb) of fuel. Of the 3892 kg (8,581 lb) of fuel left onboard, approximately 900 kg (2000 lb) was loaded as extra fuel, part of which is considered bias to ensure the burning of any extra LOX in the event it is usable and thereby assuring LOX depletion. If the same cutoff timer had been used on SA-3, as was used on SA-1 and SA-2, cutoff would have occurred 6 seconds after IECO and the LOX and fuel residuals would have been 4,765 kg (10,504 lb) and 3443 kg (7,591 lb) respectively, showing a substantial increase in performance for a depletion type cutoff.

In order to check overall vehicle propellant utilization, twelve liquid level probes were located in each tank to indicate discrete propellant levels during the

flight. However, the most useful information obtained from the flight was the weight of propellant onboard at the end of flight. Flow information during flight, based on the liquid level probes, has not been entirely satisfactory. Various techniques are being investigated to obtain reliable continuous flow information from the liquid level probe signals.

A propellant utilization (PU) system was carried on the SA-3 flight test, as on SA-1 and SA-2, to determine system performance and reliability, and was not a control feature of the Saturn first stage. Results from the PU system indicate that the propellant consumption rate was close to predicted. IECO was initiated by the level cutoff probe in LOX tank 04 at 141.66 seconds range time, or 1.32 seconds later than predicted. The late cutoff might be attributed to dispersion in performance parameters such as variables in engine calibration, container pressures, propellant loading and densities.

LOX container ΔP transducer output indicated a higher-than-predicted differential pressure throughout powered flight except during the time from 110 to 135 seconds. The fuel container ΔP transducer output indicated a higher-than-predicted differential pressure throughout powered flight. The ΔP ratio calculated from the LOX and fuel container ΔP data were generally below predicted, particularly in the period of 90 to 140 seconds. However, this correlates with the individual propellant level and ΔP data and may, therefore, be attributed to performance dispersion.

Data from the liquid level probes in the propellant tank may be used to compare PU system performance. Fuel level probe data correlates well with the PU system data. However, LOX level probe data indicated that the PU system results do not correlate up to approximately 100 seconds. This difference in system results might be attributed to difficulty in determining a valid LOX density, since the density error on the PU system results would be greatest during the first portion of flight, where the liquid column is highest, and would tend to diminish near the end of powered flight, where the liquid column is lowest.

Overall propellant utilization system performance was considered satisfactory although some disagreement was prevalent from the LOX discrete level probe data. Some PU system performance data also varies from predicted data; however, this may be attributed to performance dispersion.

5.6 HYDRAULIC SYSTEM

The telemetered data from SA-3 flight indicated that the operation of all four hydraulic systems was satisfactory. All temperature, level, and pressure measurements remained within acceptable operating limits.

5.7 RETRO ROCKET PERFORMANCE

Four solid propellant retro rockets were flown on Saturn SA-3 vehicle; these retro rockets were the only

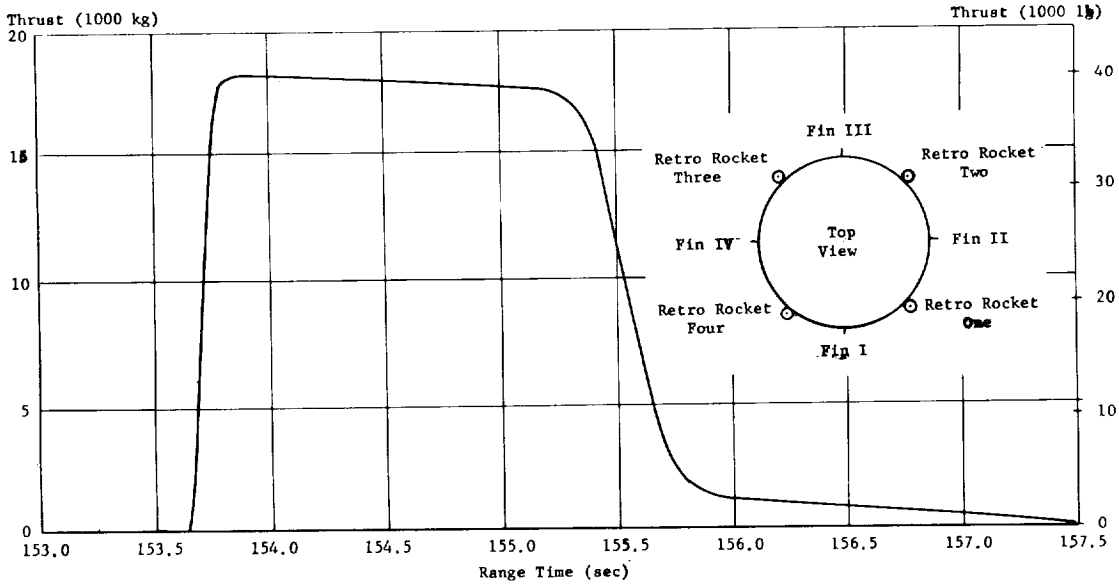

FIGURE 5-7. TYPICAL RETRO ROCKET CHAMBER THRUST

active part of the S-I/S-IV stage separation system flight tested on SA-3. The retro rockets were mounted 90 degrees apart on the spider beam at the top of the S-I stage. Retro rocket thrust vectors were directed through the S-I stage center of pressure. The rocket motors were directed downward and canted 12 degrees from the vehicle centerline. Retro rocket locations are shown in Figure 5-7. Retro rocket firing command (153.66 seconds range time) was given as scheduled, 12 seconds after IECO on SA-3.

A typical retro rocket thrust curve is shown in Figure 5-7. Telemetered retro rocket chamber pressure data indicated satisfactory retro rocket performance and approximately equal performance levels for the four retro rockets. The performance of the retro rockets was within expected limits of the predicted, with total impulse as calculated from measured chamber pressures being about 1.7 percent higher than predicted. The performance, as calculated from chamber pressures, is substantiated by flight mechanical measurements (Section IV Paragraph 4.4). Measured and calculated retro rocket performance parameters are listed in Table 5-IV, along with some predicted values.

During retro rocket operation, a vehicle roll (clockwise viewed from the rear) of approximately 4.3 deg/s occurred, and is attributed to an effective retro rocket misalignment of approximately 0.3 degree for each rocket, caused by twisting of the spider beam and/or misalignment of the rockets to the vehicle centerline. The ST-90 platform roll limit of 15 degrees was reached at 158.4 seconds range time. Retro rocket specifications did not require alignment to prevent roll moments on the SA-3. The effective misalignment of retro rockets on SA-3 is not considered significant because S-I/S-IV separation was not scheduled. Proper alignment of retro rockets on future Saturn vehicles scheduling S-I/S-IV stage separation will be significant in preventing possible S-I/S-IV stage interaction during separation.

TABLE 5-IV. RETRO ROCKET PARAMETERS

Retro Rocket	Predicted*	Actual				
		1	2	3	4	Total
Duration (sec)	2.15	2.105	2.065	2.080	2.070	—
Total Impulse (kg-sec)	33,800	34,630	34,100	34,300	34,400	137,430
(lb-sec)	74,500	76,350	75,200	75,700	75,900	303,150
Average Thrust (kg)	15,720	16,450	16,520	16,510	16,630	66,110
(lb)	34,650	36,270	36,420	36,390	36,670	145,750
Nozzle C_F		1.628	1.628	1.628	1.628	—
Throat Area (m^2)		0.0103	0.0103	0.0103	0.0103	
(in^2)		15.904	15.904	15.904	15.904	—
Maximum Pressure (kg/cm^2)		110	108	108	108	
(psi)**		1,560	1,530	1,533	1,530	—
Maximum Thrust (kg)		18,300	18,000	18,000	18,000	—
(lb)		40,400	39,600	39,700	39,600	
Average Pressure (kg/cm^2)		98	99	99	100	
(psi)		1,400	1,406	1,405	1,416	—
Firing Command (sec range time)		153.66	153.66	153.66	153.66	—
Time of Pressure Build-Up (sec range time)		153.66	153.66	153.66	153.66	—

* Propellant Temperature 15.5°C and Altitude of 76.2 km
** Excluding Ignition Peak

SECTION VI. MASS CHARACTERISTICS

6.1 VEHICLE WEIGHTS

The total vehicle weight was approximately 500,137 kg (1,102,614 lb) at ignition command. Approximately 348,219 kg (767,692 lb) of propellant was consumed during the S-I powered phase of flight (Figure 6-1). Table 6-I indicates weights at various flight events.

6.2 VEHICLE CENTER OF GRAVITY AND MOMENTS OF INERTIA

Longitudinal and radial center of gravity and pitch and roll moments of inertia are given in Table 6-II. These parameters are also plotted versus range time in Figure 6-1.

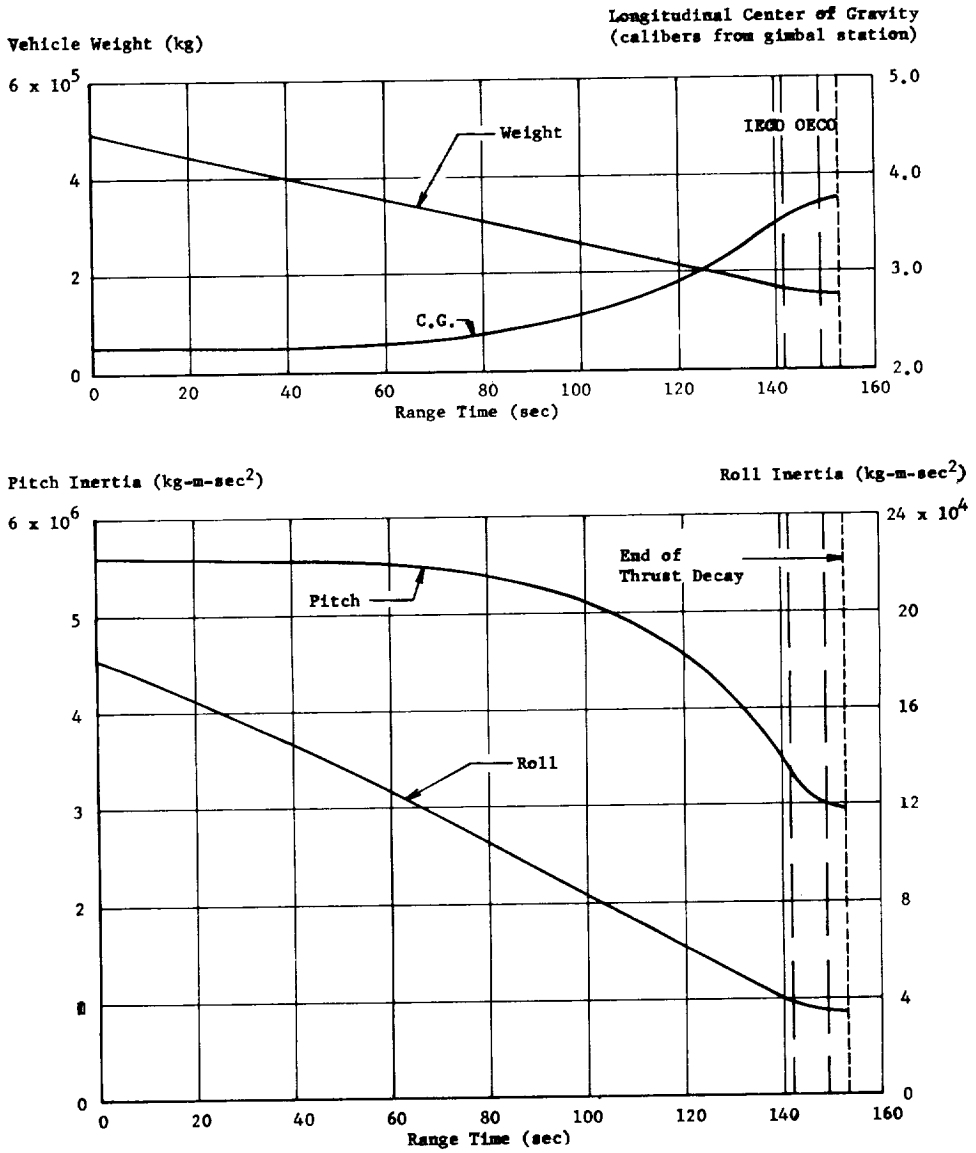

FIGURE 6-1 VEHICLE WEIGHT, LONGITUDINAL CENTER OF GRAVITY AND MASS MOMENTS OF INERTIA VERSUS RANGE TIME

TABLE 6-I. SA-3 VEHICLE WEIGHTS

EVENT	IGNITION COMMAND		FIRST MOTION		INBOARD ENGINE CUTOFF		OUTBOARD ENGINE CUTOFF		END OF THRUST DECAY	
	Pred*	Flight	Pred*	Flight	Pred*	Flight	Pred*	Flight	Pred*	Flight
RANGE TIME (sec)	-3.57	-3.79	0.10	0.10	140.33	141.66	147.90	149.09	150.48	152.78
WEIGHTS (kg)										
Dry Vehicle	143,488	143,598	143,488	143,598	143,488	143,598	143,488	143,598	143,488	143,598
LOX	245,815	244,851	240,505	239,413	8,034	8,295**	1,710	2,355**	1,450	2,145**
Fuel	109,788	110,750	107,771	108,675	5,703	7,264**	2,617	4,266**	2,248	3,892**
Gas in LOX Container	116	113	127	125	1,407	1,403	1,459	1,456	1,461	1,458
GN_2	344	344	344	344	344	344	344	344	344	344
Hydraulic Oil	27	27	27	27	27	27	27	27	27	27
TOTAL	499,578	499,683	492,262	492,182	159,003	160,931	149,645	152,046	149,018	151,464
WEIGHTS (lb)										
Dry Vehicle	316,338	316,580	316,338	316,580	316,338	316,580	316,338	316,580	316,338	316,580
LOX	541,930	539,804	530,224	527,815	17,713	18,287**	3,771	5,191**	3,197	4,728**
Fuel	242,042	244,162	237,594	239,587	12,572	16,015**	5,770	9,404**	4,957	8,581**
Gas in LOX Container	255	250	281	276	3,102	3,094	3,216	3,210	3,220	3,215
GN_2	758	758	758	758	758	758	758	758	758	758
Hydraulic Oil	60	60	60	60	60	60	60	60	60	60
TOTAL	1,101,383	1,101,614	1,085,255	1,085,076	350,543	354,794	329,913	335,203	328,530	333,922

NOTES:
1. Flight dry weight includes 87,329 kg (192,528 lb) water ballast.
2. Predicted dry weight includes 87,414 kg (192,716 lb) water ballast.
3. GOX vented accounted for.
4. No GN_2 vented from fuel containers.
5. Ice accumulation (Approx. 453.6 kg (1,000 lb) at Liftoff) not included.
6. Ignition weight does not include jacket prefill.
7. Predicted propellant weights based on fuel density of 808.1 kg/m^3 (50.45 lb/ft^3)
   Flight propellant weights based on fuel density of 806.6 kg/m^3 (50.356 lb/ft^3)
8. Fuel consumed includes 0.23 kg/sec (0.50 lb/sec) lube fuel flow per engine.

*Predicted Mass Characteristics are those Reported in M-P&VE-ES-91-62 and M-P&VE-ES-111-62.

**Determined from Discrete Level Probe Data

TABLE 6-II. MASS CHARACTERISTICS COMPARISON

EVENT		RANGE TIME	WEIGHT		LONGITUDINAL C.G. (X-Sta)		RADIAL C. G.		PITCH MOMENT OF INERTIA		ROLL MOMENT OF INERTIA	
		Seconds	Kg Lb	% Dev	Meters Inches	Dev	Meters Inches	Dev	$Kg\text{-}M\text{-}S^2$	% Dev	$Kg\text{-}M\text{-}S^2$	% Dev
Dry Vehicle	Pred*	N/A	143,488 316,338	0.1	27.96 1100.6	0.04 1.5	0.005 0.2	0 0	2,583,534	0.4	29,814	0.3
	Flight	N/A	143,598 316,580		27.92 1099.1		0.005 0.2		2,595,148		29,892	
Ignition Command	Pred*	-3.57	500,032 1,102,383	0.0	17.39 684.6	0.01 0.3	0.003 0.1	0 0	5,590,293	0.0	184,340	0.1
	Flight	-3.79	500,137 1,102,614		17.38 684.3		0.003 0.1		5,587,896		184,193	
First Motion	Pred*	0.10	492,717 1,086,255	0.0	17.35 682.9	0.01 0.4	0.003 0.1	0 0	5,583,505	0.0	181,130	0.3
	Flight	0.10	492,635 1,086,076		17.34 682.5		0.003 0.1		5,581,354		181,696	
Inboard Engine Cutoff	Pred*	140.33	159,004 350,543	1.2	25.86 1018.3	0.23 9.3	0.010 0.4	0.005 0.2	3,262,713	2.0	38,175	2.3
	Flight	141.66	160,932 354,794		25.63 1009.0		0.005 0.2		3,329,594		39,052	
Outboard Engine Cutoff	Pred*	147.90	149,646 329,913	1.6	27.08 1066.2	0.33 13.0	0.010 0.4	0.005 0.2	2,875,358	3.4	33,196	3.9
	Flight	149.09	152,045 335,203		26.75 1053.2		0.005 0.2		2,972,326		34,485	
End of Thrust Decay	Pred*	150.48	149,019 328,530	1.6	27.17 1069.7	0.34 13.4	0.008 0.3	0.003 0.1	2,846,605	3.5	32,871	4.3
	Flight	152.78	151,464 333,922		26.83 1056.3		0.005 0.2		2,947,283		34,272	

*Predicted Mass Characteristics are those reproted in M-P&VE-ES-91-62 and in M-P&VE-ES-111-62.

NOTES: Predicted dry weight includes 87,414 kg (192,716 lb) of water.
Flight dry weight includes 87,329 kg (192,528 lb) of water.

SECTION VII. CONTROL

7.1 SUMMARY

The control system for the Saturn vehicle SA-3 was essentially the same as that used on SA-1 and SA-2. However, the control gains (a_o and b_o) were changed because of the increased propellant loading in order to maintain the same correlation with the vehicle mass as on SA-1 and SA-2.

The tilt program for the ST-90 platform was generated by a synchronous motor driven cam as on SA-2. Transients which appeared in the pitch actuator deflections on SA-2, due to a periodic resistance encountered by the cam generating the tilt program did not occur on SA-3.

Engine deflections, attitude angles, and angles-of-attack were less than those observed on SA-1 and SA-2 flights primarily due to the trajectory shape. The greatest wind speeds occurred in the pitch plane direction and were nearly the same as experienced on SA-2.

The Statham control accelerometers, which were flown for operational study purposes for the first time on SA-3, indicated that they should be satisfactory for "closed loop" operation. Statham accelerometers will be in "closed loop" operation on SA-4. The control rate gyro package also performed properly. The usual vibration effects were present, although not detrimental with proper filtering if the rate gyro package was used as an active control sensor in its present location.

Angle-of-attack measuring systems performed satisfactorily. An "upwash effect" was noticed at subsonic speeds on the Q-ball angle-of-attack sensor. With this properly taken into account, the Q-ball could have been used for control up to 100-110 seconds of flight.

The operations of the hydraulic actuators and the control computer were satisfactory.

The attitude measurements from the ST-124P passenger platform were satisfactory except for some differences which are explained by the fact that the ST-124P was not aligned accurately in azimuth and the resolver chain was not "trimmed" as will be done for SA-4.

7.2 S-I CONTROL ANALYSIS

7.2.1 PITCH PLANE

TABLE 7-I. MAXIMUM PITCH PLANE CONTROL PARAMETERS

Parameter	Magnitude	Range Time (sec)
Attitude	1.8 (deg)	88.5
Angle-of-Attack (Free-stream)	-6.8 (deg)	115.0
Angular Velocity	-1.0 (deg/s)	101.4
Normal Acceleration	-1.1 (m/s^2)	83.3
Actuator Position	-2.8 (deg)	83.3

Pitch attitude deviations were essentially zero prior to 50 seconds and after 115 seconds (Figure 7-1). Vehicle tilting was initiated by the ST-90 tilt cam (similar to the one used on SA-2) at 10.33 seconds. The tilting program (Figure 7-2) was based on eight engines operating prior to 20 seconds and seven engines operating for the remainder of the flight in order to minimize control requirements in the event of an engine failure. According to measurements made of the ST-90 cam by LVOD, the actual tilt program cut on the cam started differing from the requested tilt, beginning around 90 seconds. Final tilt arrest occurred at 132.03 seconds, with the vehicle tilted 44.28 degrees from the launch vertical.

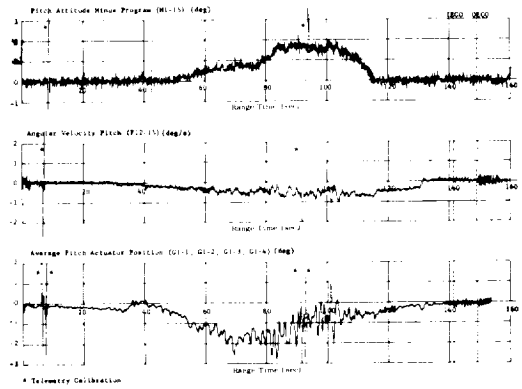

FIGURE 7-1. PITCH ATTITUDE, ANGULAR VELOCITY AND AVERAGE ACTUATOR POSITION

The cam device provided continuous tilting from the time of initiation at 10.33 seconds, until tilt arrest at 132.03 seconds, with the tilt rate varying between zero and a maximum of 0.6 deg/s at 85 seconds. Periodic transients, which occurred in the actuator position of SA-2 due to the cam device, did not occur on SA-3.

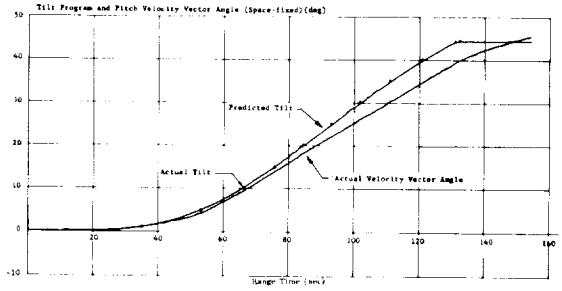

FIGURE 7-2. TILT PROGRAM AND PITCH VELOCITY VECTOR ANGLE

The maximum actuator deflection of minus 2.8 degrees occurred at 83.3 seconds (Figure 7-1) as a result of a wind gradient of 0.023/s acting over an altitude increment of 390 m. This gust had a velocity increment of 9.0 m/s as determined from the angle-of-attack winds compared to 8.7 m/s from rawinsonde measurements. The wind component variation with altitude for the pitch plane was very similar to previous Saturn flights in both magnitude and direction (tail wind). Angles-of-attack and engine deflections were lower, however, due to the different trajectory flown by SA-3 and changed control gains.

Shown in Figure 7-3 is a comparison of the pitch component winds as a function of time from three sources: rawinsonde, rocketsonde, and angle-of-attack winds. The angle-of-attack winds (solid line) were determined from attitude and angle-of-attack measurements made onboard the vehicle which were combined with trajectory angles and velocity components from tracking. Local angles-of-attack (U.S. Science meters) were used for this calculation after applying the appropriate correction for the upwash factor. Rawinsonde winds were obtained up to an altitude of 33.3 km (114.3 seconds vehicle range time). Rocketsonde winds are shown as solid points in Figure 7-3. The angle-of-attack winds are considered questionable after 117 seconds.

The maximum pitch plane wind component as measured by rawinsonde during the maximum dynamic pressure region was 30.9 m/s at 83.1 seconds (13.9 km). The free-stream angle-of-attack at this time was minus 4.1 degrees. Approximately 51 percent of this angle-of-attack can be attributed to the winds. The remaining portion is attributed to the fact that the tilt program is based on seven engines operating during this flight period.

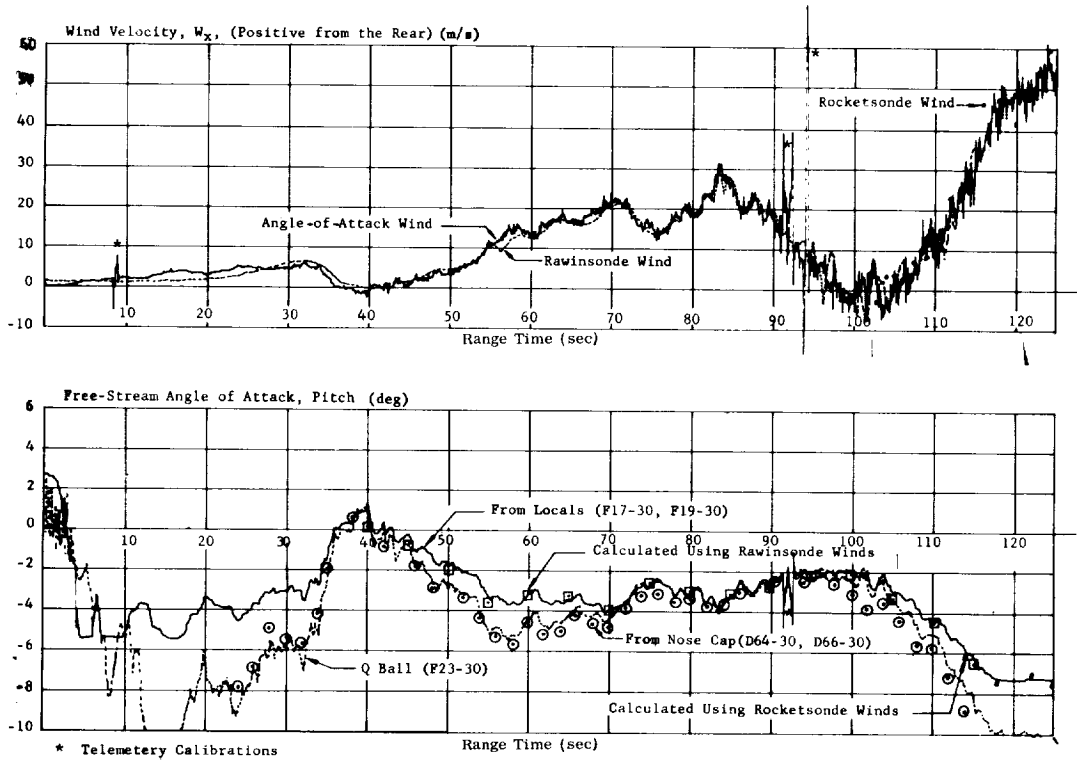

FIGURE 7-3. PITCH PLANE WIND COMPONENTS AND FREE-STREAM ANGLE-OF- ATTACK

Figure 7-4 shows an estimate of the pitch angle design criteria with eight engines operating on a seven engine tilt program for a flight time of 70 seconds. The gains used for establishing the design criteria were from the Drift Minimum Principle for the full propellant loading. The response, due to the 2σ steady-state winds, has been increased by 25 percent to account for gusts. Variations in aerodynamic parameters have been accounted for by increasing the nominal response 11 percent.

The solid lines in Figure 7-4 represent the design criteria as a function of time, and the points are the observed values from the SA-3 flight. Shown to the right of the angle-of-attack are two bar graphs which are estimates of the budgeting for the various factors. The factors considered were:

1. Seven engine tilt program
2. Effect of control gains being different from drift minimum gains
3. 2σ steady-state winds
4. Wind gusts
5. Stability ratio (C_1/B^O) variations

The actual flight values are approximately 36 percent of the design values at 70 seconds, which is near the maximum dynamic pressure region. The wind velocity at 70 seconds was 20.1 m/s. All parameters were well below the design condition.

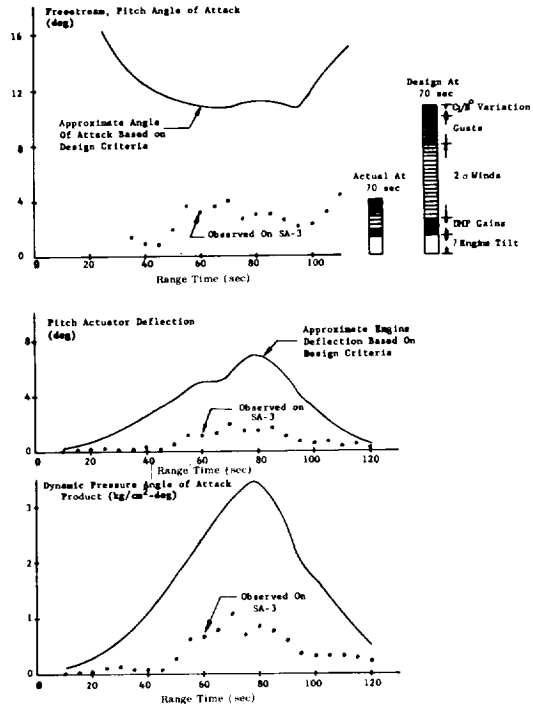

FIGURE 7-4. PITCH ANGLE DESIGN CRITERIA (8 ENGINES OPERATING WITH 7 ENGINE TILE PROGRAM

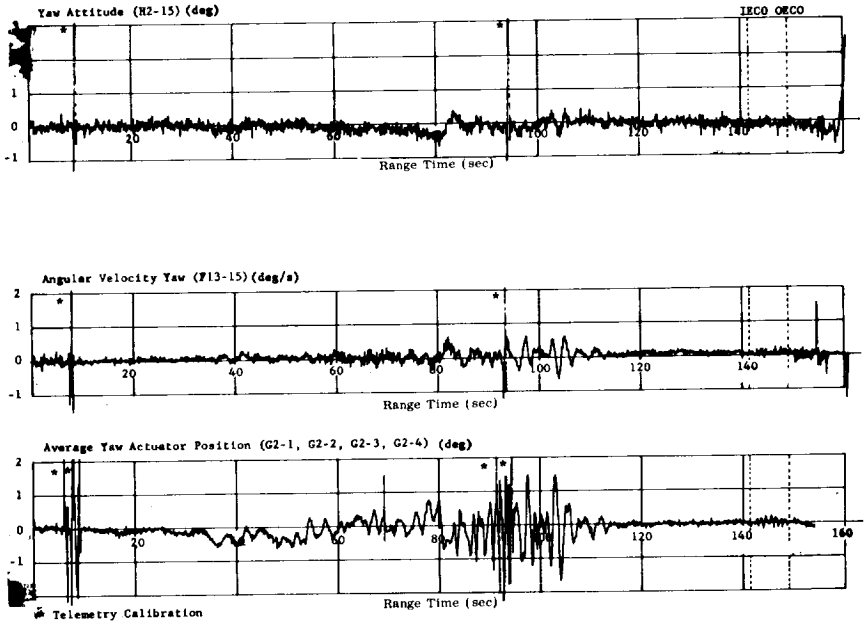

FIGURE 7-5. YAW ATTITUDE, ANGULAR VELOCITY AND AVERAGE ACTUATOR POSITION

7.2.2 YAW PLANE

TABLE 7-II. MAXIMUM YAW PLANE CONTROL PARAMETERS

Parameter	Magnitude	Range Time (sec)
Attitude	-0.4(deg)	80.6
Angle-of-attack (Free-stream)	1.3(deg)	79.5
Angular Velocity	-0.6(deg/s)	104.5
Normal Acceleration	0.5(m/s^2)	77.9
Actuator Position	-1.7(deg)	103.7

Small yaw deviations were observed throughout the powered flight (Figure 7-5). Essentially all of these deviations were the results of winds. Comparatively large actuator movements occurred around 100 seconds. The largest actuator deflection was minus 1.7 degrees at 103.7 seconds as a result of a wind gradient of 0.02/s over an altitude increment of 670 m. This wind gust had a velocity increment of 13.5 m/s as determined from angle-of-attack winds compared to 12.4 from rawinsonde winds.

Yaw plane wind components (Figure 7-6) were very light throughout the flight. The maximum yaw plane wind component was 13.2 m/s (from the left) at an altitude of 12.4 km (79.6 seconds). As in the pitch plane, good agreement existed between the angle-of-attack winds (solid lines) and the rawinsonde winds (dashed lines). Rocketsonde winds (solid points) were also in good agreement with both angle-of-attack and rawinsonde winds. The dynamic pressure at the point where the angle-of-attack winds appeared to be unreliable (122 seconds) was 0.026 kg/cm^2.

7.2.3 ROLL PLANE

TABLE 7-III. MAXIMUM ROLL PLANE CONTROL PARAMETERS

Parameter	Magnitude	Range Time (sec)
Attitude	0.7(deg)	142.1
Angular Velocity	-0.6(deg/s)	143.0
Effective Engine Deflection	-0.1(deg)	80.0

Roll attitude of the vehicle was maintained by differentially deflecting the outboard control engines in both pitch and yaw.

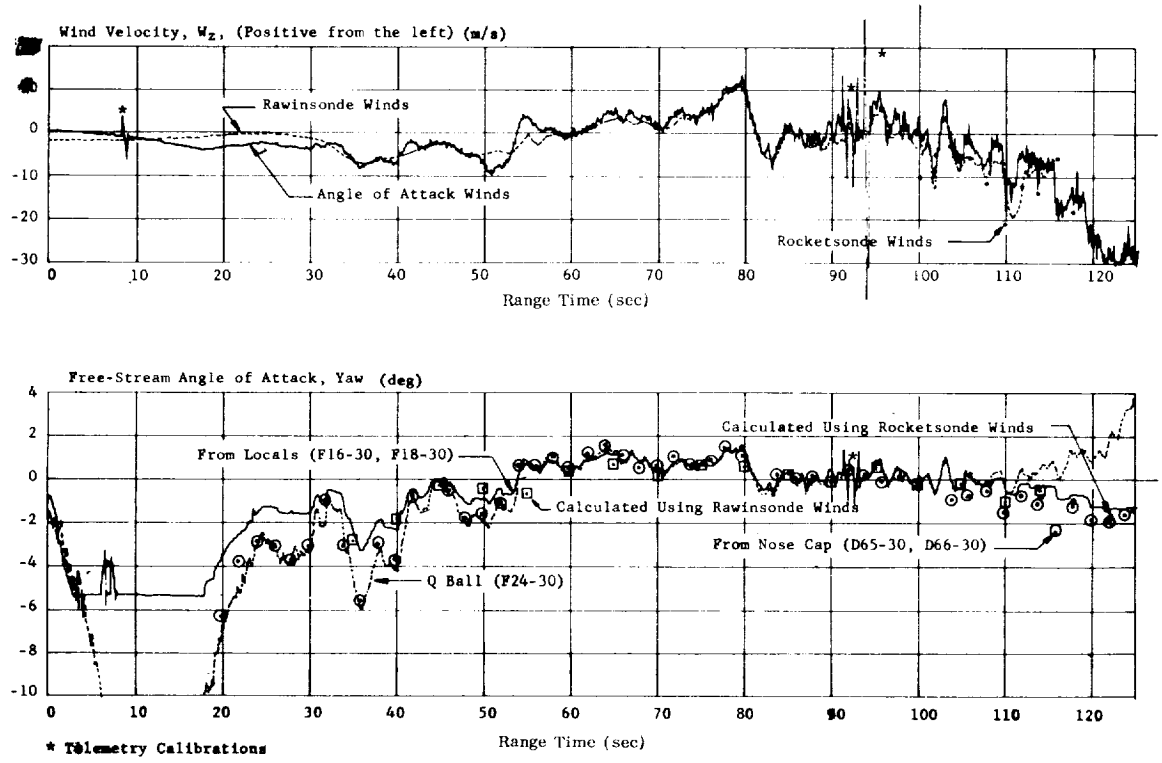

FIGURE 7-6. YAW PLANE WIND COMPONENT AND FREE-STREAM ANGLE-OF-ATTACK

The roll attitude and average roll actuator positions are shown in Figure 7-7. The roll of SA-3 exhibited what is now obviously a characteristic pattern for the Saturn vehicle. The observed roll attitude represents an equilibrium between some unknown "disturbance" moment and the control torque corresponding to the average engine deflections in the roll direction shown in Figure 7-7. The disturbing moments in roll in the cutoff period are compared for all three flights in Table 7-IV.

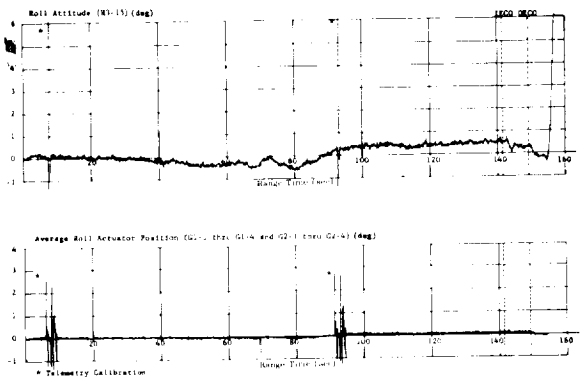

FIGURE 7-7 ROLL ATTITUDE AND AVERAGE ACTUATOR POSITIONS

TABLE 7-IV. ROLL MOMENT

Vehicle	Prior to IECO (kg-m)	Prior to OECO (kg-m)
SA-3	1553	928
SA-2	2140	713
SA-1	1490	672

SA-1 and SA-2 followed the same trajectory and had similar characteristic roll angle time histories. SA-3 flew a different trajectory, and the time history of the roll angle for SA-3 was also somewhat different from that of the first two vehicles. However, if the roll attitudes for the three flights are plotted together as a function of Mach number (Figure 7-8); the trend is almost identical and indicates a close correlation. The increase in roll (in the CW direction) after Mach 1.5 can be correlated with the longitudinal acceleration. The variations in roll between 60 and 90 seconds (prior to Mach 1.5) are most closely correlated with Mach number, indicating a possible aerodynamic effect.

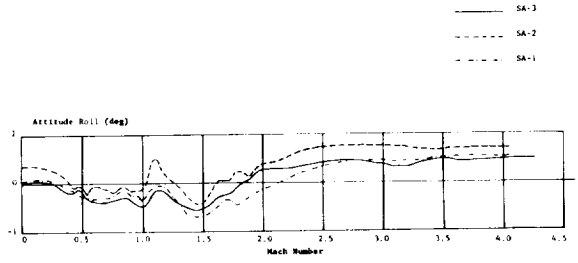

FIGURE 7-8. COMPARISON OF ROLL ANGLE DEVIATIONS FOR SA-1, SA-2 AND SA-3

The roll after Mach 1.5 appears to be more likely an inertial effect. This is also very apparent in the level changes in the roll bias after each cutoff. One possible explanation of this is that the basic trend to roll in the CW direction may be associated with a softness in the servo system and structure associated with the actuators. The center of gravity of the engines are offset in the proper direction such that, coupled with the softness and the inertial load, it could cause an angular misalignment of the thrust vectors. The actuator loads, as measured by the actuator differential pressures are consistent with this hypothesis.

The roll deviation clearly does not affect the functional performance of the vehicle, but analysis will be pursued further from a general interest viewpoint.

7.2.4 ATTITUDE AND CONTROL AFTER CUTOFF

The cutoff of the outboard engines at 149.09 seconds excited the vehicle first bending mode in both pitch and yaw at a coupled frequency of 2.6 to 2.7 cps. The damping of the bending in yaw was approximately 2 percent of critical damping. Bending in pitch initially damped until 151 seconds, after which the amplitude remained almost constant until ignition of the retro rockets at 153.66 seconds. After this, damping was essentially normal in both planes.

As the engine thrust decays, the first bending mode coupled root approaches the unstable region. A root locus analysis indicated that at zero thrust the mode in pitch would be slightly unstable, which is in agreement with the flight. There is a difference between pitch and yaw mounting constraints of the instrument canister containing the platform, such that the control feedback gain in yaw was 0.5 to 0.6 that in pitch. At zero thrust, this would give an increasing damping effect. However, this by itself would not explain the damping observed in yaw. There must be other effects. Some possibilities might be a difference in structural damping in yaw, increased phase lag of the servo system at small amplitudes, and other possible non-linearities in the complete system.

Since the effect of the thrust vector angularity of the engines during thrust decay is of interest in future design, values have been obtained for all three Saturn

vehicle flights. The largest thrust vector angularity during any portion of the decay period that has been considered occurred on SA-1, and was 0.38 degree during the 10 percent to 0 percent thrust decay period. The values obtained for the SA-3 flight are listed in Table 7-V. All values are well within the design angularity of one degree allowed for in the S-IV stage separation design. A large degree of uncertainty (estimated to be 0.75 degree) exists (Table 7-V) in the measurements due to the small deviations being analyzed.

TABLE 7-V. THRUST VECTOR ANGULARITY DURING CUTOFF DECAY

Averaging Period	Pitch (deg)	Yaw (deg)
100 to 10 Percent Thrust	0.21	0.08
10 to 0 Percent Thrust	0.08	0.14
100 to 0 Percent Thrust	0.12	0.08

Retro rockets were flown for the first time on SA-3 to test their functional performance prior to their use for separating the SI-SIV stages on Block II vehicles. Close alignment tolerances for the retros were waived for this flight and measured alignment is questionable. However, there is a possibility that the LOX stud became a load path at retro ignition, and since the LOX studs are 3.8 inches off of the spider beam centerline, an effective misalignment would result from twisting of the spider beam outside of the cross beam network. The results would be in the same direction as that observed from telemetered data.

At the time of retro rocket ignition (153.66 seconds) a sharp roll deviation began. At the end of retro rocket burning (155.73 seconds), the roll angular velocity had increased to 4.3 deg/s (Figure 7-9). To obtain this roll rate, an average misalignment of all four retro rockets of 0.285 degree perpendicular to the cant angle planes was required. If there were any misalignments of the retro rockets in the pitch or yaw planes, they were small and could not be determined. The roll attitude angle measured on the ST-90 stabilized platform reached its mechanical stop of 15 degrees at 158.5 seconds. This forced the ST-90 out of reference in yaw and no usable vehicle attitude information was obtained after this event. Figure 7-9 shows the simulation (dashed line) of this event using the telemetered retro rocket chamber pressures, with a misalignment of each retro rocket in the same direction in the roll plane of 0.285 degrees.

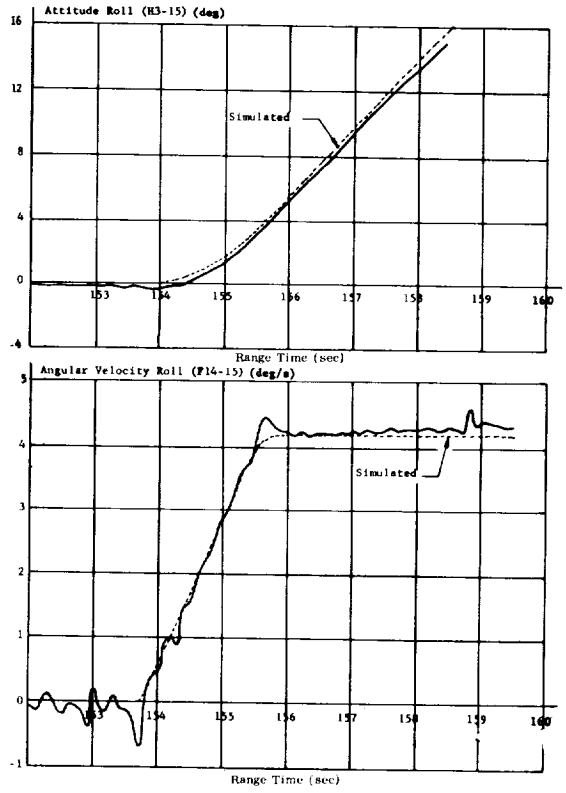

FIGURE 7-9. ROLL DURING RETRO ROCKET FIRING

7.3 FUNCTIONAL ANALYSIS

7.3.1 CONTROL SENSORS

7.3.1.1 CONTROL ACCELEROMETERS

Two Statham control accelerometers (pitch and yaw) were flown for operational study purposes for the first time on SA-3. The telemetered accelerations (Figure 7-10) show proper operation of the equipment during flight. These would have been acceptable for "closed loop" operation in the flight control system. A comparison made between the telemetered acceleration and that calculated from independent flight measurements gives satisfactory agreement, less than 0.2 m/s^2, which is within the error limits of the reduced data used in the comparison. A considerable amount of high frequency (approximately 10 to 15 cps) oscillations appear on the measurements, but they are less than were experienced from the Edcliff accelerometers flown in the same location on SA-1 and SA-2. Statham type control accelerometers will be flown in "closed loop" control on SA-4, in place of the local angle-of-attack transducers.

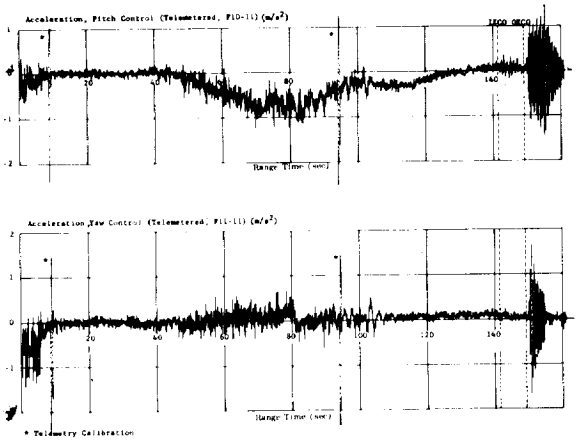

FIGURE 7-10. PITCH AND YAW CONTROL ACCELERATIONS

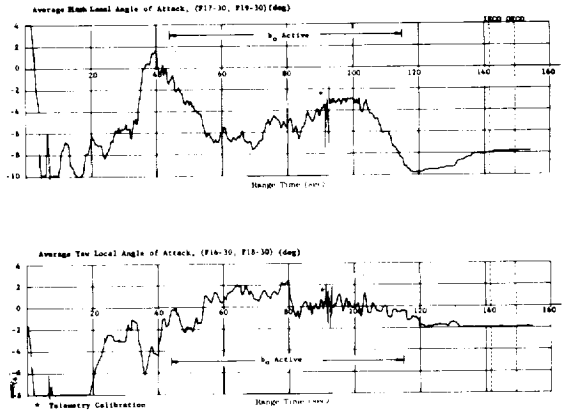

FIGURE 7-11. PITCH AND YAW LOCAL ANGLES-OF-ATTACH

7.3.1.2 RATE GYROS

Rate gyro packages were located in both the instrument canister (a 3-axis Minneapolis Honeywell control package) and in the tail of the S-I stage (a 2-axis Kearfott "measuring" package for pitch and yaw). A 3-axis large measuring range (+ 100 deg/s) rate gyro package was also onboard for vehicle failure analysis if required. All of the instruments operated properly. Some vibration effects were evident in the two sets of low range rate gyros, which were on continuous telemetry channels, but were not detrimental to the basic information. With proper filtering, the "control" package could be employed as an active control sensor in the control loop.

7.3.1.3 ANGLE-OF-ATTACK METERS

Four active control local angle-of-attack meters (U.S. Science) were used on SA-3. A Q-ball angle-of-attack device, similar to the one used on SA-2, was used for measuring purposes.

The U.S. Science meters were mounted radially 90 degrees apart in the payload body surface at station 1841. Two of these meters measure in the pitch plane and two in the yaw plane. The average of the two pitch measurements and the two yaw measurements are shown in Figure 7-11. Since these meters are located on the body, they are influenced by the body upwash. Free-stream angles-of-attack, resulting from correcting the local meters for upwash, are presented in Figures 7-3 and 7-6.

From the comparison of the calculated angles-of-attack from rawinsonde (square points) and rocketsonde wind data (solid points) and the angles-of-attack from the local meters, it can be concluded that these meters functioned properly when the dynamic pressure was greater than 0.026 kg/cm^2. Information from these meters is probably unreliable after this time. The pitch meter reached its measuring limit of 10 degrees at 117 seconds.

Shown in Figures 7-3 and 7-6, as dashed lines, are the direct measurements of angle-of-attack from the Q-ball indicator. Good agreement is obtained between the Q-ball angle-of-attack and the angle-of-attack from the locals after approximately 65 seconds (Mach 1) and up to 105 seconds. At speeds below Mach 1 there is probably an upwash effect influencing the measurement of angle-of-attack from the Q-ball.

The angle-of-attack was also calculated from the telemetered individual differential pressures and dynamic pressure correction factor as measured by the Q-ball. These are shown as circled points in Figures 7-3 and 7-6. The agreement with the direct measurement of angle-of-attack from the Q-ball in the pitch plane is quite good up to 65 seconds, where a deviation of about 0.25 degree starts, and which continues for essentially the remainder of the time. The yaw plane agrees very well with the direct measurement of angle-of-attack from the Q-ball prior to 105 seconds. At this time, an increasing deviation between the direct measurement from the Q-ball and the calculated angle-of-attack from the differential pressure starts. The latter follows essentially the angle-of-attack from the locals and the winds.

The deviations prior to 105 seconds may possibly be attributed to telemetry inaccuracies. Based on these comparisons, the use of the Q-ball angle-of-attack

system appears to be feasible up to at least 105 seconds.

7.3.2 CONTROL COMPUTER

The operation of the control computer on this flight was entirely satisfactory. Comparisons of the telemetered outputs of the computer and calculations of the output values based on the static control equation gives an agreement within ± 0.6 degree or better for all three axes, as was expected.

7.3.3 ACTUATORS

The operation of the hydraulic actuators was satisfactory. An investigation of actuator loading during the flight was made by analyzing the actuator differential pressure measurements. Thrust vector misalignments and inertial loads were determined for all actuators. An investigation of curtain and gimbal friction torques was not made since reliable data was not available for periods when these torques could be isolated.

Thrust misalignment forces, as determined from the differential pressure measurements, are shown in the upper portion of Figure 7-12. These were determined by subtracting the telemetered differential pressure values just prior to engine ignition from the values just after ignition. Thrust misalignment forces were less than 250 kg on all actuators except engine 2 yaw. The force on this actuator was about 435 kg (Figure 7-12). The indicated direction of the net thrust misalignment in roll is in a consistent direction to explain the systematic roll deviation (Section VII Paragraph 7.2.3). However, this explanation appears unsatisfactory with regard to the fact that the roll deviations were so similar in all three Saturn flights (Figure 7-8). As yet, it has not been determined if the magnitude of the misalignment is sufficient.

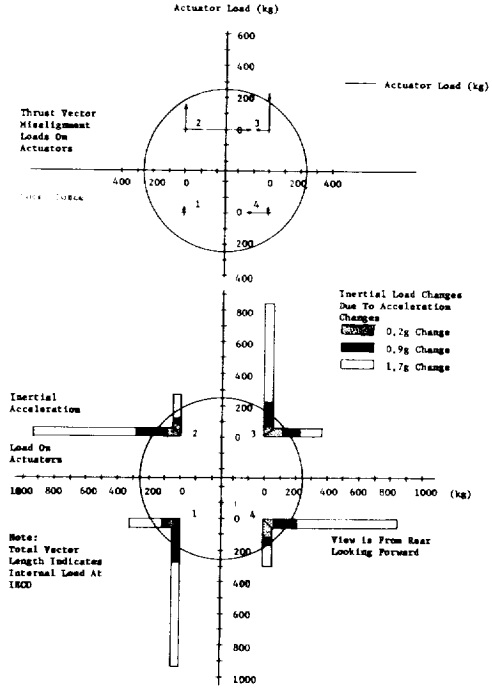

FIGURE 7-12. NON-CONTROL ACTUATOR LOADS, SA-3

The differential pressure measurements indicate maximum actuator loads of 1,433 kg (design load 5,230 kg) occurred just prior to IECO (Figure 7-13). Variable loads up to 689 kg appeared during the high dynamic pressure region of flight. The center of gravity of each of the outboard engines is displaced radially from the engine center line, approximately 20 cm, primarily due to the turbopump assembly. The increasing acceleration of the vehicle, coupled with this offset center of gravity location, puts a load on each of the engines tending to swing them outboard. The increase in actuator loads to counteract this inertial load can readily be observed in the vector diagram in the lower portion of Figure 7-12. The maximum inertial loading occurred just prior to IECO and was 970 kg. Gravitational loading effects prior to liftoff are not clearly indicated since curtain loads and the exact zero point of the ΔP measurements interfere with the determination.

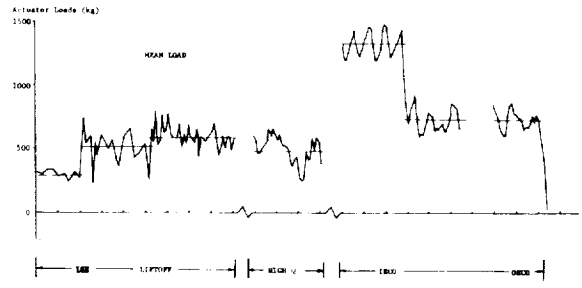

FIGURE 7-13. REPRESENTATIVE ACTUATOR LOADS

The maximum demands on the actuators occurred during the 90 to 104 seconds time period, where all actuators experienced peak deflection rate demands of 4.5 to 5.5 deg/s. The nominal level of demand was less than 1 deg/s.

After OECO there were several periods where first mode bending oscillations were excited. The stability of this mode is influenced by the movement

of the control engines. When the engines are swiveled in response to control commands at the first mode bending frequency and at a zero thrust condition, the inertia effect of the engines tends to decrease the bending mode stability (as discussed in Section VII Paragraph 7.2.4). This swiveling requires power to move the actuators. Figure 7-14 shows representative curves for one typical engine hydraulic supply after OECO. This indicates that complete depletion of hydraulic pressure occurred at 158.5 seconds. Between OECO and this time, for the control system used on SA-3, energy could be fed into a bending oscillation, decreasing the stability.

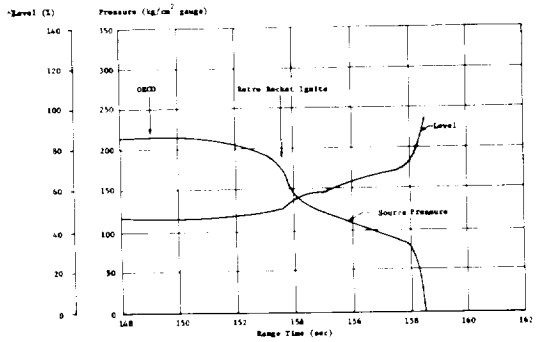

FIGURE 7-14. HYDRAULIC SOURCE PRESSURE AND LEVEL

7.3.4 ST-124P STABILIZED PLATFORM, ATTITUDES

The ST-124P stabilized platform (prototype model) was flown as a passenger on SA-3. The ST-124P is planned for use on the operational vehicles and will be flown in "closed loop" on Block II vehicles beginning with SA-7.

A comparison of the attitude measurements from the two platforms (ST-90 and ST-124P) shows some difference in all three axes (Figure 7-15). The systematic deviation, shown between the yaw and roll attitude measurements from the two platforms is due to the misalignment of the ST-124P platform azimuth reacting, through the vehicle tilting, as mentioned in Section VIII Paragraph 8.3.3. The additional small differences are felt to be due to excess backlash in the servo gear trains in the ST-124P and telemetry and data reduction errors. The much larger systematic difference between the pitch attitude angles is due to an impedance mismatch in the ST-124P resolver chain. This pitch angular error (φ_e) is a function of the impedance mismatch and the sine of twice the resolved angle (i.e. φ_e - M sin 2χ). χ is the tilt angle of the ST-124P outer pitch resolver. The dashed line in Figure 7-15 shows the remaining difference in the pitch angles after a correction for a 1.3 Ω (approximately 0.3 percent) impedance mismatch error has been made.

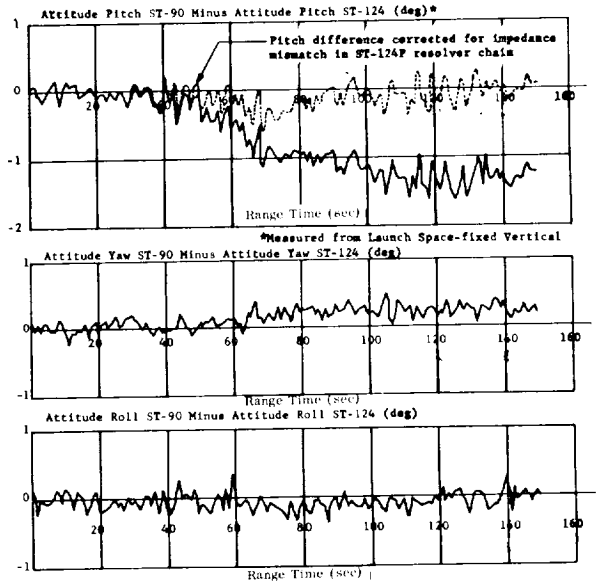

FIGURE 7-15. ATTITUDE DIFFERENCES BETWEEN ST-90 AND ST-124P

To substantiate the mismatch assumption, the platform for SA-4 was tested and found to have a similar error buildup as the tilt program was run in. The error for a tilt angle of 44 degrees amounted to 1.75 degrees. This will be reduced to less than 0.25 degree by balancing out the major portion of the mismatch before the platform is flown.

7.4 PROPELLANT SLOSHING

The same baffle configurations were used in the outer propellant tanks as used on SA-2. These baffles again proved effective in keeping sloshing amplitudes at low levels. However, some oscillations at the sloshing frequency were noted in the engine positions. A peak amplitude of ± 0.2 degree occurred in the pitch actuator positions at 145 seconds, being damped out by OECO.

Sloshing in three of the nine propellant tanks was measured by means of differential pressure measurements. Slosh measurements were made in the center LOX tank, LOX tank 04 and fuel tank F2. Measurements D6-OC (in center LOX tank) and D6-04 (LOX tank 04) were telemetered on continuous telemetry channels.

All of the measurements apparently functioned properly during most of the flight except during the

first few seconds, which is characteristic. The first apparently valid information was obtained at the times indicated in the table below. Comparable times for SA-2 are also shown.

Start Times of Valid Slosh Measurements

	SA-3	SA-2
D4-F2	0 sec	-
D5-F2	0	3 sec
D6-04	8	20
D7-04	29	18
D6-OC	0	15
D7-OC	18	14

The telemetered sloshing differential pressures must be multiplied by a conversion factor to obtain the sloshing height in centimeters. This factor is a function of many parameters, including the liquid level in the tank, longitudinal acceleration, propellant damping, and frequency of oscillations. The converted propellant slosh heights for the center LOX tank are shown in Figure 7-16. The best information was obtained by measurement D6-OC which was telemetered on the continuous channel. The results are extremely sensitive to many parameters, especially the height of the propellant surface in the tank and the exciting frequency. The results shown here are believed to be the best results to be obtained at this time. Presently, ground tests of this slosh differential pressure measuring system are being analyzed to verify the conversion procedures being used or to develop more exact methods.

The largest amplitudes of sloshing occurred around the time of maximum dynamic pressure (80 seconds). Table 7-VI compares the peak sloshing amplitudes observed on SA-3 with those of SA-2

TABLE 7-VI. PEAK SLOSHING AMPLITUDES

Tank	Plane	Meas. No.	Peak-to-Peak Amplitudes (cm) SA-3	SA-2
Fuel 2	Pitch	D4-F2	15	-
Fuel 2	Yaw	D5-F2	8	13
LOX 4	Pitch	D6-04	24	10
LOX 4	Yaw	D7-04	20	11
Center LOX	Pitch	D6-OC	10	11
Center LOX	Yaw	D7-OC	10	10

The most noticeable sloshing near the end of powered flight was detected on measurement D6-OC in the center tank. A pronounced regular oscillation started around 120 seconds, which was before the propellant surface went below the baffles (Figure 7-16). The amplitude amounted to only about ± 1 cm up to the time

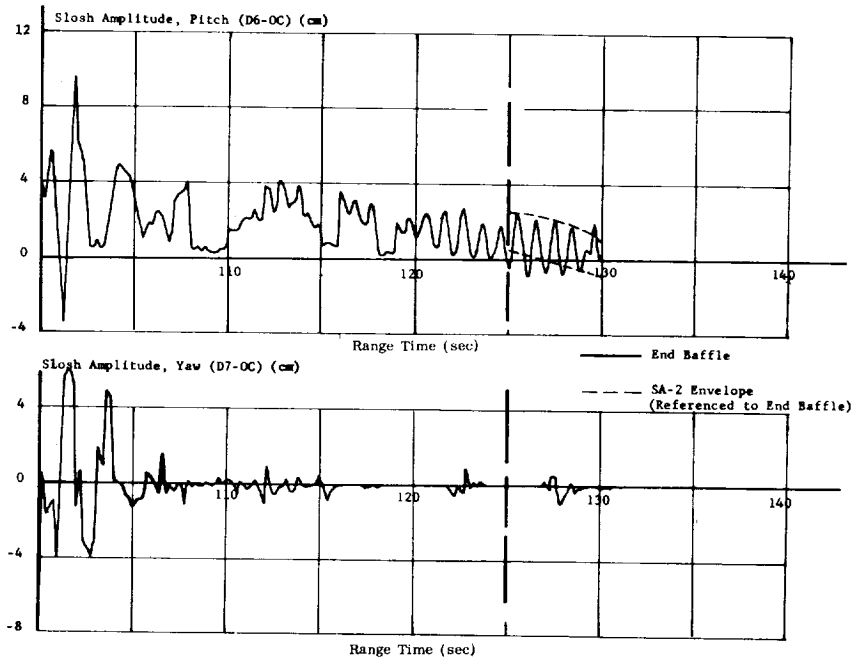

FIGURE 7-16. CENTER LOX TANK TELEMETERED SLOSHING AMPLITUDES AFTER 100 SECONDS

the fluid surface went below the slosh probe and the measurement ended. The dashed lines in Figure 7-16 show the envelope of the slosh amplitude observed in the center tank on SA-2. This has been referenced to the location at the end of the baffles, since the time history of the two flights was different due to the propellant loading differences. The sloshing in the center tank was similar in magnitude on SA-2 and SA-3. However, it appeared that sloshing started somewhat earlier on SA-3. Also, the vehicle was driven more at the sloshing frequency as mentioned previously, than SA-2.

Figure 7-17 shows a comparison of some of the frequencies detected in the sloshing measurements compared to the predicted. The square points shown after IECO are frequencies detected in some of the accelerometers, which indicate that the vehicle was being forced by the sloshing. The pitch actuator positions also indicated this. In this case, in contrast to SA-1, the vehicle appears to be driven at the natural frequency of the propellant, rather than at some coupled frequency. Whether this is consistent or not, is not known at this time.

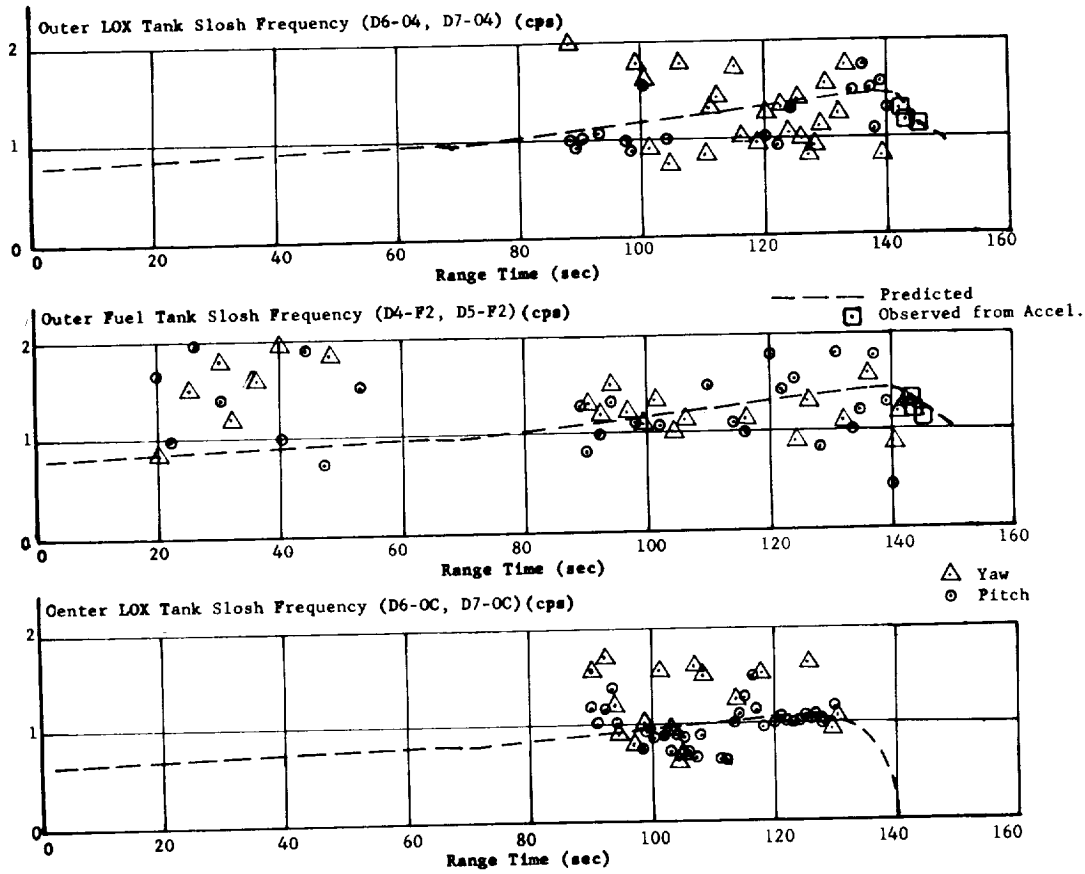

FIGURE 7-17. SLOSHING FREQUENCIES

SECTION VIII. GUIDANCE

8.1 SUMMARY

The Saturn SA-3 vehicle was flown without active path guidance or velocity cutoff. However, passenger hardware for both ST-90 and ST-124P (Prototype) guidance systems was onboard to establish the operational capabilities of the guidance equipment in the Saturn flight environment. The telemetered data as well as a trajectory comparison confirm satisfactory performance of the ST-90 guidance equipment throughout powered flight.

Erroneous outputs from the cross range accelerometer system mounted on the ST-124P platform were noted before ignition. No correction was made and the cross range measurement contained extraneous signals throughout flight. These extraneous signals could be eliminated from the telemetered accelerometer output and valid cross range information was deduced from the measurement.

The output of the altitude accelerometer mounted on the ST-124P platform was satisfactory. Comparisons with both calculated and ST-90 guidance data indicated a velocity difference of approximately 0.2 m/s at end of thrust, after the altitude velocity was corrected for a 0.09 percent scale factor error.

The Saturn SA-3 vehicle experienced a high roll rate after ignition of the retro rockets at about 153.6 seconds. Both the ST-90 and ST-124P platforms reached their mechanical limits at approximately 158.4 seconds and 159.2 seconds respectively. Guidance data past these points were invalid.

8.2 DESCRIPTION OF GUIDANCE SYSTEM

8.2.1 ST-90 GUIDANCE SYSTEM

The ST-90 guidance system was similar to that flown on SA-2 (Reference 3). Three integrating accelerometers (AMAB-3) were mounted on the stable element to measure velocities in the slant range, slant altitude, and cross range directions. The slant range accelerometer was oriented in the firing direction and 41 degrees up from the launch horizontal; the slant altitude accelerometer was 41 degrees from the launch vertical; the cross range measuring direction was in the launch horizontal plane and completed a right handed coordinate system. This orientation remained fixed during flight until the platform was forced out of its frame of reference in roll at 158.4 seconds.

8.2.2 ST-124P GUIDANCE SYSTEM

The ST-124P is a four gimbal system utilizing two AMAB-3 integrating accelerometers mounted on the stabilized element. Platform orientation is maintained by three AB-5 stabilizing gyros. The accelerometers were oriented to measure the vehicle velocities in the vertical and cross range directions. The altitude accelerometer was aligned along the local vertical at launch; the cross range axis lay in the launch horizontal plane and normal to the firing azimuth. This orientation remained essentially fixed in space until the stable element was forced out of its frame of reference.

Mechanical limits and times when both platforms reached the indicated stops are listed below:

Platform	Mechanical Stop	Limit	Time (sec) Computed	Time (sec) Record
ST-90	Roll	±15 deg	158.4	158.4
ST-124P	Yaw or X-gimbal	±11 deg	158.54	158.9 to 159.4*

* Indication of loss of platform reference from the yaw gyro pickup measurement (H19-12) occurred during a calibration period.

The vehicle was flying at an angle of approximately 45 degrees measured from the platform X-axis. Therefore, the component of motion about the platform X-axis due to roll about the vehicle longitudinal axis is approximately given by:

$$\theta_y \approx - \sin 45^\circ \int_{t_o}^{t} \dot{\varphi}_{roll}\, dt$$

A rotation of 11 degrees about the ST-124P X-axis at 158.54 seconds was computed by inserting the telemetered values for $\dot{\varphi}_{roll}$ in the above equation and performing the integration from the time of retro rocket ignition. The yaw gyro servo signal (measurement H19-12) indicated that a bias shift to full scale measurement occurred during a calibration period between 158.9 and 159.4 seconds. The time at which this measurement departs from its normal level should be the true indication that the platform is no longer space-fixed. The difference in the computed and observed times is due to truncation of the equation for θ_y, errors in data used in the computations, response of the various telemetry channels, and prototype hardware components for the ST-124P system.

It should be emphasized that the ST-124P platform was only an engineering test model, and gimbal limits existing in this system will not apply to the ST-124P equipment to be flown in the Block II vehicles.

8.3 OPERATIONAL ANALYSIS

8.3.1 GUIDANCE INTELLIGENCE ERRORS

The guidance intelligence errors are defined as deviations in the guidance measurements resulting from platform and accelerometer errors, and may be found by comparing the guidance system measurements with the vehicle trajectory.

The errors presented in Figures 8-1 and 8-2 include errors in tracking and data reduction as well as guidance hardware errors. ST-90 guidance intelligence errors, shown in Figure 8-1, are within the data noise level and one sigma hardware errors.

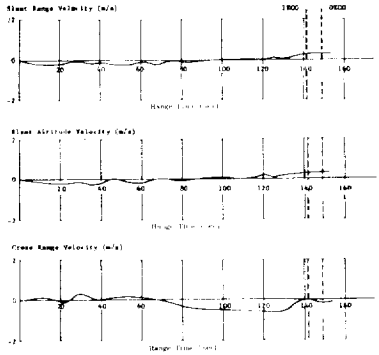

FIGURE 8-1. GUIDANCE VELOCITY COMPARISON (ST-90) (TELEMETERED - CALCULATED)

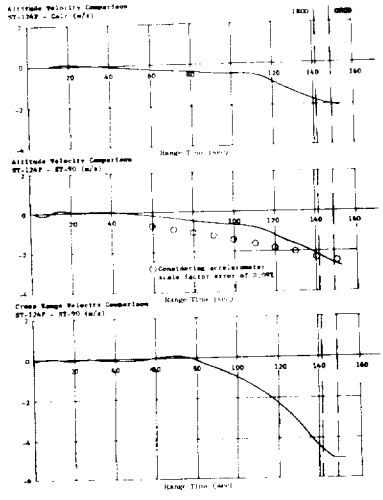

FIGURE 8-2. GUIDANCE COMPARISONS, ST-124P GUIDANCE SYSTEM

The errors made by the ST-124P guidance equipment in measuring the vertical and cross range velocities are discussed in Section VIII Paragraph 8.3.3.

8.3.2 ACCELEROMETER OUTPUTS (ST-90)

The inertial velocity outputs of the integrating accelerometers represent the vehicle motion as sensed by the guidance system. The data from both the ST-90 and ST-124P guidance systems were reduced and compared with corresponding velocities computed from external tracking data. Ideal alignments of the guidance hardware were assumed for the guidance calculations. The comparisons indicated a favorable agreement of the data, especially for the ST-90 system. The small errors observed may be attributed to errors in the telemetered data reduction, tracking, and hardware errors. The accelerometer outputs were monitored prior to ignition. The velocity errors, averaged over several time points, corresponded to accelerometer angular misalignments of:

ST-90

Slant Range	+0.003 deg
Slant Altitude	-0.002 deg
Cross Range	-0.009 deg

where a positive angle represents a positive output error. The ST-90 platform remained in its reference established at liftoff with essentially no errors greater than the established one sigma deviations, until reference was lost in roll at about 158.4 seconds.

Slant Range Velocity (ST-90)

The outputs of the slant range accelerometer were compared with corresponding values computed from earth-fixed trajectory data assuming ideal alignment of the platform and accelerometers. These differences are plotted versus time in the upper portion of Figure 8-1. The errors oscillate around zero for the entire powered flight. The small errors observed are the results of errors in the data compared and the one sigma errors of the guidance hardware.

Cross Range Velocity (ST-90)

The cross range velocity, as measured by the ST-90 guidance system, is plotted versus time in the upper portion of Figure 8-3. Extraneous incremental outputs were noted on the telemeter trace of the cross range velocity from minus 2.82 seconds to about 3.9 seconds. However, the data were manually reduced with little difficulty. The azimuth of the ST-90 platform and the Fin I - Fin III launch position of the vehicle were 100.011 degrees and 100.381 degrees East of North respectively. This alignment difference

produced the cross range velocity observed by both the accelerometer and the external tracking. The overall velocity profile also reflects the changes in the cross range wind velocity.

Cross range guidance velocity was about minus 2.2 m/s at 40 seconds of flight when b_o (angle-of-attack control coefficient) entered the control loop. The cross range velocity increased from minus 2.2 m/s at 40 seconds to minus 3.0 m/s at 50 seconds and remained relatively constant to about 85 seconds. From this time the ST-90 cross range velocity increased to minus 7.5 m/s at outboard engine cutoff. The term b_o was taken out of the control loop at 115 seconds of flight time.

Differences between the telemetered and calculated ST-90 cross range velocities are plotted versus time in the lower portion of Figure 8-1. The differences oscillate around the zero reference until after 70 seconds. From this time the differences increase to about minus 0.5 m/s at 90 seconds and remain practically constant to 130 seconds. The differences go to essentially zero by 140 seconds. The error profile presents no definite trend and the differences are probably due to bias shifts in tracking data rather than the ST-90 guidance equipment. However, the cross range velocity errors are within the usual noise level of the guidance hardware.

Slant Altitude Velocity (ST-90)

The telemetered slant altitude velocity was the actual velocity as sensed by the ST-90 guidance accelerometer. The lower portion of Figure 8-3 presents the telemetered and precalculated slant altitude velocities plotted versus time. Telemetered velocity was generally lower than precalculated values, particularly after tilt arrest, resulting from approximately 1.2 percent lower flow rates and about 0.28 degrees extra tilt. At end of thrust, the slant altitude velocity was 1241.4 m/s, or 12 m/s lower than precalculated.

The differences between telemetered and calculated slant altitude velocities are plotted versus time in the middle portion of Figure 8-1. The differences oscillate around the zero reference within ±0.3 m/s, indicating very good agreement of the data compared.

Table 8-I presents a comparison of the guidance velocities at some significant flight events. Telemetered ST-90 guidance velocities and those calculated from external tracking data are in close agreement. The deviations in the ST-124P measurements are discussed in Section VIII Paragraph 8.3.3.

TABLE 8-I. GUIDANCE COMPARISONS

Flight Event		ST-90			ST-124P	
		Slant Range Vel. (m/s)	Slant Altitude Vel. (m/s)	Cross Range Vel. (m/s)	Altitude Vel. (m/s)	Cross Range Vel. (m/s)
First Motion	Telem	0	0	0	0	0
	Calc	0	0	0	0	0
	Precal	0	0	0	0	0
Inboard Engine Cutoff	Telem	2601.7	1227.5	-7.2	2630.4	-11.8
	Calc	2601.2	1227.0	-7.2	2632.2	-7.2
	Precal	2571.8	1237.9	-0.25	2621.5	-0.25
Outboard Engine Cutoff	Telem	2762.6	1240.6	-7.5	2745.6	-12.4
	Calc	2762.3	1239.7	-7.3	2747.3	-7.3
	Precal	2740.4	1252.6	-0.26	2743.2	-0.26
End of Thrust	Telem	2770.5	1241.4	-7.5	2752.0	-12.4
	Calc	2770.7	1240.7	-7.3	2754.2	-7.3
	Precal	2748.0	1253.3	-0.26	2748.7	-0.26

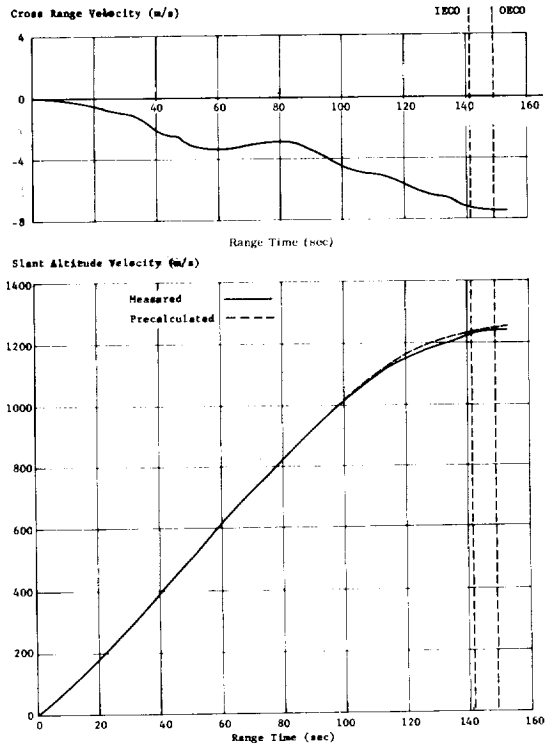

FIGURE 8-3. TELEMETERED CROSS RANGE AND SLANT ALTITUDE VELOCITY, ST-90 GUIDANCE SYSTEM

8.3.3 ACCELEROMETER OUTPUTS (ST-124P)

Measurements were made by the ST-124P guidance system in the vertical and cross range directions. The vertical telemetered data were easily reduced, but much difficulty was experienced in reducing the cross range outputs. This difficulty is discussed in Section VIII Paragraph 8.4.2.

Altitude Velocity (ST-124P)

The upper portion of Figure 8-2 presents differences between the telemetered and calculated altitude velocities. The differences are essentially zero until about 40 seconds. From this time, the differences increased until the end of thrust to a value of about minus 2.1 m/s.

A similar comparison was made between the outputs of the vertical accelerometer (ST-124P) and corresponding values determined from the slant range and slant altitude accelerometers carried on the ST-90 platform. This comparison is presented in the middle portion of Figure 8-2. Both comparisons indicate an error of approximately 2.5 m/s in the altitude velocity telemetered from the ST-124P system.

A scale factor error of about minus 0.1 percent was noted in the vertical accelerometer about 90 minutes prior to launch. An error of this magnitude would produce the observed velocity error. After correcting for the scale factor error, the altitude velocities from the two guidance systems are in agreement, indicating maintenance of proper orientation of the ST-124P platform about its Z-axis.

The circled points shown in Figure 8-2 represent the velocity difference for an accelerometer scale factor error of 0.09 percent.

Cross Range Velocity (ST-124P)

Much difficulty was experienced in reducing the cross range data; however, valid values were obtained. These data were compared with the same measurement as sensed by the ST-90 guidance system. This comparison is presented on the lower portion of Figure 8-2. The differences are essentially zero until about 80 seconds. From this time, the differences increased until IECO to a value of about 5.0 m/s. This difference may be attributed to a difference of azimuth alignment of the ST-124P platform and the ST-90 platform. The ST-124P platform was not optically aligned to azimuth as was the ST-90. Instead, it was referenced to a vehicle Fin I - Fin III position.

The azimuth of the ST-124P is acceptable since the platform could not be optically aligned. Precise azimuth alignment for the ST-124P, to be flown on SA-4, will not be possible since the mounting arrangement on SA-4 will be the same as SA-3. However, this will be no problem for the Block II vehicles.

The cross range velocity comparison shows a constant azimuth difference between the platforms. The ST-124P platform was oriented approximately 0.27 degree South of the optically aligned ST-90. Essentially no platform rotations occurred about the X or Y axes until after retro firings, when the platform reached its mechanical limit.

8.4 FUNCTIONAL ANALYSIS

8.4.1 GUIDANCE SENSORS

The operation of the five AMAB-3 guidance accelerometers, (three on ST-90, two on ST-124P) flown as passenger items on SA-3, was as expected, with the single exception of the cross range accelerometer on the ST-124P stabilized platform. Telemetry measurements of the servo pickup voltage for this accelerometer indicate a continuous oscillation of the system at about 60 to 65 cps from before liftoff (approximately T minus 140 seconds) to the end of flight. Laboratory

tests following the flight indicate that the gain adjustment of the servo amplifier was probably set in a critical area, where the system is stable unless subjected to a fairly large electrical or mechanical disturbance; at a setting in this critical area, once the required disturbance occurs, the system goes into a self-sustained oscillation. The critical area of gain setting is just below the maximum gain capability of the servo amplifier. The servo loop signals for the remaining accelerometers were normal.

8.4.2 VELOCITY ENCODERS AND SIGNAL PROCESSOR REPEATERS

The operation of the accelerometer velocity encoders was satisfactory. Five encoders were flown, three with the ST-90 system accelerometers and two with the ST-124P system accelerometers.

Two Guidance Signal Processor Repeaters were flown on SA-3, one for each stabilized platform. The processor for the ST-90 system operated satisfactorily throughout the flight; the second unit, for the ST-124P system, had a failure in a buffer amplifier stage, causing loss of one of the DC logic signals used in sensing the polarity of the cross range velocity increments. This malfunction occurred early in the countdown. A second disturbance in this processor occurred intermittently in both channels during the time period from 113 to 125 seconds. The disturbance is believed to be due to voltage transients on the processor B+ line.

Ground recording, and inflight telemetry records showed a disturbed condition of the ST-124P cross range velocity system, which appeared to indicate that the accelerometer was wandering randomly. This has been shown to be incorrect after a detailed study of the ground and inflight records, the logic network of the signal processor, and the 65 cps oscillation observed in the accelerometer servo loop.

Oscillation of the accelerometer system would normally result in both positive and negative incremental velocity pulses, which cancel each other except for actual velocity change. However, with a loss of one DC logic signal used in sensing the polarity of the velocity increment, the output would be a continuous pulse pattern as shown in pattern 1 of Figure 8-4. As the system changes position, intermediate pulse patterns occur as shown in the even numbered patterns of Figure 8-4. When the pulse pattern on the telemetry record changes from one pattern to a second distinct pattern, a velocity change of 0.1 m/s has occurred. The pulse patterns result from a combination of three conditions:

1. A small true acceleration.
2. Accelerometer servo loop oscillation.
3. Loss of one logic signal in the signal processor.

The lower portion of Figure 8-4 shows the incremental velocity pulses as they should occur if the system was operating properly.

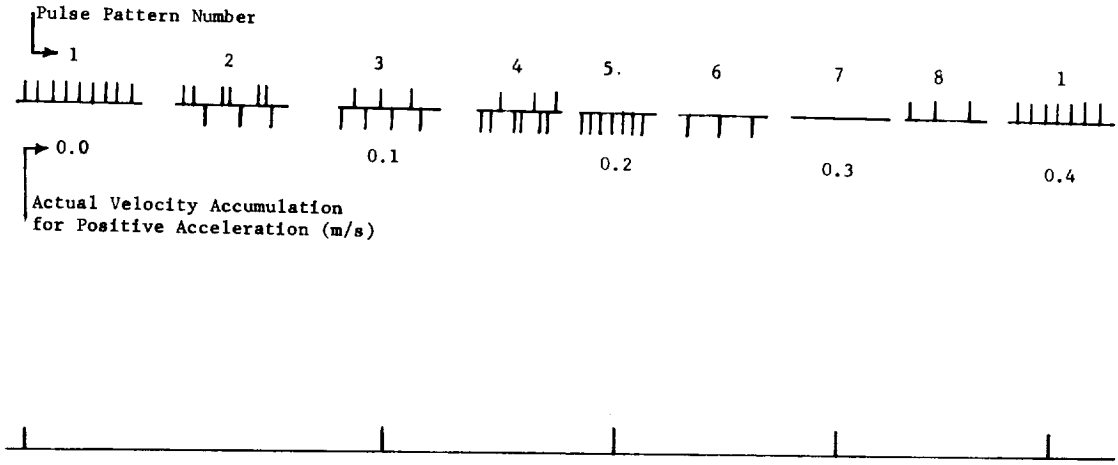

FIGURE 8-4. INCREMENTAL VELOCITY PULSE PATTERNS, ST-124P CROSS RANGE

It was concluded from this study that the loss of one DC logic signal input to the rotation sensor logic circuits, combined with the 65 cps modulation of the true accelerometer output, could produce the patterns of incremental velocity pulses observed on the telemetry and ground recordings (Figure 8-4 and 8-5). Laboratory tests confirmed the above conclusion. The pulse pattern sequences were used to reduce the actual telemetered cross range velocity from the ST-124P system. The second disturbance to the signal processor occurred intermittently from 113 to 125 seconds range time, and was characterized by improper shifting of the bias voltage for the coarse velocity indication in both cross range altitude channels. Short term voltage transients of fairly large amplitude on the B+ line are believed to be the source of this extraneous switching of the bias flip-flop. The source of the transients could not be determined, but could have originated either on the D21 buss, in the static inverter, or in the signal processor power supply.

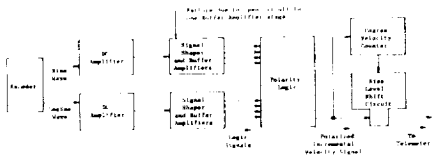

FIGURE 8-5. SIMPLIFIED SCHEMATIC OF CROSS RANGE SIGNAL PROCESSOR

The improper switching of the bias flip-flop did not cause any error in the incremental velocity values.

8.4.3 ST-90 STABILIZED PLATFORM

The ST-90 stabilized platform flown on SA-3 utilized similar components and systems as the platform flown on SA-2, with the exception that AMAB-3 accelerometers replaced the usual AMAB-4 units. All systems operated properly, with the air bearing supply pressure relatively constant at 2.4 kg/cm^2 (34 psi) and the compartment pressure varying from 1.10 to 0.98 kg/cm^2 (15.6 to 14.0 psi).

The final tilt angle of the ST-90 platform at tilt arrest was 44.28 degrees as compared with the intended 44 degrees (Section VII Paragraph 7.2.1).

ST-124P

The ST-124P system (consisting of platform, resolvers, and associated mechanical and electrical circuitry), flown on SA-3, was a prototype or engineering test model. Many of the components were not optimized for high accuracy, and are not the same as those to be flown on Block II vehicles. SA-3 was the first flight test of this system (also to be flown on SA-4). The primary test objectives of the system were the observation of its functional operation and familiarization with the resolver chain and the 5 kc/s servo systems in an operational environment. The operation of the system as an engineering test was quite satisfactory.

The resolvers used with the ST-124P system were not trimmed; therefore some error in their output must be expected. The error in the output of the pitch resolver is a function of, and increases with, the programmed pitch angle. The incremental differences in pitch attitude data obtained from the ST-124P and ST-90 systems is primarily attributed to this effect. A laboratory test of the ST-124P system to be used on SA-4 indicated that the error for the pitch resolver for this system was about the same as that experienced on SA-3 (Section VII Paragraph 7.3.4).

During flight, the air bearing air supply pressure was a constant 2.2 kg/cm^2 (32 psi) and the air temperature was 24.6 degrees centigrade. The compartment air pressure varied from 1.03 to 0.98 kg/cm^2 (14.7 to 14.0 psi), while the temperature was 24.7 degrees centigrade.

9.1 SUMMARY

All vehicle networks performed satisfactorily except for the failure of measuring supply number 5.

9.2 FLIGHT RESULTS

The voltage and current for battery D20 and its corresponding buss (D21) were constant at 28.5 volts and 165 amps. A total of 898 amp-minutes was used for the flight or approximately 33.9 percent of battery capacity. Figure 9-1 shows the connections for the 9 inflight distributors.

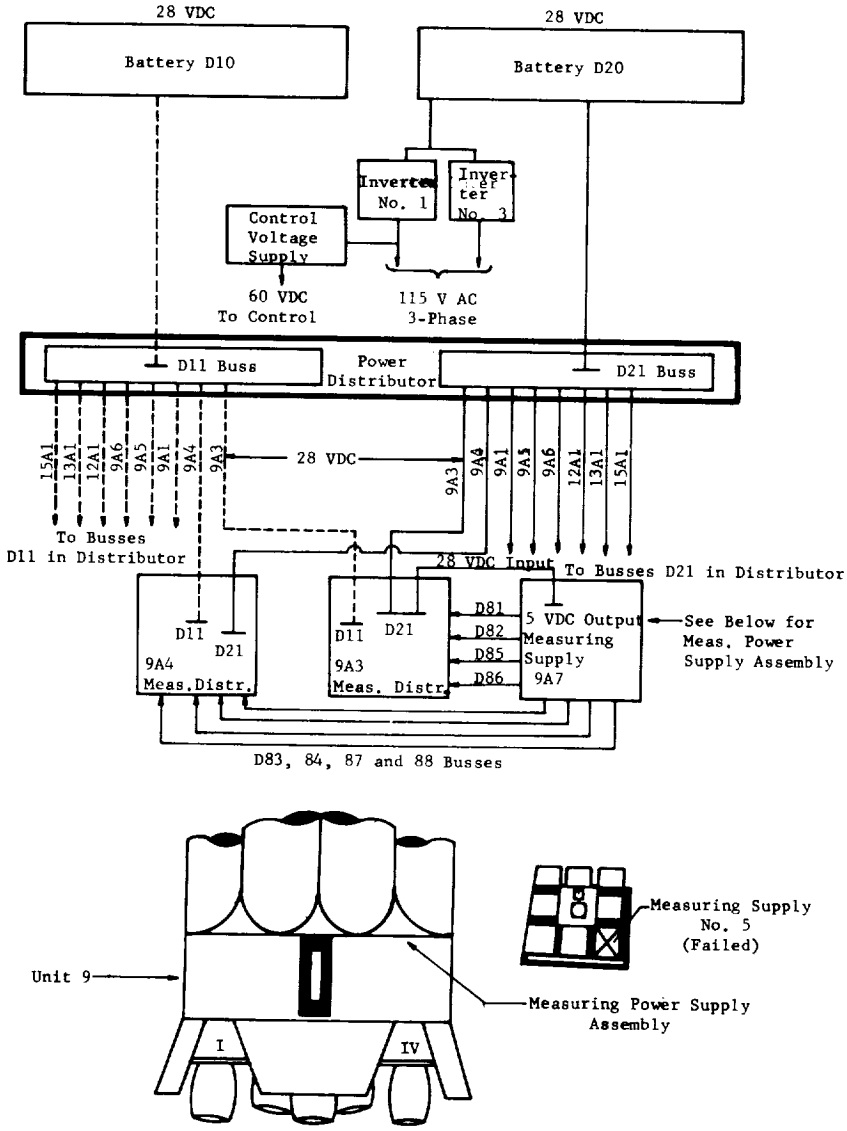

FIGURE 9-1. DISTRIBUTOR CONNECTIONS AND UNIT 9 MEASURING SUPPLY

The variable load for battery D10 and its corresponding buss (D11) caused the voltage and current to vary from 27.6 volts, 165 amps at liftoff to 28.0 volts, 95 amps at end of flight. These voltages and currents varied as expected, with 0.4 volt increases when the continuous lights and the angle-of-attack heaters were switched off.

The frequency of the precision inverter on SA-3 was 399.788 to 400.225 cps over the flight period. The usual frequency disturbance caused by ignition was within minus 0.202 cps of the inverter frequency. All frequencies were within allowable tolerances.

Measuring voltages of the eight "slave" units off busses D81 through D88, located in the measuring distributors, operated within the 5 volts ±5 percent limits, except for D85. Measuring supply number 5, which supplies buss D85, failed before liftoff.

Measuring supply number 5 failed on SA-3 at minus 2.17 seconds prior to liftoff. Since this time period is associated with the initial shock due to ignition of the engines, investigations have been made to correlate the failure with this time period. Simulated shaker tests indicate a possibility of transistor failure during this period.

The measuring voltage supply assembly has a volume of approximately 208 cubic inches, weighs 7.05 pounds, and is located in the thrust frame area of the vehicle above the firewall (Figure 9-1). The assembly consists of eight individually isolated power supplies and one input filter. Each power supply contains seven transistors. Five of the seven transistors were ultra-high-reliability type transistors obtained through Engineering Magnetics from Pacific Semi Conductors Incorporated. The two remaining transistors consisted of one Fairchild type and one Texas Instrument type. Shaker tests indicate that the Pacific Semi Conductors type (EM 113531) transistor was the probable cause of failure in measuring voltage supply number 5. Additional tests are being conducted to determine more detailed information. However, this type of transistor will be replaced on SA-4

Main fuel and LOX valve position signals (start open, open, and closed) operated satisfactorily with the exception of measurements A6-5 and A11-5. These measurements were lost because of the failure of measuring supply number 5.

Cutoff signals (inboard) and flight sequence signals were as expected. Outboard cutoff was initiated by LOX depletion.

10.1 SUMMARY

The instrumentation for SA-3 included strain measurements on the truss members and on the LOX pins from which pitch and yaw moments and longitudinal forces were computed at various significant flight times. The results compared well with predicted values.

Instrumentation for detecting vehicle body bending consisted of ten bending accelerometers at five vehicle stations. The accelerometers showed response at frequencies in the range of first and second vehicle bending. These frequencies were present in both pitch and yaw directions, with a maximum amplitude at liftoff on the nose cone of 0.016 g's single amplitude for first mode of 2.0 cps. At OECO, a forced response of 0.095 g's single amplitude occurred at a coupled frequency of 2.7 cps. The response is lower than on SA-2 before OECO.

The flight data indicated that the SA-3 vibration levels were generally similar to those recorded during the previous two Saturn flights.

10.2 BENDING MOMENTS AND NORMAL LOAD FACTORS

10.2.1 INSTRUMENTATION

Instrumentation for determining bending moments and normal load factors consisted of eight strain gauges on the main compression members and sixteen strain gauges on the tension members of the interstage truss at station 979. In addition, eight LOX tank studs at station 869 were gauged. However, five of the eight LOX tank stud gauges were lost prior to ignition and hence offered very little information. The telemetered data were obtained as decommutated oscillograph traces and also in digitized form. Flight evaluation consisted of determining the instantaneous load and bending moments about the pitch and yaw axes for numerous time slices.

10.2.2 MOMENT LOADS

Maximum bending moment at station 979 occurred at 69.2 seconds range time, approximately Mach 1. At Mach 1, a vehicle bending moment diagram could not be constructed since there were no aerodynamic loads data available. However, the highest strain gauge moments were observed at this time. A vehicle bending moment diagram was constructed at time point 81.6 seconds, where another relatively high moment occurred and reliable aerodynamic loads were available (Figure 10-1). In Figure 10-1 the strain gauge moment is shown by a cross at the gauge location, station 979. Good agreement existed between this strain gauge moment and the predicted bending moment distribution. Also shown in Figure 10-1, is the normal load factor compared with the accelerometer reading from flight.

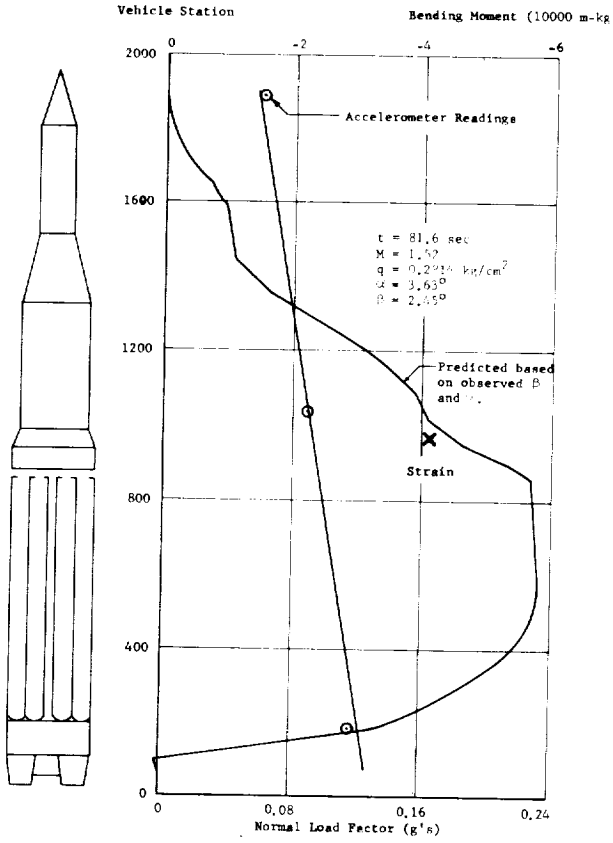

FIGURE 10-1. BENDING MOMENT AND NORMAL LOAD FACTOR

Because five of the eight stud gauges of the 1.8 m (70 inch) LOX tanks (station 869) were lost, no bending moments about the pitch and yaw axes could be calculated at that station. However, the three gauges which functioned properly gave some check on the bending moment at station 979. These three gauges were found to be in agreement with predicted values.

The vehicle bending moment about the pitch axis at station 979 is shown in the 75 to 85 seconds range

time interval in Figure 10-2. Also shown on this graph are the angle-of-attack (α) and gimbal angle (β) about the pitch axis. Close agreement in frequency of oscillation between the three values is evident.

10.3 LONGITUDINAL LOADS

Multiplication of the actual telemetered strain by the calibration factor results in the loads shown in Figure 10-3 (circled points). The solid line in Figure 10-3 was obtained by using the differential strains and adding the 101,290 kg (223,300 lbs) of load which was lost when the gauges were set to zero. The calculated load was determined from SA-3 thrust and acceleration data and theoretical drag data.

During firing of the engines, before launch command, dynamic forces arise in the deflecting masses of the system. These forces can be amplified and cause large vibrations of the vehicle. A staggering time of 100 ms between engine pairs was expected to keep the vibratory force lower or equal to 20 percent of the maximum static thrust. Figure 10-4 presents the results of an investigation made to see if the actual staggering times of the engines still keep the vibratory force below the above value. The frequencies of the system were measured by potentiometers (YL-1, YL-2) located on the support arms. From these frequency measurements and from single engine thrust curves, the maximum vibrating force was obtained as shown by the maximum theoretical response (calculated) on Figure 10-4. These results show that the maximum response was sixteen percent of the maximum static thrust.

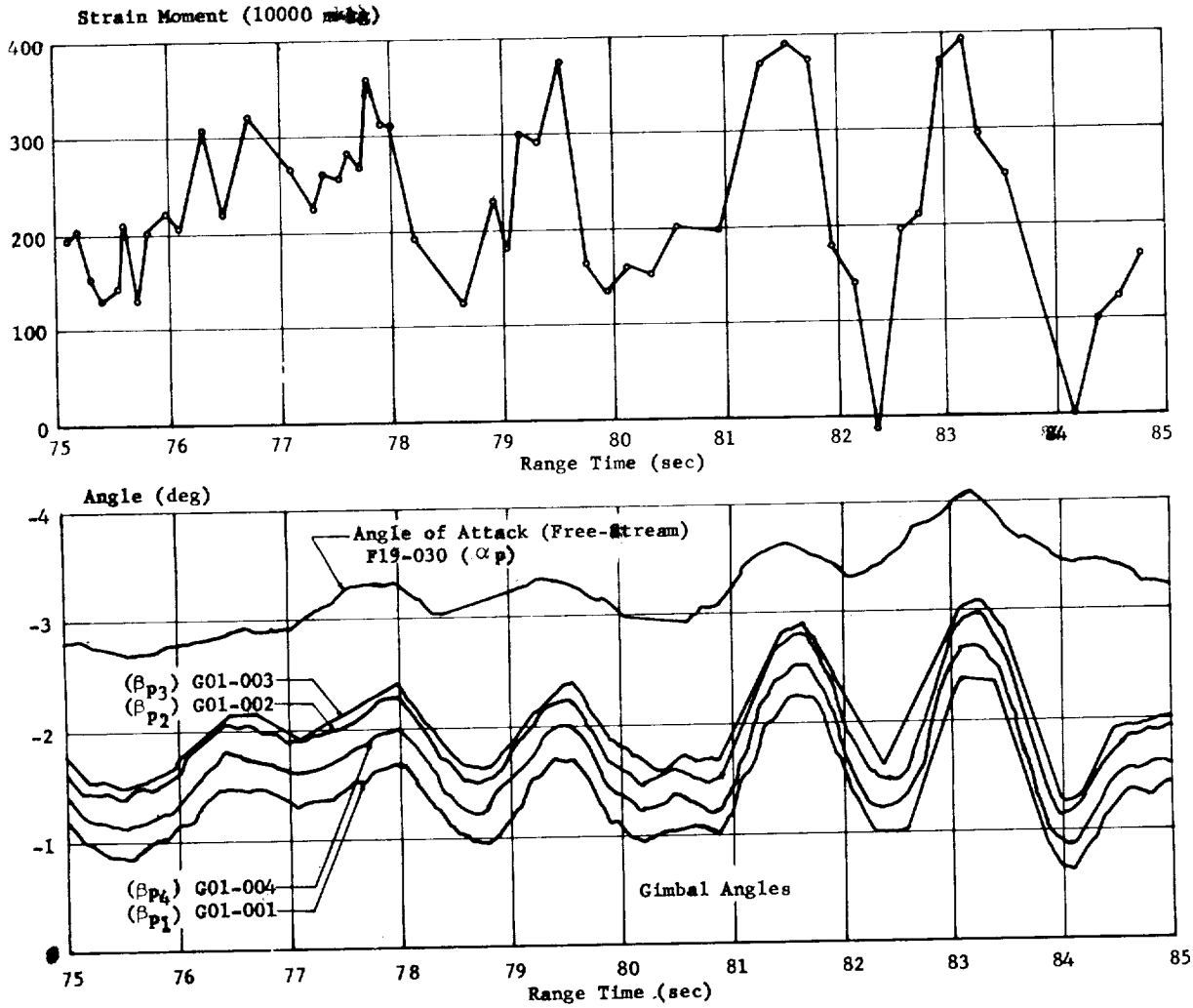

FIGURE 10-2. BENDING MOMENT AT STATION 979, ANGLE-OF-ATTACK, AND GIMBAL ANGLE VERSUS RANGE TIME

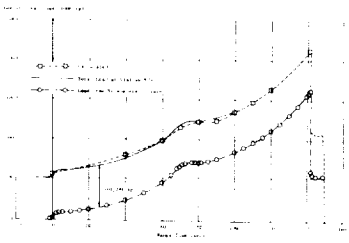

FIGURE 10-3. LONGITUDINAL LOAD AT STATION 979

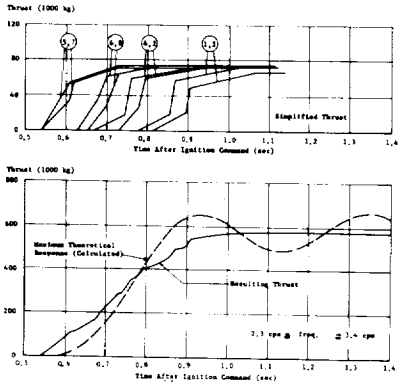

FIGURE 10-4. MAXIMUM DYNAMIC RESPONSE

10.4 BENDING OSCILLATIONS

All accelerometers appeared to have responded properly and have polarity as reported before flight.

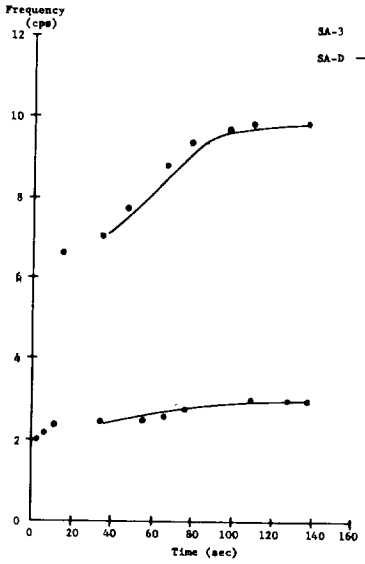

FIGURE 10-5. SA-3 SYSTEM FREQUENCY TREND

The frequencies presented as flight results vary slightly in accuracy, but all are considered to be within ±0.15 cps.

The oscillographs showed a predominant frequency content of approximately 12 to 20 cps throughout the flight, with increases in amplitude at liftoff and the two engine cutoffs. This could possibly be caused by the natural frequency of the accelerometers which is about 17 cps. In addition to the high frequencies, analysis of the data showed frequencies in the control and propellant sloshing range.

The trend of the vehicle first mode follows the first mode trends from SA-D tests for similar fill conditions (Figure 10-5), and is further substantiated by the mode shapes shown in Figures 10-6 and 10-7. The second mode frequency trend is present, but cannot be shown by second mode shapes due to low amplitude of response. After OECO, a predominant frequency of 2.7 cps is present (Figure 10-8) and is a forced response due to engine gimbaling (Section VII Paragraph 7.2.4).

Other frequencies were present in the analysis, all of which cannot be identified with known natural frequencies of the system. Some of these frequencies can be attributed to local structural response, coupled tank, vehicle torsion, and vehicle bending modes for which no comparison data is available.

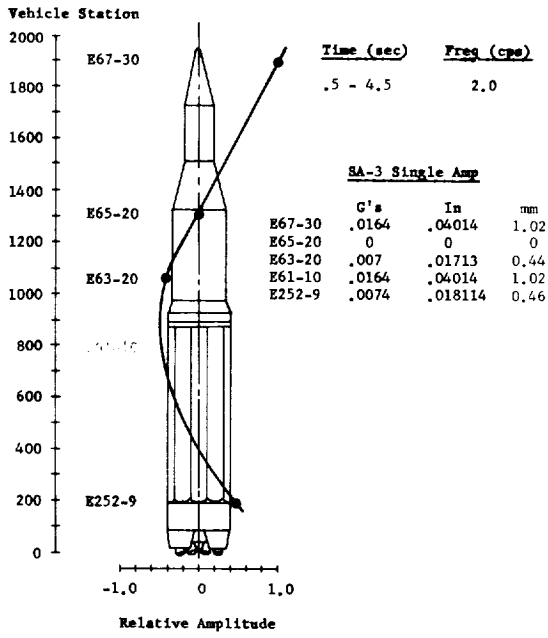

FIGURE 10-6. SA-3 BENDING MODE - FIRST MODE, YAW AT LIFTOFF

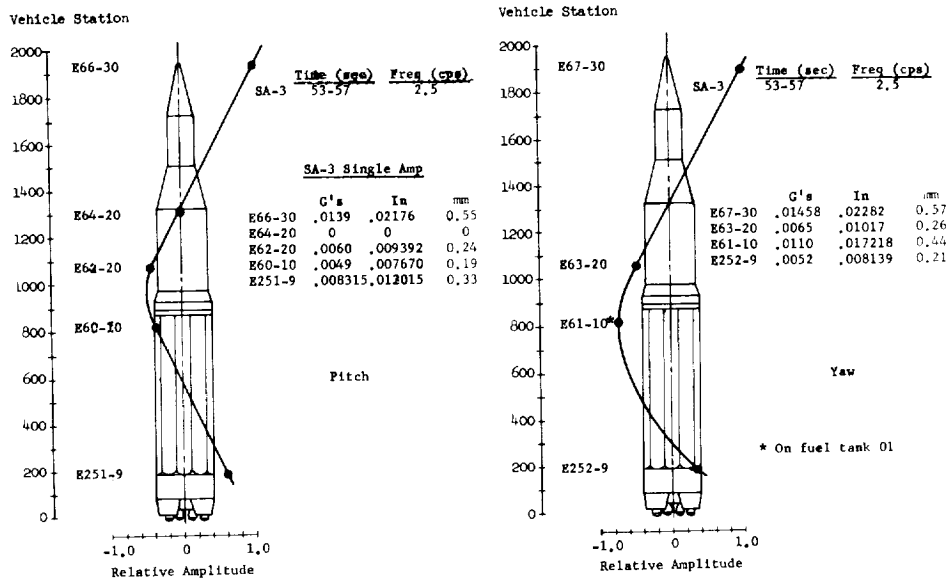

FIGURE 10-7. SA-3 BENDING MODE-FIRST MODE, PITCH AND YAW (53 to 57 sec)

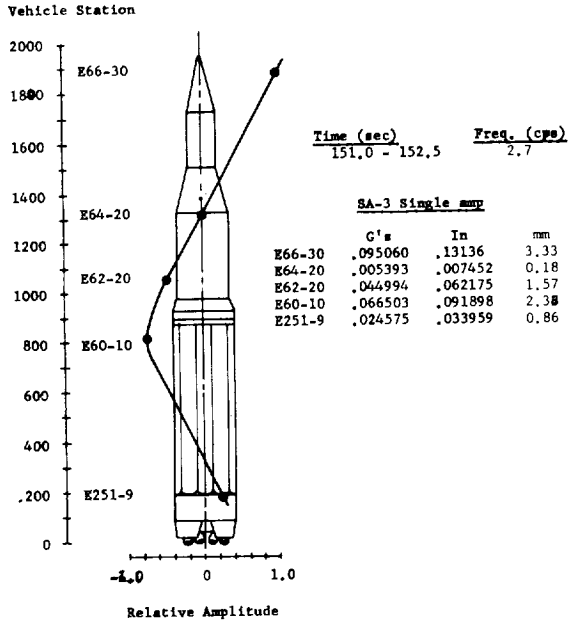

FIGURE 10-8. BENDING MODE - FIRST MODE, PITCH (151 to 152.5 sec)

10.5 VIBRATIONS

10.5.1 SUMMARY OF VIBRATION DATA

The flight data indicated that the SA-3 vibration levels were generally similar to those recorded during the previous two Saturn flights (Reference 2 and 3). The major deviations observed in the flight data are summarized as follows:

a. Three combustion chamber dome measurements contained erratic data.

b. A measurement on the fuel suction line which feeds engine position eight indicated significantly higher vibration levels than previous flights.

c. Transients were observed in several measurements, for which a satisfactory explanation has not yet been determined. An intensive analysis of the flight data is presently in progress in order to determine the causes of these transients.

10.5.2 INSTRUMENTATION

The SA-3 space vehicle was instrumented with 40 vibration measurements. The vibration data were transmitted by two telemetry systems. Five

canister area measurements were transmitted on FM/FM channels with a data frequency range varying from 0 to 330 cps or 0 to 1050 cps, depending upon the specific telemetry channel. The remaining 35 measurements were transmitted by SS-FM with an approximate data frequency range of 50 cps to 3 kc. The eight hydraulic actuator vibration measurements were transmitted on a time-shared basis with four measurements on each of two telemetry channels.

10.5.3 DISCUSSION OF VIBRATION MEASUREMENTS

Structural Vibrations

Five structural measurements were monitored during SA-3 flight. The two measurements on the spider beam (E99-11 and E100-11) varied considerably, being much more sensitive than the engine measurements to the events of flight (i.e., ignition, Mach 1, max Q, cutoffs, and retro firing). This same characteristic was experienced during both previous flights.

The engine gimbal point support measurements (E40-1 and E40-7) displayed high level transients at ignition, then immediately decayed to the mainstage level. These measurements remained relatively constant throughout the remainder of flight until cutoff, responding much like engine measurements due to their near-engine location.

The heat shield measurement (E47-1) showed a maximum buildup at ignition, then decreased gradually to a very low level at approximately 95 seconds flight time. This measurement did show a slight increase in vibration level at Mach 1 and max Q similar to SA-2 flight.

The upper part of Figure 10-9 displays the maximum and minimum acceleration time histories of the structural measurements. The upper portion of the envelope was established by the data from the gimbal point support measurements and heat shield measurement, which were previously noted to have remained constant throughout flight. The lower portion of the envelope, characterized by the spider beam measurements, shows an increase in vibration level in the region of Mach 1 and max Q.

Propulsion System Vibrations

Twelve engine vibration measurements were monitored during the SA-3 flight. These measurements showed considerable buildup at or immediately after ignition, followed by a decay to a steady state level. There was no significant change in the engine vibration levels during the mainstage portion of powered flight

Increased vibration levels were noted at cutoff, followed immediately by a decay to zero. Data were available only intermittently on the thrust chamber dome longitudinal measurements, therefore they were considered to be only partially successful.

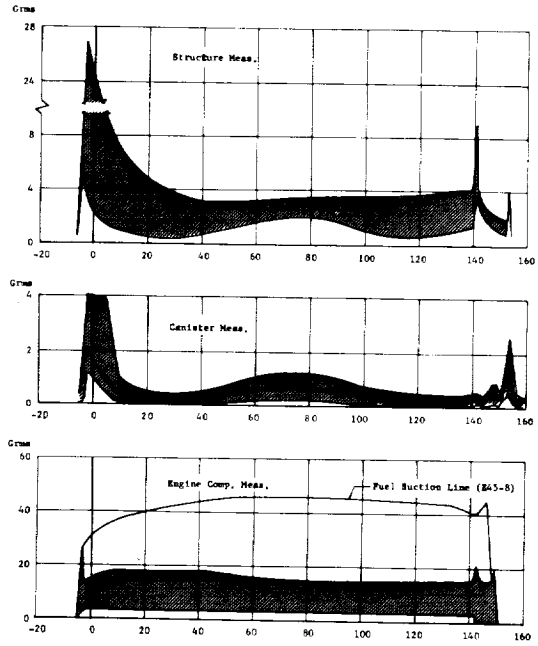

FIGURE 10-9. VIBRATION ENVELOPE OF STRUCTURE, CANISTER AND ENGINE COMPARTMENT MEASUREMENTS

All engine vibration data from SA-3 flight compared very well to SA-1 and SA-2 data, except measurement E45-8 (fuel suction line long't), which was about twice as high on SA-3 flight as compared to SA-2 flight. However, no evidence of structural failure was indicated in this area. An investigation is being made to determine the cause of these high levels. Because of the high levels indicated, measurement E45-8 was not included in the maximum and minimum acceleration time histories as shown in the lower part of Figure 10-9. However, it is felt that the measurement is valid.

Component Vibrations

The hydraulic actuators, ST-90, ST-124P, retro rocket number 1, canister 14 lower support, instrument panel in canister 14, and propulsion unit distributor were monitored by a total of 22 vibration measurements.

The hydraulic actuators were instrumented with

eight vibration measurements. The only erratic data were recorded from the yaw actuator measurement on engine four. Vibration amplitudes appeared to be very similar to the data recorded during previous flights.

The center part of Figure 10-9 presents an envelope of the RMS acceleration time histories obtained from the canister area. This envelope does not reflect erratic transients which occurred on some of the measurements. As the envelope indicates, all the canister area measurements recorded buildup during the Mach 1 and max Q region.

Quasi-periodic transients were recorded throughout recorded flight on the ST-90 gimbal and on the ST-124 measurements. These transients did not appear on all the six ST-124 measurements. Transients were recorded intermittently by the three measurements on the ST-124 roll gimbal between 110 and 126 seconds, but were not observed on the ST-124 mounting frame. An example of this is shown below.

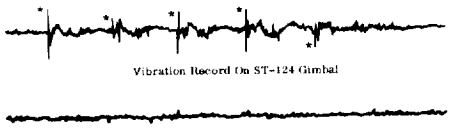

A relatively high transient was recorded at 138.8 seconds on the ST-90 gimbal, two panel measurements in canister 14, and at the canister 14 support on the spider beam. Additional study is required to determine the cause of these transients.

Retro rocket number 1 was instrumented with three vibration measurements. The vibration levels inidcated a gradual increase to the periods of Mach 1 and max Q. No effects were noted at engine cutoff, although an expected sudden increase in vibration amplitude occurred at the time of retro firing. Several periods of erratic data were noted on all the measurements. The cause of these transients is presently under investigation.

One vibration measurement was located on the propulsion unit distributor. This measurement was very smooth indicating only a slight buildup at approximately 60 seconds and at engine cutoffs and retro firing.

10.6 VEHICLE ACOUSTIC MEASUREMENTS

The SA-3 vehicle had one inflight acoustic measurement (L10-11) and four trailing wire measurements (XL24-9, XL25-9, XL26-11, XL27-13). The inflight measurement was located at station 889 on fin line IV and followed the general expected trend (Figure 10-10). The preliminary purpose of this measurement was to obtain "inflight" acoustic data. To obtain this type of data, the calibration range of the recording system was 120 to 140 db; consequently, the higher level "on-pad" acoustic data were sacrificed for the inflight data.

The inflight measurement recorded a disturbance at 138.8 seconds range time (see component vibrations Section X Paragraph 10.5.3) and caused the measurement to appear unusual throughout the rest of the flight. The source of this disturbance is unexplained at this time.

The trailing wire acoustic measurements on SA-3 recorded data between minus 3 and plus 6 seconds range time. This period was sufficient to obtain useful "on-pad" acoustic data. The maximum levels recorded on these measurements are presented in Table 10-I.

TABLE 10-I. MAXIMUM ON-PAD OVERALL SOUND PRESSURE LEVELS

Meas. No.	Location	Max OA-SPL (db)	
XL 24-9	Inside Shroud Sta. 167 off Fin II toward Fin I	149.0	Liftoff
XL 25-9	Outside Shroud Sta. 167 off Fin II toward Fin I	157.5	
XL 26-11	Sta. 889 on Fin IV Adjacent to Canister 13	149.5	Liftoff and 6 sec
XL 27-13	Sta. 889 Inside Canister 13	132.0	

The time histories of these measurements are shown in the lower part of Figure 10-10. The maximum overall sound pressure levels (OA SPL), recorded on measurements XL 24-9 and XL 25-9, indicated that the shroud provided a noise reduction of about 8.5 db at liftoff. Measurement XL 25-9 then remained fairly constant during the remaining time duration of data acquisition, while XL 24-9 decreased somewhat during the last 3 seconds of data due to a change in the spectral characteristics of the external sound field.

The difference in the maximum overall sound

pressure levels of measurements XL 26-11 and XL 27-13 indicated a noise reduction across the wall of canister 13 of 17.5 db. This noise reduction existed throughout the period during which data were obtained.

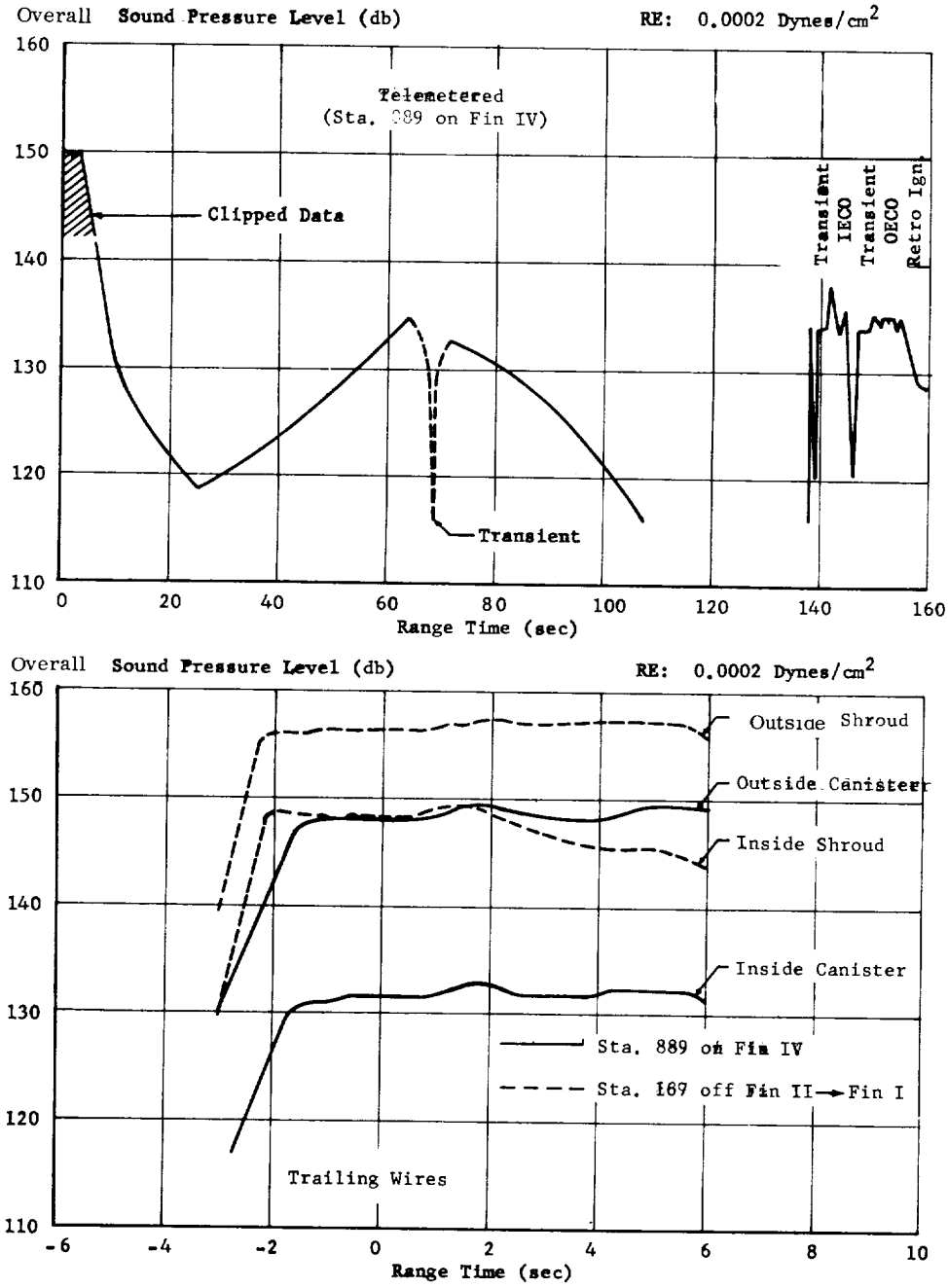

FIGURE 10-10. SA-3 VEHICLE ACOUSTICS

SECTION XI. ENVIRONMENTAL TEMPERATURES AND PRESSURES

11.1 SUMMARY

The base region environment during the SA-3 flight was similar to that encountered on the two previous flights. Radiative heating rates on SA-3 are considered representative for the Saturn I, Block I vehicle. Absolute values of the total heating environment after 90 seconds of flight are considered questionable at this time. The heat shield and flame shield thermal insulation scheme was the same for SA-1, SA-2, and SA-3, except for one panel on the heat shield which was insulated with the Block II insulation material (M-31). Measurements made forward of the heat shield (except the temperature measurement on the M-31 insulated panel which failed prior to liftoff) indicated the insulation to be entirely adequate.

The base pressure measurements on SA-3 indicated a slightly higher pressure gradient across the heat shield than indicated on previous flights. However, results from all three flights are within the telemetry error band.

Skin temperatures on the propellant tanks were generally lower on SA-3 than on previous flights due to the higher propellant level in the tanks. Skin temperatures on the dummy S-IV stage and interstage fairing indicated no significant temperature rises except on the conical portion of the interstage fairing where maximum skin temperatures of 71 degrees centigrade to 159 degrees centigrade were indicated. Skin temperatures in the vicinity of the S-IV stage protuberance were within expected levels.

Instrument canister pressure was maintained within the required level (0.7 to 1.2 kg/cm^2) throughout flight. The canister temperatures were maintained within an accpetable range (10 to 40 degrees centigrade) during both prelaunch and during flight. Both the ST-90 and the ST-124P guidance platform compartment temperatures were in an acceptable temperature range (25 ± 2 degrees centigrade) at liftoff.

11.2 TAIL SECTION

11.2.1 BASE ENVIRONMENT

11.2.1.1 BASE PRESSURE

Absolute base pressure instrumentation on SA-3 was identical to that on SA-1 and SA-2. In addition, one instrument was installed on the SA-3 vehicle to measure the pressure difference between the lower compartment (forward of heat shield) and the region aft of the heat shield. This pressure differential measurement failed just after ignition and prior to liftoff, due to a malfunction of a power unit supply (Section IX).

The difference between base pressure and ambient pressure for both the heat shield and flame shield is presented in Figure 11-1. All measurements on the heat shield were generally consistent with each other throughout the powered phase of flight. A minimum pressure differential of minus 0.03 kg/cm^2 was observed at an altitude of 6 km (60 seconds of flight) in the area between the outboard engines. A maximum value of 0.03 kg/cm^2 was observed at an altitude of 17 km (90 seconds of flight) between the outboard engine and the engine shroud. There appears to be an indication of a higher pressure gradient across the heat shield than indicated on previous flights. Although this occurrence may be a direct consequence of the different trajectory followed by SA-3, results from all three flights are within the error margin which can be attributed to telemetry error.

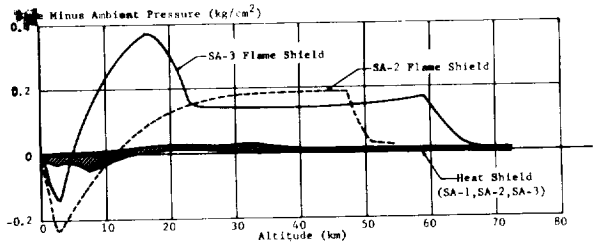

FIGURE 11-1. BASE PRESSURE MINUS AMBIENT PRESSURE VERSUS ALTITUDE

The largest magnitude of base pressure minus ambient pressure occurred in the flame shield region where extreme values ranged from minus 0.15 kg/cm^2 at an altitude of 2.5 km to 0.37 kg/cm^2 at 17.2 km (Figure 11-1). The telemetered data indicated a different behavior in the flame shield region than was observed on the first two Saturn flights (Figure 11-2). At an altitude of approximately 3 km, the pressure in the flame shield area stabilized with only a slight decrease between 3 and 17 km. Then it rapidly decreased to the expected level. A sharp decrease in the center star base pressure occurred at IECO (61.5 km) as expected. At this time, no definite conclusions have been drawn in regard to this unusual phenomenon in the flame shield pressure. Close investigation of the pressure data in the center star region has not revealed any reason to suspect the telemetry or measurement.

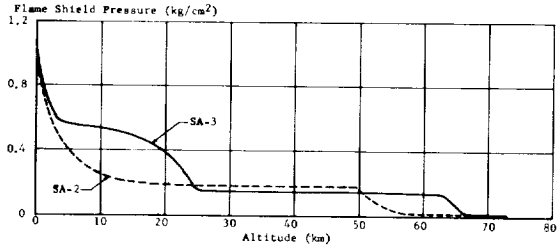

FIGURE 11-2. FLAME SHIELD PRESSURE COMPARISON VERSUS ALTITUDE

Average values of the ratio of base pressure to ambient pressure, p_b/p_a, for both the heat shield and flame shield (center star) are plotted versus Mach number in Figure 11-3. Wind tunnel test data from the Rocket Test Facility, AEDC, are also shown for comparison.

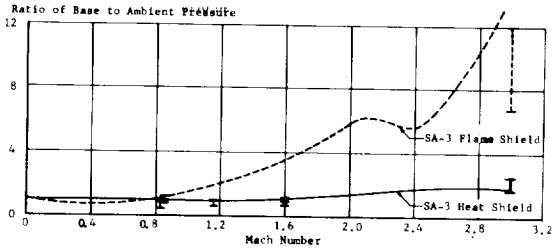

FIGURE 11-3. RATIOS OF BASE PRESSURE TO AMBIENT PRESSURE VERSUS MACH NUMBER

The absolute pressure measurement in the lower compartment, D27-5, and four differential pressure measurements, D143-2, D143-4, D144-9, and D145-9, for measuring the difference between lower and upper compartment pressures, failed prior to liftoff. All of these failures are attributed to loss of the inboard power supply.

The forward compartment pressure lagged the ambient pressure except at altitudes below 2 km, as expected. The maximum difference between the forward compartment pressure and ambient pressure was approximately minus 0.023 kg/cm^2 at an altitude of 21 km.

11.2.1.2 BASE TEMPERATURES

Gas temperature in the SA-3 base region was measured with a series of unshielded thermocouples. The thermocouples were distributed over the area to ensure valid information.

The bands of gas temperature and associated areas of the base region for SA-2 and SA-3 flights are shown in Figure 11-4. Gas temperatures measured during the SA-3 flight compare favorably with those measured during the SA-2 flight at the same altitude. Measured gas temperatures from the SA-1 flight are not included in these bands because of the necessary correction factor required to compensate for the shielding of the gauges; however, the corrected SA-1 gas temperatures also compared well with the SA-3 measurements.

The maximum gas temperature measured on the heat shield, 1150 degrees centigrade, occurred at approximately 25 km (or 103 seconds range time for SA-3); this was the same as the maximum measured on SA-2. The gas temperature measured between the inboard engines, near the heat shield, and between the shroud and outboard engines reached a maximum of 700 degrees centigrade on SA-3, approximately 50 degrees centigrade below that of SA-2. High temperatures measured between the outboard engine and the shroud, labeled SA-2 in Figure 11-4, did not appear during the SA-3 flight.

The gas temperature in the heat shield region appears to be the result of reversed gases leaving the flame shield and circulating in the base region. The latter would indicate that the scoops tend to lose their ability to flush the base region above 15 or 20 km.

The slight decrease in the gas temperatures above 25 km can possibly be attributed to the inability of the thermocouple to measure the true gas temperature at these high altitudes and low densities, rather than a real trend.

Surface temperatures of the outboard engine shroud's stringer and skin respectively, are shown as the lowest band in Figure 11-4. Although the shroud stringer temperature is a structural measurement, the temperature-time history of the two measurements show similar trends since both are subjected to the same base heating. On the SA-3 vehicle, these instruments were covered by reflective aluminum tape. Both measurements, however, show a trend similar to that measured on SA-2, with the stringer measurement reaching a maximum, which was approximately 100 degrees centigrade lower than the SA-2 maximum.

Shown also in Figure 11-4 is the gas temperature measurement, C67-7, which was located on the flame shield. This gas temperature probe extended approximately 8 cm below the surface of the flame shield. The maximum temperature measured by this probe (1600 to 1650 degrees centigrade) is only an estimated value as the measurement went off scale during this period. Beyond approximately 15 to 20 km, the flame shield gas temperature remained constant at 1500 degrees centigrade (approximately 50 percent of engine chamber temperature), indicating a choked flow condition.

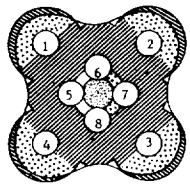

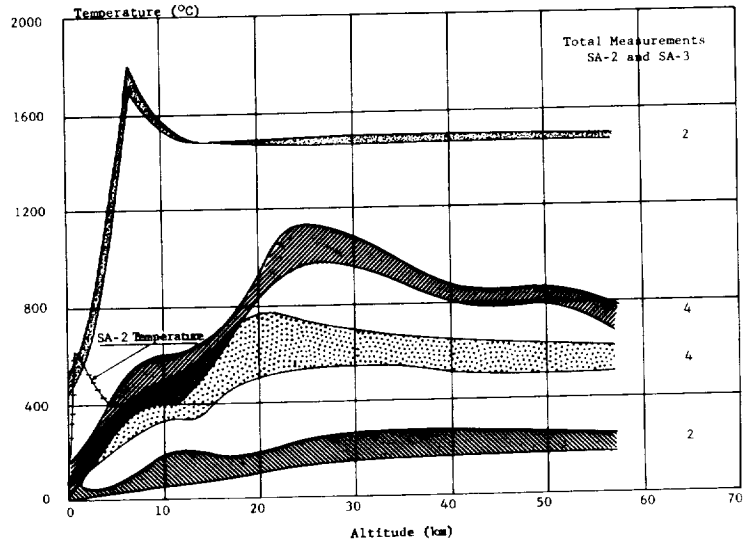

FIGURE 11-4. COMPARISON OF GAS TEMPERATURES ON HEAT AND FLAME SHIELD, SA-2 AND SA-3

11.2.1.3 HEATING RATES

Four total heating calorimeters were located on the SA-3 vehicle base. Two of these calorimeters, C76-3 and C63-1 were mounted approximately 26 cm aft of the heat shield and one calorimeter, C77-5 was mounted flush on the Saturn I, Block II heat shield panel (M-31) which was flown as an experiment on the SA-3 flight. The remaining calorimeter was mounted on the flame shield.

The total heat flux (radiation plus convection) to the calorimeters C76-3 and C63-1 measured during the SA-3 flight is shown in Figure 11-5. The total heat flux measured by these two calorimeters show good agreement with that measured during the SA-1

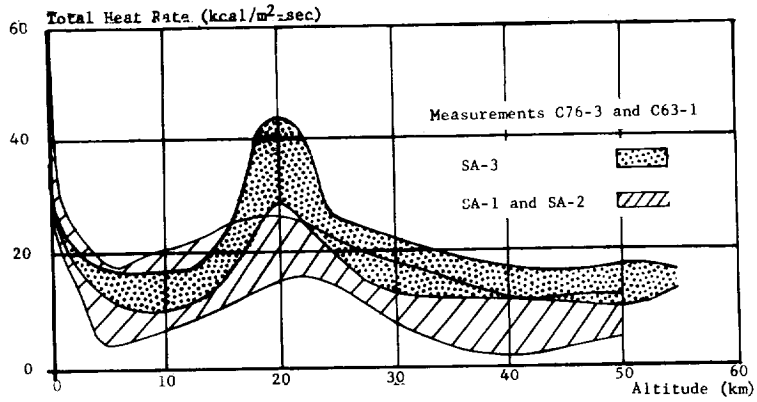

FIGURE 11-5. TOTAL HEAT RATE TO SA-3 BASE

and SA-2 flights up to approximately 16 km. Between 16 and 25 km, these measurements indicated heating rates approximately two times that measured on the SA-1 and SA-2 flights. From 25 km until OECO, the SA-3 heating rates were also higher than those of SA-1 and SA-2.

The total heat flux measured by C77-5, the calorimeter mounted flush with the panel insulated with M-31, is shown in Figure 11-6. With the exception of a high transient just after liftoff, the SA-3 heat flux in this area agrees, as expected, with SA-1 and SA-2 heat flux up to 32 km. The relatively wide heat flux band from 32 km to cutoff is the result of applying two independent calibration techniques. One technique considers only the temperature-time decay following cutoff for the determination of the calorimeter loss coefficient to be applied throughout flight. The other technique utilizes a laboratory calibration method to determine the inflight corrections.

This particular calorimeter, even though it showed almost identical efficiency as calorimeters C76-3 and C63-1 in laboratory calibration, had a loss after cutoff (based on the temperature-time history) of almost twice the rate encountered on C76-3, C63-1, or on previous flights' total calorimeter measurements (Figure 11-7).

A second degree polynomial was used to smooth through the temperature data shown in Figure 11-7. The heating decay does not appear to be affected by OECO; i.e., there is no inflection point in the temperature decay. This indicates that the major heating source at high altitudes is either the inboard engines or the turbine exhaust ducts.

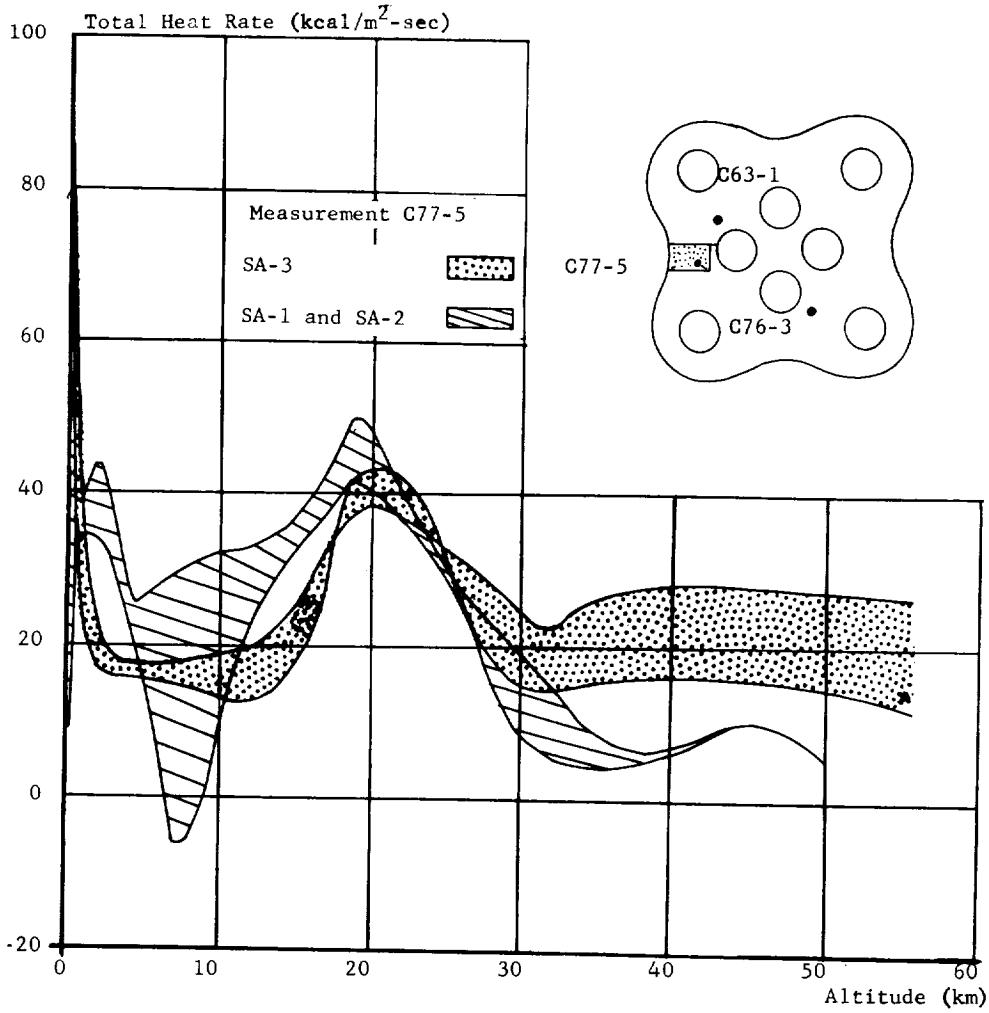

FIGURE 11-6. TOTAL HEAT RATE TO M-31 PANEL COMPARED TO SA-1 AND SA-2 RATES

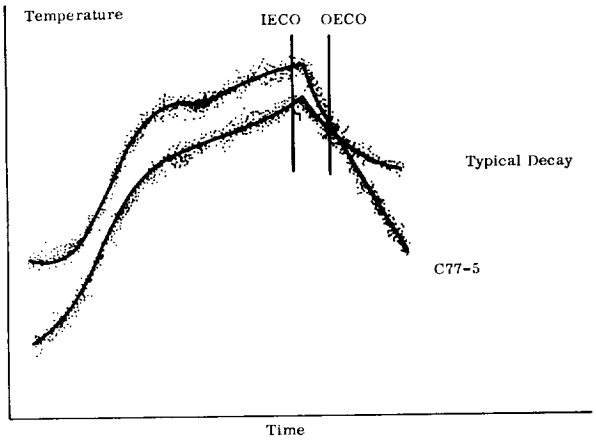

FIGURE 11-7. COMPARISON OF CUTOFF DECAY FOR C77-5 WITH A TYPICAL DECAY

At this time, no explanation as to the cause of this rapid temperature decay is available, but preliminary evaluation indicates the following possibilities: 1) a difference in the heating and cooling cycles possibly exists, whereby the correction factor obtained after cutoff is possibly not valid for the entire flight, 2) possible conduction losses during flight higher than indicated by the laboratory calibration method, and 3) a possibility of a convective cooling source hitting the calorimeter surface at cutoff could exist.

Differences existed between the height, mounting, and insulation in the immediate vicinity of the SA-1, SA-2, and SA-3 calorimeters. These differences should be considered before firm conclusions are reached as to the relative comparison of heating rates. Even though the total heating rates appeared to be higher on SA-3, this did not influence the heat shield forward side temperature which was approximately the same as SA-1 and SA-2. Further evaluation of these measurements will be performed in an effort to obtain a truer loss coefficient.

In general, the total calorimeter heating values on the heat shield should only be used as relative values, since preliminary evaluation has indicated the possible error sources stated above. As these error sources could conceivably become significant near the end of flight, one should not attempt a conclusion as to whether convective heating or cooling was dominant to the calorimeter surfaces.

The total heat flux measured by the flame shield calorimeter C78-8 is shown in Figure 11-8. The SA-3 inflight heat flux to the flame shield is in good agreement with that measured during the SA-1 and SA-2 flights, and absolute values are considered valid. The maximum heat flux measured near liftoff on SA-3 was slightly higher than that of SA-1 or SA-2. The heat flux measured at approximately 8 km (the altitude where the heat flux appears to be most strongly influenced by exhaust jet flow reversal) was slightly lower on SA-3 than on SA-1 or SA-2. Beyond approximately 25 km until IECO, the heat flux remained relatively constant.

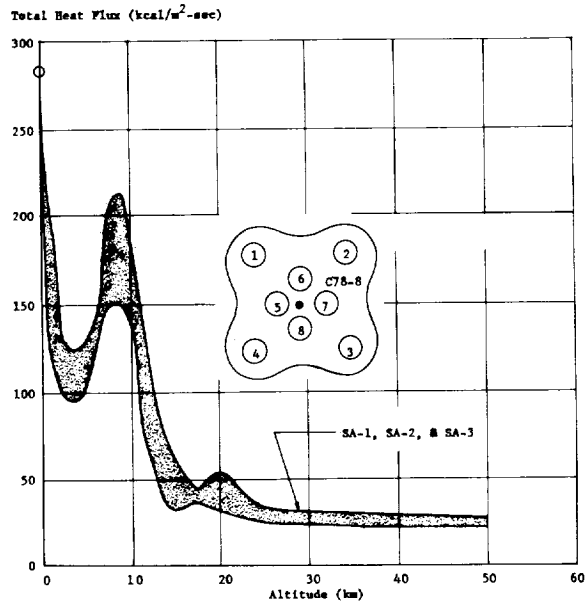

FIGURE 11-8. TOTAL HEATING RATE ON FLAME SHIELD, SA-1, SA-2 AND SA-3

Two thermal radiation calorimeters were located 26 cm aft of the heat shield on the SA-3 vehicle. Both calorimeters were located between an outboard and two inboard engines in approximately symmetrical positions. These calorimeters differed considerably in design.

Thermal radiation levels which were measured on the SA-3 flight are shown in Figure 11-9. Corrections were made to the telemetered data by two different techniques, both of which consider the calorimeter slug temperature history. The data in the upper band was obtained by varying the calorimeter slug heat input and measuring the temperature-time history of the slug to obtain the proper correction. The lower band of data was corrected by evaluating the losses after engine cutoff using the temperature-time slope and defining a heat balance assuming no heat input. This second method assumes that the correction factor is constant throughout flight; i.e., the loss coefficient will be the same for both the heating and the cooling cycles. However, this point has not been proven at this time, and based on the laboratory calibration

technique, this loss coefficient varies throughout flight.

A point of interest concerning the two methods is that values obtained at both liftoff and cutoff agree within the accuracy of the data. At liftoff, this would be expected since the calorimeter losses should be negligible compared to the sensible heat input. At cutoff, it appears that the two techniques also yield approximately the same results. Intermediate values between liftoff and cutoff differ due to the methods utilized.

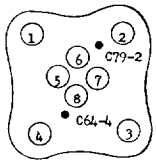

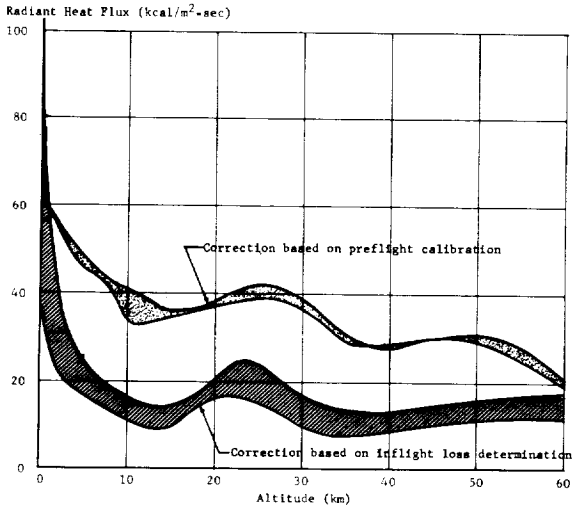

FIGURE 11-9. RADIANT HEATING RATES FOR SA-3 FLIGHT COMPARING PREFLIGHT AND INFLIGHT DATA CORRECTION TECHNIQUES

11.2.2 ENGINE COMPARTMENT

The engine compartment experienced no extreme temperature environment during the flight. Ambient air temperature within each engine area was measured, and no temperature above 0 degree centigrade or below minus 50 degrees centigrade was indicated. The upper limit of the engine compartment temperature of SA-3 was slightly below that of SA-2 flight (Figure 11-10).

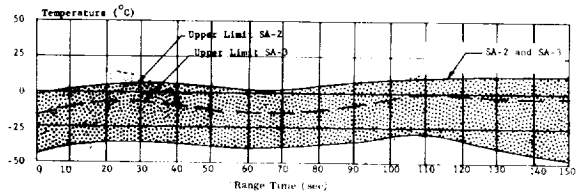

FIGURE 11-10. ENGINE COMPARTMENT STRUCTURAL TEMPERATURES

11.2.3 FORWARD HEAT AND FLAME SHIELD

Two other temperatures are also shown in Figure 11-11; measurement C20-5, attached to the flame support strut, and C21-5, attached to the flame shield seal support. The temperature level in this area is as expected.

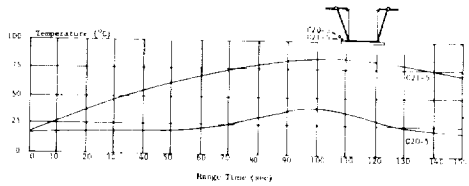

FIGURE 11-11. ENVIRONMENT, FORWARD SIDE OF FLAME SHIELD

Temperatures recorded on the forward side of the heat shield are presented as a band in Figure 11-12. The heat shield measurements on SA-3 agree well with those of SA-1 and SA-2, ranging from minus 25 to plus 25 degrees centigrade. The high temperature measured by C70-7 during the SA-2 flight (Reference 3) cannot be explained; however, based upon the SA-1 and SA-3 results, it follows that it is not characteristic of the heat shield temperature. The maximum temperature of 25 degrees centigrade, measured during the SA-3 flight, indicated that the heat shield insulation was more than adequate. Due to the failure of the measurement in back of the M-31 insulated panel, the relative adequacy of the two insulation materials cannot be assessed.

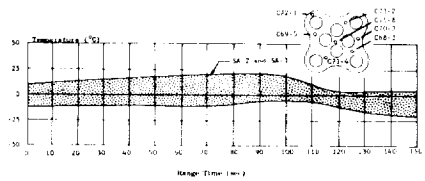

FIGURE 11-12. BASE ENVIRONMENT, FORWARD SIDE OF HEAT SHIELD

11.3 SKIN

The skin temperatures at various positions on the propellant tanks for the SA-3 vehicle were measured by ten thermocouples. Generally, the skin temperatures measured during the SA-3 flight were lower than those indicated during the SA-1 and SA-2

flights (Figure 11-13), due to the higher propellant level in the tanks; however, the measured temperatures were within the anticipated range of skin temperatures. Shown in Figure 11-14 are the skin temperature measurements of the fuel tank, C50-F3, and the LOX shroud at station 835. The latter measurements were in good agreement with those of the SA-1 and SA-2 flights.

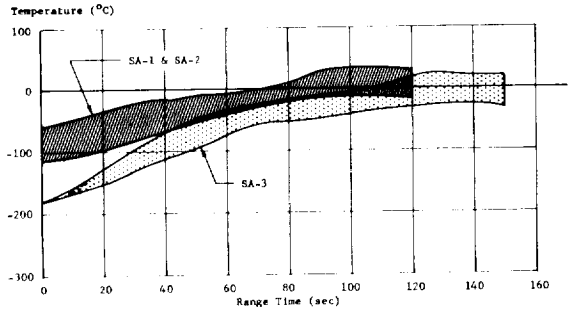

FIGURE 11-13. PROPELLANT TANK SKIN TEMPERATURE AT STATION 745

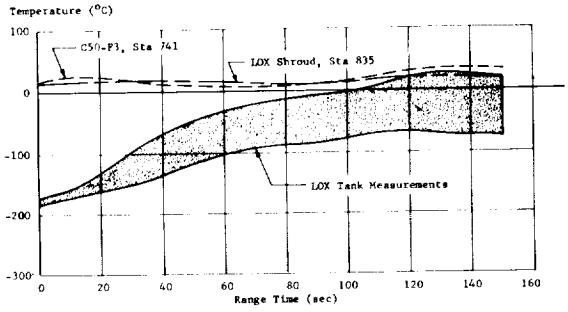

FIGURE 11-14. PROPELLANT TANK SKIN TEMPERATURE AT STATION 835

The skin temperatures at various positions on the dummy S-IV stage and the interstage fairing were measured by 18 thermocouples. Twelve of the thermocouples (requested by DAC) were located on the dummy S-IV stage to supplement the analytical determination of structures in the vicinity of protuberances and separated regions. The other six measurements on the interstage fairing were located to monitor any skin temperature rise during retro rocket firing.

No significant rise in skin temperature due to aerodynamic heating was indicated, except on the conical portion of the interstage fairing where maximum skin temperatures prior to retro rocket firing of 71 degrees centigrade to 159 degrees centigrade were indicated (measurements C128-11 and C133-11 shown in Figures 11-15 and 11-16).

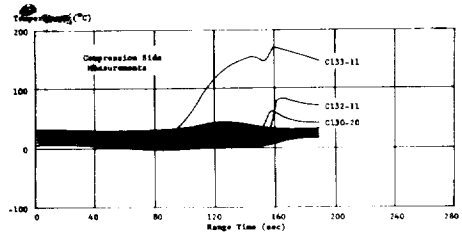

FIGURE 11-15. TEMPERATURE MEASUREMENT ON DUMMY S-IV STAGE AND INTERSTAGE

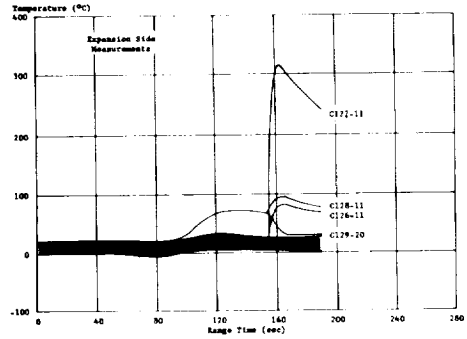

FIGURE 11-16. TEMPERATURE MEASUREMENT ON DUMMY S-IV STAGE AND INTERSTAGE

The retro rockets were ignited at approximately 153 seconds range time, and the response due to the heating from the retro rockets' plume impingement is shown in Figures 11-15 and 11-16. Measurement C127-11 (Figure 11-16) indicated the maximum temperature increase during retro rocket firing (from 10 degrees centigrade at 154 seconds to 315 degrees centigrade at 161 seconds). An investigation is being made to determine any secondary effects (thermocouple attachment, nearby structural members, etc.) that may have prevented an indication of the actual skin temperatures.

Temperatures in the vicinity of the S-IV stage protuberance were within expected levels, although a heating rate of approximately twice that predicted by theory was encountered.

Further analysis is being performed to determine the factors which may have influenced the temperatures indicated by these measurements.

11.4 INSTRUMENT CANISTER

11.4.1 CANISTER PRESSURE

Instrumentation and guidance components located in the canisters required the canister pressure

to be maintained between 0.7 and 1.2 kg/cm^2 during flight. Three canister pressures were measured during flight and gave indications that the pressure was maintained within this range. Canister pressure decayed approximately 0.1 kg/cm^2 from 0 to 150 seconds range time.

11.4.2 CANISTER TEMPERATURE

Temperature in the canisters was controlled by an external cooler package mounted on the swing arm. After the umbilical swing arm was retracted there was no additional canister cooling. The acceptable range of canister temperature was 10 to 40 degrees centigrade. All canisters were within the acceptable range at liftoff.

Specifications call for ambient air temperatures in the ST-90 and ST-124P guidance platform compartments to be controlled at 25 ± 2 degrees centigrade. Both ST-90 and ST-124P guidance platform compartment temperatures were in the acceptable range at liftoff. The ST-124P compartment temperature measurement indicated that the temperature stayed within the acceptable range throughout flight. ST-90 ambient temperature was not monitored during flight.

12.1 SUMMARY

Aerodynamic static stability ratio, gradient of normal force coefficient, and the center of pressure location were determined from the SA-3 telemetered data. The flight results were in agreement with predicted values. However, the gradient of normal force coefficient and the center of pressure location for the SA-3 flight had larger error margins than did results from previous flights, as expected, due to lower values of angle-of-attack and dynamic pressure.

Surface pressure data for the SA-3 flight are presented as a ratio of surface pressure to ambient pressure. SA-3 pressure data agreed well with data from wind tunnel tests.

Pressure data on the simulated Centaur weather shield are in excellent agreement with wind tunnel results. The flight results indicate a maximum low pressure region (Cp = minus 1.74 at mach 0.7) right behind the shoulder in the subsonic region.

12.2 RATIO OF GRADIENTS OF ANGULAR ACCELERATION (STABILITY RATIO)

The ratio of the gradients of angular acceleration (stability ratio C_l/B°) was determined from the average telemetered pitch plane engine deflection (β_p) and the free-stream angle-of-attack (α_p).

The values of C_l/B° obtained for the SA-3 vehicle and predicted values agreed well when plotted versus time (Figure 12-1). A minimum value of minus 0.58 was obtained at the time of maximum dynamic pressure (79.6 seconds) compared to a predicted value of minus 0.55. An estimate of the possible error margin in the flight-determined stability ratio is also shown in Figure 12.1.

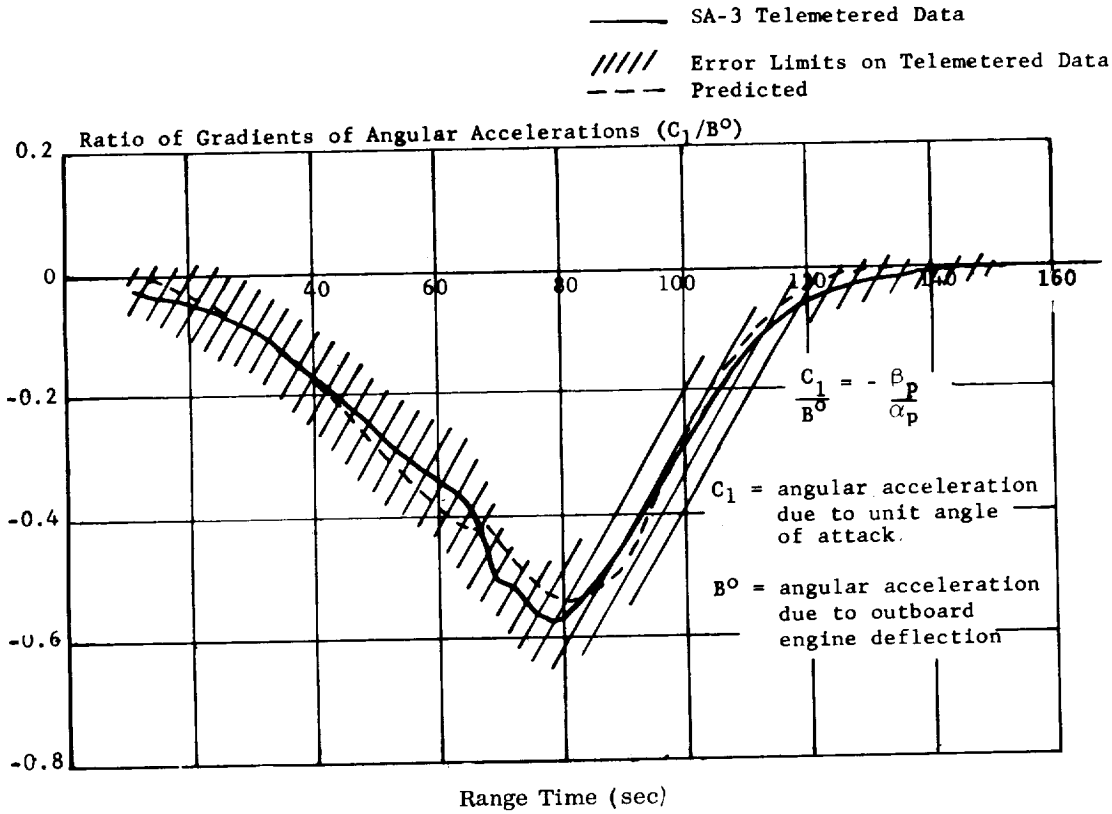

FIGURE 12-1. RATIO OF GRADIENTS OF ANGULAR ACCELERATIONS VERSUS RANGE TIME

12.3 GRADIENT OF NORMAL FORCE COEFFICIENT AND CENTER OF PRESSURE LOCATION

The gradient of the normal force coefficient (C_z') and the center of pressure location (CP/D) were obtained using telemetered values of angle-of-attack, normal acceleration, and engine deflection.

Calculated values of C_z' and CP/D are in fair agreement with predicted values and previous flights' results when plotted versus Mach number (Figure 12-2). SA-3 data has a broader error margin than SA-1 or SA-2, which is attributed to the generally lower values of angle-of-attack and dynamic pressure experienced on the SA-3 trajectory. The unreliability and wide scatter of data at higher Mach numbers limited the SA-3 analysis to the transonic and low supersonic region. In this region, predicted values as well as SA-1 and SA-2 flight results were within the error margin of the SA-3 results.

12.4 SURFACE PRESSURE

12.4.1 STATION 205 MEASUREMENTS

All four surface pressure pick-ups at Station 205 on SA-3 were located on the fillets of the flared-out region adjacent to the extreme lower portion of the fuel and LOX tanks, similar to SA-2. Figure 12-3 is a plot of surface-to-ambient-pressure ratio versus Mach number for all four individual measurements. Also shown are their approximate radial locations at this station.

Except for measurement D78-10, the pressures rose steadily above ambient at this station after a Mach number of approximately 0.4, reaching a maximum pressure ratio of 1.5 at Mach 2. Excellent agreement (Figure 12-3) is also shown with SA-2 values and wind tunnel test data.

The validity of the data from measurement D78-10 had been previously questioned after the SA-2 flight on the grounds that it differed widely from wind tunnel results and from the consistent trend exhibited by the other three measurements. As shown in Figure 12-3, SA-3 data for measurement D78-10 was very similar to SA-2, thereby adding some validity to the results from SA-2.

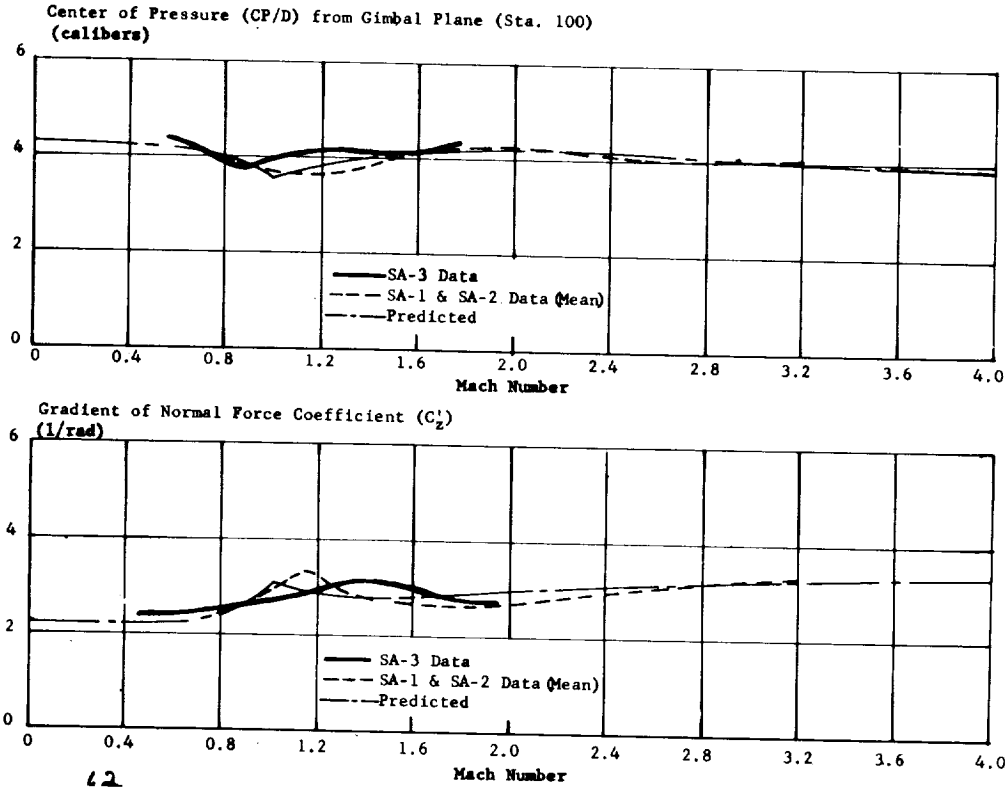

FIGURE 12-2. CENTER OF PRESSURE LOCATION AND GRADIENT OF NORMAL FORCE COEFFICIENT VERSUS MACH NUMBER

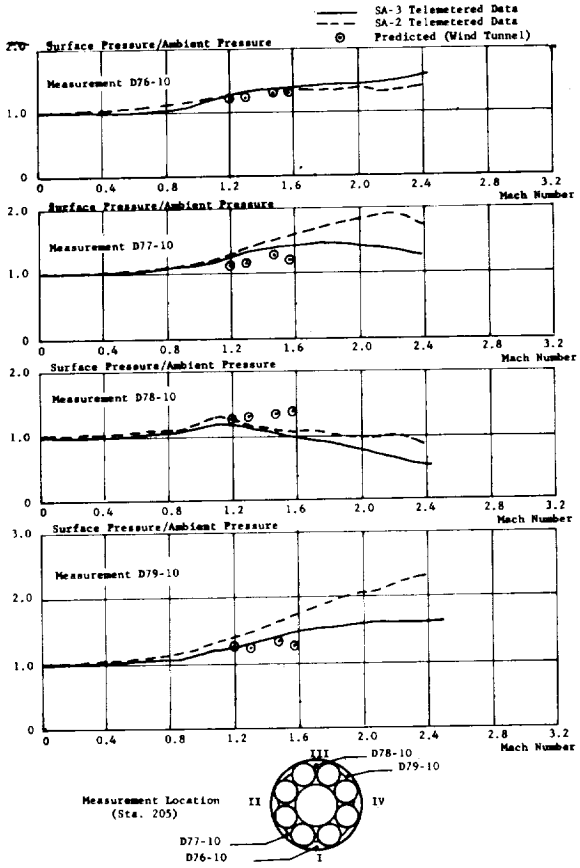

FIGURE 12-3. RATIOS OF SURFACE PRESSURE TO AMBIENT PRESSURE VERSUS MACH NUMBER

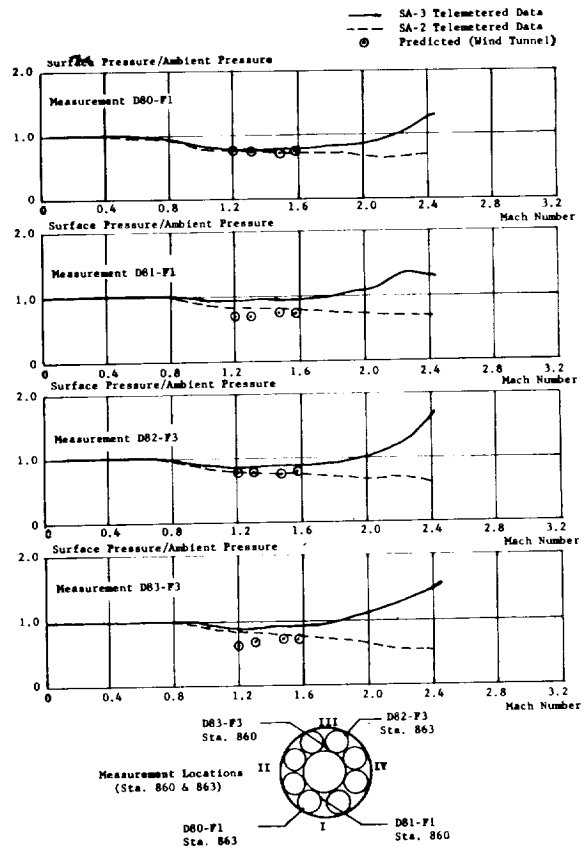

FIGURE 12-4. RATIOS OF SURFACE PRESSURE TO AMBIENT PRESSURE VERSUS MACH NUMBER

12.4.2 STATION 860 AND 863 MEASUREMENTS

Pressure ratios (surface to ambient) obtained from the four measurements (same as on SA-2), located at Stations 860 and 863, are plotted versus Mach number in Figure 12-4, with a sketch indicating the radial location of each individual measurement. Surface pressure measurements D80-F1 and D82-F3, situated at station 863, were located on the extreme upper portion of the fuel tanks facing the flight direction. Measurements D81-F1 and D83-F3 were located facing the center of the cluster at Station 860, slightly above the fuel tanks. Observed flight readings indicated that the pressure dropped to a minimum of 80 percent of ambient at Mach 1.2 and gradually increased to ambient around Mach 2. SA-3 data is in good agreement with results from wind tunnel tests conducted in the Langley 8-foot TPT and 4-foot UPWT. SA-2 data, shown for comparison in Figure 12-4, indicates slightly lower pressure than SA-3, but both results are within the error margin of the telemetered data.

12.4.3 STATION 989 AND 1019

Pressure ratios (surface to ambient) obtained from the four measurements on the interstage are plotted versus Mach number in Figure 12-5. These surface pressure measurements were obtained for the first time on SA-3. Measurements D84-20 and D86-20 are located at Station 989.3, approximately 7 degrees from fin locations III and I, respectively; D85-20 and D87-20 are located at Station 1019.3, also at approximately 7 degrees from fin locations III and I. Values of the ratio of surface to ambient pressure at Station 989.3 increased from 1.0 at Mach 0.3 to approximately 2.1 at Mach 2. Data from wind tunnel tests at Langley ($\alpha = 0$) agreed well with the flight data.

Measurements D85-20 and D87-20, at Station 1019.3 indicated slightly lower pressures than at Station 989.3, as expected, since the orifices are located closer to the expansion corner on the frustrum of the S-IV stage. Readings from measurement D85-20

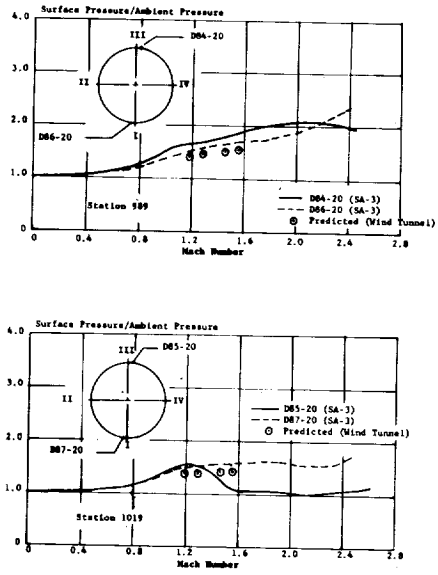

FIGURE 12-5. RATIOS OF SURFACE PRESSURE TO AMBIENT PRESSURE VERSUS MACH NUMBER ON INTERSTAGE

dropped from 1.5 at Mach 1.2 to a value slightly above ambient at Mach 1.6. It is conjectured at this time that the local shock wave moving downstream caused this drop in pressure. Wind tunnel measurements at locations in close proximity to the flight measurement do not indicate this drop. However, the value obtained from the wind tunnel tests was a faired value, and the possibility exists that the faired value is not correct.

12.4.4 CENTAUR SIMULATION PRESSURES

An experiment was flown on SA-3 to simulate the Centaur shoulder configuration behind the nose fairing. The failure on the first Centaur flight was possibly attributed to an adverse pressure distribution in the vicinity of the shoulder with respect to a venting arrangement. To gain some full scale flight information in support of this hypothesis, two panels were mounted on SA-3 to simulate a portion of the Centaur configuration. Two 2.3-cm thick panels were installed on the payload surface of the vehicle, one between fin locations III and IV (designated panel III - IV) and the other between fin locations I and III (designated panel I - II). The panels were approximately 60 degrees wide in circumference and extended from Station 1968 to 1731. The shoulder of the nose cone was moved back 10 cm to station 1727 on the area encompassed by panels. A total of 11 surface pressure measurements were located longitudinally on the centerline surface of the panels. The Centaur vented in an area similar to the base of the simulation panels installed on SA-3. Base pressures were measured on each one of the panels during the SA-3 flight.

Figure 12-6 is a representative plot of surface pressure coefficients versus Mach number which were obtained from the six measurements on panel III-IV. A configuration sketch and the location of each measurement is also shown in Figure 12-6. The largest pressure coefficient occurred at Station 1726, 2.5 cm from the shoulder, where a value of minus 1.74 was obtained at Mach 0.7.

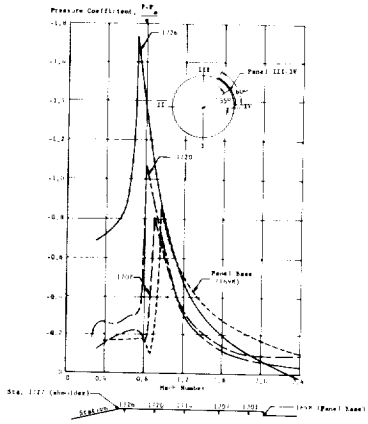

FIGURE 12-6. PRESSURE COEFFICIENT VERSUS MACH NUMBER ON CENTAUR - SIMULATION PANEL

Values of pressure coefficients at various Mach numbers are plotted versus vehicle station in Figure 12-7. Results show excellent agreement with wind tunnel results (Reference 4) on the Centaur shoulder configuration tests at Ames Research Center for the Mach numbers available. The flight results indicated a very low pressure region directly behind the shoulder in the subsonic region.

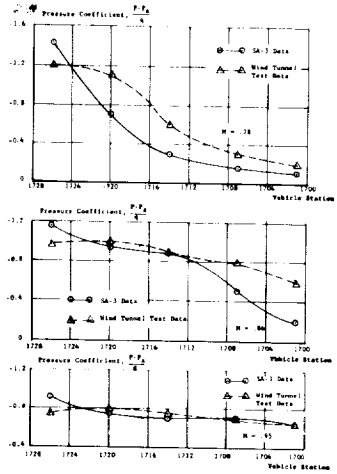

FIGURE 12-7. PRESSURE COEFFICIENT VERSUS VEHICLE STATION AT VARIOUS MACH NUMBERS ON CENTAUR - SIMULATION PANEL

SECTION XIII. INSTRUMENTATION

13.1 SUMMARY

Overall reliability of the SA-3 measuring system was 97.0 percent. All commutators performed satisfactorily with no deviation from normal operation. All preflight and inflight calibrations were normal.

Transmitted RF power from all telemetry links was sufficient to produce good data during the flight time of approximately 292 seconds. Indications are that the entire system performed without significant failure.

The signal strength of all RF systems, except C-Band Radar, was very close to the expected values. Even though the C-Band Radar received a lower-than-normal signal, tracking information from this system, the UDOP system, and the Azusa system was sufficient for good trajectory information.

This flight has again proven the usefulness of redundant tracking systems. As pointed out in Section XIII Paragraph 13.4, some periods of flight exist when data from one system may be insufficient to provide good tracking information, but these periods may be filled using data from redundant systems.

The engineering sequential camera coverage for the SA-3 flight was comparable to that of SA-2.

13.2 MEASURING ANALYSIS

Measurement Malfunctions

There were 607 flight measurements made on the SA-3 vehicle. Of these measurements, fourteen were found to be completely unusable, six were partially usable, and one was questionable.

Two types of malfunctions occurred on the flight. First, there were seven pressure transducers and one temperature measurement lost because of a malfunction in the power supply serving the direct measurements in area five. Second, there were six other measurements in which the measuring components had apparent failures.

The eight measurements that were lost because of measuring voltage failure were: C69-5, Temperature Radiation Shield; D12-5, Pressure Fuel Pump Inlet; D13-5, Pressure LOX Pump Inlet; D14-5, Pressure Turbine Inlet; D18-5, Pressure Gear Case Top; D19-5, Pressure Gear Case Lub, Hi; D20-5, Pressure Gear Case Lub, Lo; and D27-5, Pressure Inside Tail. These failures occurred 3.2 seconds after ignition command. All of these measurements had responded to their various systems prior to the power failure.

Measurement M27-12, Frequency Static Inverter, showed no output even though this inverter did function.

The pressure measurement D3-01, Pressure of Gas in LOX Tank No. 1, became intermittent 1.6 seconds after ignition. The signal was completely lost 3.9 seconds later.

The strain measurement E21-02, Strain, Mounting Stud, had no output. This failure is believed to be in the strain gauges. There were four other gauge failures on similar measurements before launch day.

The pressure measurements D143-2, D144-9, and D145-9, ΔP Across Shroud, were lost 0.5 seconds after ignition. These measurements are believed to have received a very high "g" load at this time. There is also a large amount of displacement in this area at ignition.

Pressure measurement D1-4, Pressure Combustion Chamber, failed at 73 seconds range time. This measurement became extremely noisy at this time. A normal output was observed after cutoff.

Three of the 108 discrete level probes did not function. They were probes number 6, 2, and 11 on measurements A19-OC, A19-01, and A19-03 respectively.

Partial failures were also observed on A6-5 and A11-5, Main Fuel and LOX Valve respectively. These measurements recorded the valves' opening, but failed to record the valves' closing because of the measuring voltage failure mentioned previously.

The measurement D18-2, Pressure Gear Case Top, showed an unusually high pressure. This is a gauge type pressure transducer. A systems analysis does not support this high pressure. It is believed that the orifice to the pressure port of the transducer was obstructed, thus trapping the nitrogen gas sometime during the launch. As the vehicle rose into the atmosphere, the pressure on the vent side of the transducer decreased, thereby showing an increase in the gas trapped at the pressure port. The pressure rise in this case was the same as the drop in the

atmospheric pressure. This obstruction was relieved shortly before cutoff.

Measurement Reliability

Overall reliability of the SA-3 measuring system was 97.0 percent; this is assuming eighteen failures for 598 measurements, plus three failures of the 108 discrete level probes which are the remaining nine measurements.

The optical type liquid level probes, used for the first time on this flight, performed very satisfactorily. The reliability of these probes was 97.2 percent, whereas the reliability of the impedance type probes on SA-2 was approximately 56 percent.

The pressure transducers that recorded the residual pressure in the combustion chamber after cutoff performed satisfactorily. Also, the pressure transducers on the surface areas and retro rockets performed as expected.

The temperature measurements gave a 100 percent performance as they did on the SA-2 flight, except for the measurement on the M31 panel which did not operate due to the measuring voltage failure.

13.3 TELEMETRY SYSTEM ANALYSIS

Data transmission for flight testing Saturn vehicle SA-3 was effected by eight radio telemetry system links, and a TM auxiliary equipment assembly. In addition, two experimental systems, a PCM system (link 6) and a UHF RF assembly (link 9), were flight tested for the first time. All systems operated satisfactorily.

The overall performance of link 6 was found to be excellent, and indications are that the PCM/FM system will provide very accurate data. The signal strength from this link was very good. A few nulls were noted, but these were most likely antenna nulls. The PCM package showed a 30 to 35 dbm drop during retro rocket firing, but still remained at a level high enough for good data.

The overall performance of the UHF link 9 was found to be satisfactory. Possibly, the UHF band will be used more extensively in the future for transmitting telemetry data.

The Block II antenna panel (located between the propellant tanks at the forward portion of the S-I stage) showed good results, with the signal strength being higher and somewhat more constant than other recordings. The attenuation at retro rocket firing was about the same as for the Block I antenna; however, the flame attenuation was less (probably as much as 10 db) than that noted on the Block I type.

13.4 RF SYSTEMS ANALYSIS

13.4.1 TELEMETRY

Cape Telemetry 2 Station (1.7 km at approximately 240 degrees from pad 34)

Telemetry signal strength (Figure 13-1) at this station appears to be above the receiver threshold at all times. The lowest signal was received during retro rocket firing. The signal level dropped 25 to 35 dbm at this time to approximately minus 65 to minus 75 dbm.

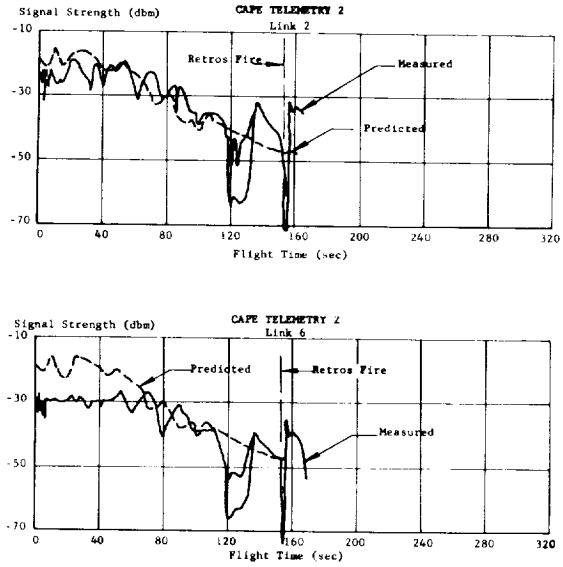

FIGURE 13-1. TELEMETRY SIGNAL STRENGTH (CAPE TELEMETRY 2)

Other decreases in signal strength were present, but they were less intense. These may be attributed to multipath, cross polarization, antenna nulls, small aspect angle, and flame attenuation.

Flame attenuation was present at this station from approximately 98 to 138 seconds. However, the signal was not noisy until approximately 118 seconds. Maximum attenuation occurred between 120 and 130 seconds, and caused a signal drop of approximately 10 to 25 db below normal, which was expected. However, it wasn't expected that the attenuation would end prior to engine cutoff. This was caused by the changing aspect angle.

Signal attenuation due to the roll of the vehicle, resulting from retro firing, can be seen on these records although it is not very pronounced. This

means that the vehicle antenna gain at this aspect angle is relatively constant.

Cape Telemetry 3 Station (6.9 km at approximately 200 degrees from Pad 34).

Preliminary investigation shows that the signal strength from this station was sufficient to prevent signal dropout at any time. Some difference existed between this station and Cape Telemetry 2 station. There was more signal fluctuation from multipath propagation during the first few seconds of flight. Flame attenuation was less, and began 5 to 10 seconds later than at Cape Telemetry 2 station. Link 10 experienced less flame attenuation than other links. Even though flame attenuation was less, this station recorded a short decrease in signal after outboard engine cutoff. This was probably due to the final expulsion of exhaust gases. Some of the signal strength decreases were more intense than the decreases at Cape Telemetry 2 station, especially after the vehicle began to roll.

Signal attenuation, due to retro rocket firing, was about the same as the Cape Telemetry 2 station.

Green Mountain Telemetry Station (near MSFC).

The telemetry signal (Figure 13-2) was received at this station approximately 128 seconds after liftoff. Average signal strength was approximately 15 to 18 db higher than on SA-2. The reason for this has not yet been determined, but is under investigation at this time. The difference could possibly be caused by an error in calibration or by a difference in propagation due to the different weather conditions of the SA-2 and SA-3 flights.

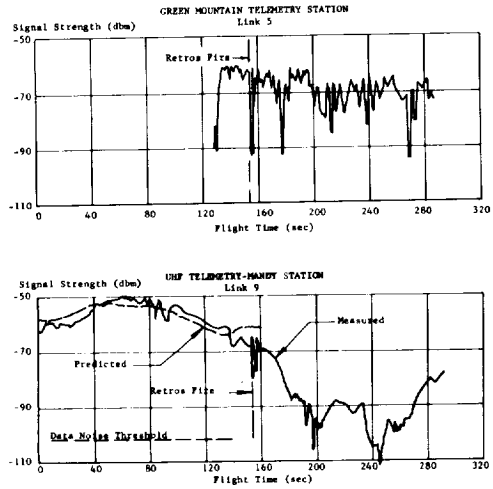

FIGURE 13-2. TELEMETRY SIGNAL STRENGTH (GREEN MOUNTAIN AND MANDY)

GBI Telemetry Station (Grand Bahama Island).

Signal was received at this station between 48 and 55 seconds. All links functioned normally until the retro rockets fired. At this time, the signal on some links dropped low enough to cause noise in the reduced data. Also, some decreases due to roll were large enough to cause signal noise. No flame attenuation was present at this station.

Hangar D Station (4.3 km at approximately 210 degrees from Pad 34).

The signal at this station was generally low and experienced dropouts at retro rocket firing and at intervals during the vehicle roll. This may be attributed partially to a low gain system and partially to hand tracking used by this station.

UHF Telemetry - Mandy Station (7.7 km at approximately 200 degrees from Pad 34).

This is the first time that UHF telemetry has been used on a Saturn flight. The signal strength during powered flight was excellent, and as shown in Figure 13-2, it followed the predicted curve almost perfectly. There was no evidence of flame effects from the engine exhaust, and the retro rockets affected this system less than the VHF systems. The signal was low after the vehicle began to roll, but this could be expected because the system was using only one antenna and it was turned away from the station much of the time. The data noise threshold was minus 102 dbm and the signal dropped below this value only two times for short periods.

13.4.2 UDOP

Mandy Station (7.7 km at approximately 200 degrees from Pad 34).

The AGC voltage at this station was constant until 125 seconds, with one exception between 78 and 79 seconds. Signal attenuation, probably caused by flame, began at approximately 125 seconds and continued until IECO. Maximum attenuation (12 to 15 dbm below normal) occurred between 125 and 133 seconds. Retro rocket firing produced a signal attenuation of approximately 25 dbm for their duration.

Signal variation occurred between retro rocket firing and destruct, caused by nulls in the antenna pattern as the vehicle rolled.

Signal was received until 465 seconds after liftoff, but it was noisy and attenuated after destruct.

Tango Station (Titusville - Cocoa Airport, 22.9 km at 270 degrees from Pad 34).

Average signal strength was higher than preliminary predictions (Figure 13-3). Some signal attenuation was experienced due to antenna nulls, especially after the vehicle began to roll.

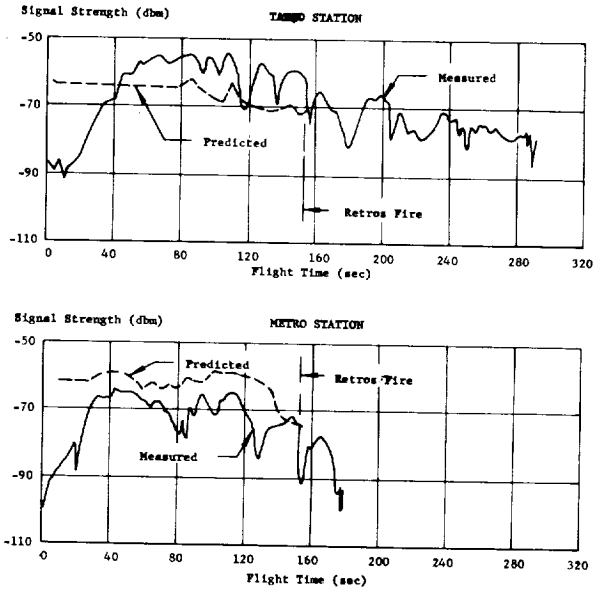

FIGURE 13-3. UDOP SIGNAL STRENGTH

Retro rocket firing produced an attenuation of 10 to 15 db below the average signal. No flame attenuation was experienced at this station. Signal was received until approximately 464 seconds after liftoff, but it was very noisy and attenuated after destruct.

Other Stations

AGC records were received from several other stations, including the Green Mountain Station. They all compared favorably with Tango and Mandy records. The signal strength from Metro Station (Merritt Island Airport, 23.4 km at approximately 214 degrees from Pad 34) is presented in Figure 13-3.

13.4.3 AZUSA

Records from the MK II station (12.4 km at approximately 194 degrees from Pad 34) indicated that the system operated as expected for the first 160 to 170 seconds. The signal (Figure 13-4) was fluctuating between 5 and 12 db for the first 80 seconds. The Azusa signal normally fluctuates due to multipath propagation and antenna lobing for the first part of the flight. These effects lasted longer than on previous flights because of the slower liftoff velocity of the vehicle. However, the signal remained above minus 95 dbm, which meets the range data commitments. From 160 seconds to destruct, the signal was attenuated as much as 35 to 40 dbm at times. This is probably due to the roll of the vehicle, since the system has only one antenna. However, records indicate that the MK II system was passive from 160 until 220 seconds, and from 225 until 270 seconds, while the MK I station was tracking. The signal was attenuated most during these periods.

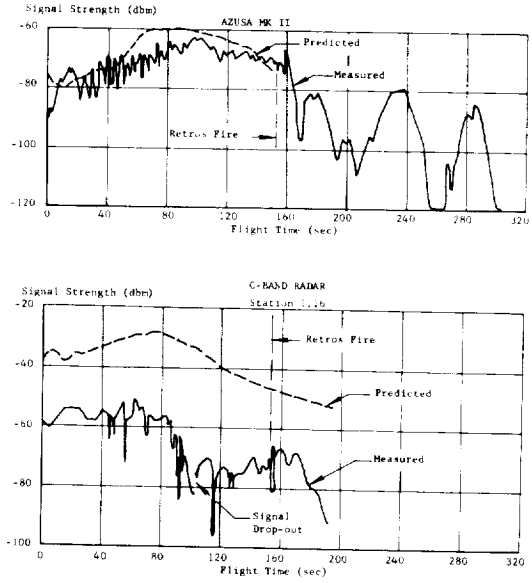

FIGURE 13-4. AZUSA AND RADAR SIGNAL STRENGTH

13.4.4 C-BAND RADAR

Station 1.16 (4.7 km at approximately 199 degrees from Pad 34).

Prior to liftoff, it was noticed that the C-Band Beacon was frequency moding and giving a double pulse output. This was causing erratic range lock-on, so the receiver was detuned to get a single narrow pulse. This detuning caused a lower signal level than would normally be received at this station, but it was felt that it was adequate because skin tracking could be used if the beacon proved to be inadequate. The signal strength from this station is shown in Figure 13-4.

Automatic beacon tracking was acquired at liftoff and used for 92 seconds. The signal followed a smooth pattern during this time, but was 20 to 30 dbm lower than predictions. Records show that the signal began decreasing at about 85 seconds; then the system began

hunting at about 91 seconds and was switched to automatic skin tracking from 92 to 103 seconds. Beacon tracking was used from 103 until 196.5 seconds. During this time, the signal-to-noise ratio was 20 to 30 db which is sufficient for high accuracy tracking. Some noise was present between 115 and 132 seconds which may have been caused by flame, but it wasn't enough to cause concern. However, retro rocket firing caused disturbances of 10 to 15 db which drove the signal-to-noise ratio down to 12 to 15 db. This disturbance probably would have been insignificant if the signal level had been normal.

After retro rocket firing, the signal dropped below the noise level at about 194 seconds and the system was switched to skin tracking from 197 to 202 seconds. This happened again around 235 seconds and the system was switched to automatic skin tracking from 241 seconds until destruct. After destruct, this station tracked pieces of the vehicle and the cloud formed by Project Highwater.

Station 0.16 (Patrick AFB, 32.9 km south of Pad 34).

This station used the MK 51 optical tracking until T plus 22 seconds, at which time it switched to automatic beacon tracking. AGC at the ground station appeared normal for the first 53 seconds. After this, it had a 2 to 3 db jitter for the remainder of the flight. Records show that this station also had trouble with narrow pulse width, double pulsing, and countdown from the beacon. Apparently it had not prepared for this by detuning its beacon as station 1.16 had done and therefore experienced more difficulty.

This station lost track three times during the flight. The first time was at 140 seconds and may have been a combination of poor beacon response and flame attenuation. The other two times were after the retro rockets had fired and may have been caused by roll. The system switched back and forth between automatic beacon tracking and automatic skin tracking from 140 to 187 seconds and ended up using automatic skin tracking from 187 seconds until destruct. It tracked the water cloud after destruct.

GBI Station (Grand Bahama Island).

The signal was received at GBI 65 seconds after liftoff. It experienced the same trouble as the other stations. No flame attenuation was present at this station, but retro rocket firing caused a signal attenuation of approximately 5 db.

Even though response was below normal, this station was able to track the beacon all the way, except for one period between 192 and 228 seconds.

SECTION XIV. SUMMARY OF MALFUNCTIONS AND DEVIATIONS

The flight test of Saturn SA-3 did not reveal any malfunctions or deviations which could be considered a serious system failure or design deficiency. However, a number of minor deviations did occur and are summarized here for documentary purposes.

Corrective measures were recommended by the division for some of the items listed. These are marked with an asterisk. Each item is listed in the area where the malfunction occurred.

Launch Operations

1. A ground generator power failure caused a 45-minute hold at T minus 75 minutes (Section III Paragraph 3.4).

2. The digital output computer for the sequence records malfunctioned (Section III Paragraph 3.4).

3. The "Support Retrack Pressure OK" switches cycled several times about 500 ms after all engines were running (Section III Paragraph 3.5).

4. A measuring error indicated that the LOX bubbling valve stayed open for 137 seconds instead of the expected 60 seconds (Section III Paragraph 3.5).

5. The LOX fill mast failed to retract on command (Section III Paragraph 3.6)*

Trajectory

6. The burning time for SA-3 was 1.3 seconds longer than expected (Section IV Paragraph 4.3.1).

7. Cross range displacement was to the left of nominal due to a difference in alignment between the platform and vehicle, and also due to winds (Section IV Paragraph 4.3.1).

Propulsion

8. The vehicle specific impulse was 1.1 percent higher than predicted (Section V Paragraph 5.3).

9. The gear case pressure measurement on engine position 2 exceeded its limits (Section V Paragraph 5.2).

10. The retro rockets were misaligned, causing a vehicle roll motion (Section V Paragraph 5.7).*

11. The pressure drop across the orifices between the center and outboard LOX tanks was 0.09 kg/cm^2 (1.3 psi) lower than predicted at IECO (Section V Paragraph 5.4.2).

Control

12. An error in tilt cam resulted in a maximum tilt angle of 44.28 degrees at tilt arrest as compared to the desired angle of 44 degrees (Section VII Paragraph 7.2.1).*

13. A clockwise roll moment of 1553 kg-m was observed at IECO (Section VII Paragraph 7.2.3).

14. Increased sloshing was observed in LOX tank 04 compared to that on the SA-2 flight. A maximum sloshing amplitude of 24 cm was observed in pitch on SA-3, as compared to 10 cm on SA-2 (Section VII paragraph 7.4).

Guidance

15. Erroneous outputs from the cross range accelerometer system on the ST-124P Platform were observed (Section VIII Paragraph 8.3.3).

16. The ST-124P platform was not aligned in azimuth and the resolver chain was not trimmed (Section VIII Paragraph 8.3.3 and Paragraph 8.4.2).*

17. A failure due to an open circuit in one buffer amplifier stage of the ST-124P guidance signal processor repeater was encountered (Section VIII Paragraph 8.4.2).

18. A disturbance was observed in the signal processor between 113 and 125 seconds (Section VIII Paragraph 8.4.2).

Electrical System

19. Number 5 measuring supply voltage failed prior to liftoff (Section IX Paragraph 9.2).*

Structures

20. A high vibration level was observed on the fuel suction line, longitudinal; measurement E45-8 (Section X Paragraph 10.5.3).

21. Systematic transients were observed in eight measures (Section X Paragraph 10.5.3 and Paragraph 10.6).

Environmental Temperatures and Pressures

22. Total calorimeter measurement (C77-5) indicated losses twice as great as previously noted (Section XI Paragraph 11.2.1.3).

23. Heating rate on the S-IV skin was twice as much as would be predicted by theory (Section XI Paragraph 11.3).

24. Flame shield pressure was unusual (Section XI Paragraph 11.2.1.1).

25. Base pressure on the heat shield had a higher gradient than previous flights (Section XI Paragraph 11.2.1.1).

Instrumentation

26. Fourteen measurements were unusuable, six were partially usable, and one was questionable (Section XIII Paragraph 13.2).

27. The C-Band Radar signal strength was lower than predicted (Section XIII Paragraph 13.4.4).

15.1 PROJECT HIGHWATER

A water cloud experiment (similar to the experiment conducted on SA-2) was accomplished successfully on SA-3. At 292 seconds range time the upper stages' water ballasts were ruptured with primacord, injecting 86.7 m^3 (22,900 gal) of water into the upper atmosphere. At the time of Project Highwater, the vehicle was at an altitude of 167.22 km (0.45 km higher than predicted) and at a range of 211.41 km (3.76 km above predicted).

The Saturn water release experiment was conducted on the SA-3 flight in order to compare the cloud formation with that observed on the SA-2 experiment; to investigate the effects of perturbing the ionosphere by the release of 86.7 m^3 (22,900 gal) of water and to monitor the ionosphere's return to an equilibrium state, and to passively monitor radio noise through a frequency range from 300 cps to 400 megacycles.

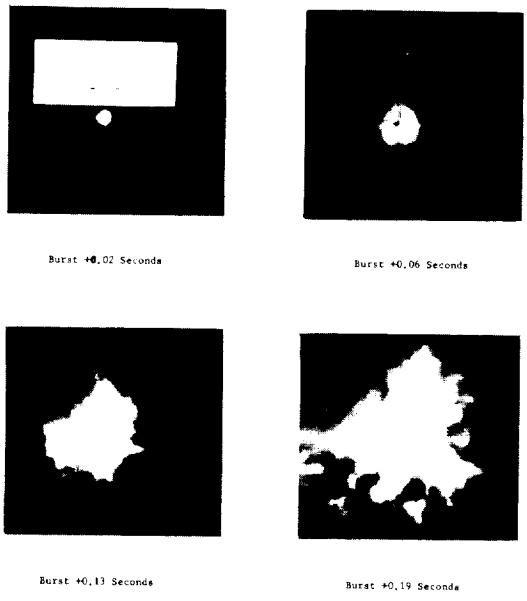

FIGURE 15-1. PICTURE SEQUENCE OF PROJECT HIGHWATER EXPERIMENT

Film from the long range camera at Vero Beach showed that the S-1 booster remained intact after destruct of the upper dummy stages. The tumbling motion of the booster was observed for an extended time. A few booster measurements continued to be transmitted on telemetry. Telemetry signals on links 3, 4, and 8 were temporarily lost after project Highwater, but were regained between 335 and 360 seconds and continued until after 400 seconds. Link 7 telemetry signals were not lost until 420 seconds; whereas link 6 (PCM) continued to transmit until approximately 600 seconds. It is questionable, however, if any of the data would represent reliable measurements. The booster was out of camera range when breakup occurred. Figure 15-1 presents camera coverage during various periods of Project Highwater.

15.2 HORIZON SCANNER

Usable data from the horizon scanner were obtained between 100 and 130 seconds range time. The data during this period were within ±5 degrees of expected values. Data in other portions of the flight were erratic and unusable. No data was expected until 100 seconds; however, the data would have continued to be usable until retro fire at 153.6 seconds.

15.3 OTHER SPECIAL MISSIONS

In addition to Project Highwater and the horizon scanner output, a number of special missions were flown as tests on SA-3. The results of these tests have been discussed in detail in the preceding sections of this report. The following table lists the section in which special mission results are discussed:

	Reference Section
a. M-31 Heat Shield Panel (Block II Type)	XI Paragraph 11.2.1.3
b. LOX Depletion	V Paragraph 5.2
c. Full Propellant Loading	V Paragraph 5.4
d. Block II Antenna Panel	XIII Paragraph 13.3
e. Passenger ST-124P	VIII Paragraph 8.2.2
f. PCM Telemetry	XIII Paragraph 13.3
g. Centaur Pressure Study	XII Paragraph 12.4.4
h. S-IV Stage Temperature and Pressure Meas.	XI Paragraph 11.3
i. Block II Swing Arm	III Paragraph 3.6
j. Retro Rockets	V Paragraph 5.7

REFERENCES

1. M-AERO-PO-3-62; "Saturn C-1 Vehicle SA-3 Test Flight: Trajectory Corridor To Be Flown By SA-3" (U); by Hardage, O. M.; dated November 2, 1962.

2. MPR-SAT-WF-61-8; "Saturn SA-1 Flight Evaluation" (C); by Saturn Flight Evaluation Working Group; dated December 14, 1961.

3. MPR-SAT-WF-62-5; "Saturn SA-2 Flight Evaluation" (C); by Saturn Flight Evaluation Working Group; dated June 5, 1962.

4. NASA TM X-503; "Steady and Fluctuating Pressures at Transonic Speeds On Two Space Vehicle Payload Shapes" (C); by Coe, C. F.; dated March 1961.

DISTRIBUTION

DIR
Dr. von Braun

DEP-T
Dr. Rees

DEP-A
Mr. Gorman

AST-S
Dr. Lange

EY
Mr. Maus

R-DIR
Mr. Weidner
R-SA
Dr. Kuettner
Mr. Dannenberg

R-AERO-DIR
Dr. Geissler
Mr. Jean
R-AERO-P
Mr. McNair
R-AERO-A
Mr. Dahm
Mr. Wilson
R-AERO-G
Dr. Hoelker
R-AERO-F (50)
Dr. Speer
R-AERO-M
Mr. Horn
R-AERO-Y
Mr. Vaughan
Mr. Smith
R-AERO-FF
Mr. Lindberg

R-ASTR-DIR
Dr. Haeussermann
R-ASTR-N
Mr. Fichtner
R-ASTR-G
Mr. Moore
R-ASTR-I
Mr. Hoberg
Mr. Bell
Mr. Price
Mr. Avery
R-ASTR-D
Mr. Hosenthien
R-ASTR-G
Mr. McMahen

R-COMP-DIR
Dr. Hoelzer
R-COMP-R
Mr. Hubbard
R-COMP-RR
Mr. Cochran

R-ME-DIR
Mr. Kuers
R-ME-X
Mr. Wuenscher
R-ME-D
Mr. Eisenhardt
R-ME-M
Mr. Orr
R-ME-F
Mr. Franklin

R-RP-DIR
Dr. Stuhlinger

R-P&VE-DIR
Dr. Mrazek
R-P&VE-A
Mr. Goerner
R-P&VE-M
Dr. Lucas
R-P&VE-P (2)
Mr. Paul
R-P&VE-PP (2)
Mr. Heusinger
R-P&VE-S
Mr. Kroll
Mr. Hunt
Mr. Farrow
R-P&VE-D
Mr. Palaoro
R-P&VE-BA
Mr. Hoffman

R-QUAL-DIR
Mr. Grau
R-QUAL-A
Mr. Urbanski
R-QUAL-Q
Mr. Brien
R-QUAL-R
Mr. Smith
R-QUAL-P
Mr. Brooks
R-QUAL-PSC
Mr. Peck

R-TEST-DIR
Mr. Heimburg
Mr. Tessmann
R-TEST-DIR-M
Mr. Edwards
R-TEST-C
Mr. Grafton
R-TEST-I
Dr. Sieber
R-TEST-S
Mr. Driscoll
R-TEST-SB
Mr. Reilman

MS-H
Mr. Akens
MS-IP (2)
Mr. Remer
MS-IPL (15)
Miss Robinson

LVO-DIR
Dr. Gruene
LVO-G
Mr. Rigell
LVO-M
Mr. Pickett

I-DIR (8)
Mr. Young

LO-ET
Mr. Collins
LO-ED4
Mr. Jelen

EXTERNAL

Headquarters, National Aeronautics & Space Administration
Washington 25, D.C.
Assistant to the Administration: Franklyn W. Phillips
Office of Plans & Program Evaluation: Abraham Hyatt
Office of Scientific & Technical Information: Melvin S. Day
Associate Administrator: Dr. Robert C. Seamans, Jr.
Office of Programs
Director of Reliability & Quality Assurance: James T. Kopenhaver

Office of Manned Space Flight
Director: Mueller
Deputy Director (Systems): Dr. Joseph F. Shea
Director of Launch Vehicles & Propulsion: Captain Robert Freitag (USN)

Office of Space Sciences
Director: Homer E. Newell
Launch Vehicles & Propulsion Programs
Director: Donald H. Heaton (10)

Office of Advanced Research & Technology
Director: Thomas F. Dixon
Director of Propulsion and Power Generation: John L. Sloop

Office of Applications
Director: Morton J. Stoller
Morris Tepper

Goddard Space Flight Center
4555 Overlook Avenue
Washington 25, D.C.
Attn: Herman LaGow

Director, Ames Research Center: Smith J. DeFrance
National Aeronautics & Space Administration
Moffett Field, California

Manned Spacecraft Center
Houston 1, Texas - P.O. Box 1537
Attn: Director: Robert R. Gilruth
Robert Smith (5)
Alfred Mardel (3)
Charles M. Grant (2)

Director, Langley Research Center: Floyd L. Thompson
National Aeronautics & Space Administration
Langley Field, Virginia

Director, Lewis Research Center: Abe Silverstein
National Aeronautics & Space Administration
21000 Brookpark Road
Cleveland 35, Ohio

Director, Western Operations Office: Robert W. Kamm
National Aeronautics & Space Administration
150 Pico Blvd., Santa Monica, California

EXTERNAL

Director, Flight Research Center: Paul F. Bikle
National Aeronautics & Space Administration
P.O. Box 273
Edwards, California

Director, Wallops Station: R. L. Krieger
National Aeronautics & Space Administration
Wallops Island, Virginia

Jet Propulsion Lab
4800 Oak Grove Drive
Pasadena 2, California
Attn; Irl Newlan, Reports Group

Jet Propulsion Laboratories, CCMTA
Attn: H. Levy (4)

Office of the Asst. Sec. of Defense for Research & Engineering
Room 3E1065
The Pentagon
Washington 25, D. C.
Attn: Tech Library

Director of Guided Missiles
Office of the Secretary of Defense
Room 3E131
The Pentagon
Washington 25, D.C.

Commander, Armed Services Tech Info Agency (5)
Arlington Hall Station
Arlington 12, Va.
Attn: TIPCR (Transmittal per Cognizant Act. Security Instruction)

U.S. Atomic Energy Commission, Sandia Corp.
University of California Radiation Lab
Tech Info Div
P.O. Box 808
Livermore, California
Attn: Clovis Craig

U.S. Atomic Energy Commission, Sandia Corp.
Livermore Br, P.O. Box 969
Livermore, California
Attn: James McMinn, Document Control Sec.

Central Intelligence Agency (2)
2430 E Street, N. W.
Washington 25, D.C.
Attn: Liaison Div. OCD

Director, National Security Agency
Ft. George Mead, Maryland
Attn: C3/TDL

Commanding General (3)
White Sands Proving Ground
New Mexico
Attn: ORDBS-OMTIO-TL

Commander, AF Missile Test Center (3)
Patrick AFB, Florida
Attn: Tech Info Intelligence Office, MTGRY

Chief of Staff, U.S. Air Force (2)
The Pentagon
Washington 25, D.C.
1 Cpy marked for DCS/D AFDRD
1 Cpy marked for DCS/D AFDRD-EX

Commander (5)
Wright Air Development Center
Wright-Patterson Air Force Base, Ohio
Attn: WCOSI-3

Commander
Air Force Flight Test Center
Edwards AFB, California
Attn: FTOTL

Rocketdyne
6633 Canoga Avenue
Canoga Park, California
Attn: O.I. Thorsen (3)

Commander-in-Chief
Strategic Air Command
Offutt AFB, Nebraska
Attn: Dir of Opns, Missile Division

Commander (2)
Arnold Engineering Development Center
Arnold Air Force Station, Tennessee
Attn: Tech. Library

Commander
Air Force Missile Development Center
Holloman Air Force Base
New Mexico
Attn: Tech Library (SRLT)

EXTERNAL

Commander
U.S. Naval Air Missile Test Center
Point Mugu, California

Chief, Bureau of Weapons (4)
Dept. of Navy
Washington 25, D.C.
1 Cpy to RESI, 1 Cpy to SP,
1 Cpy to AD3, 1 Cpy to REW3

Chief of Naval Research
Department of Navy
Washington 25, D.C.
Code 463

Director (2)
U.S. Naval Research Lab
Washington 25, D.C.
Attn: Code 2027

Douglas Aircraft Company, Inc.
Missile and Space Systems Engineering
Santa Monica, California
Attn: H.M. Thomas (1)
A.J. German (5)
D.A. Petty (2)

AMSMI-RBLD;RSIC
Bldg 4488

Aerospace Corporation
2400 East El Segundo
El Segundo, California
Attn: D.C. Bakeman

Arinc Research Corporation
1700 K Street, N.W.
Washington 6, D.C.
Attn: W.J. Willoughby

The Boeing Company
Saturn Booster Branch
P.O. Box 26088
New Orleans 26, Louisiana
Attn: R.H. Nelson (3)

North American Aviation
Space & Information Division Systems
12214 Lakewood Boulevard
Downey, California
Attn: A. Shimizu (2)
W.F. Parker (1)

Chrysler Space Division
Michoud Operations
Attn: H.C. Calahan (11)

Huntsville Operations
Attn: H. Bader, Jr. (3)

Headquarters
6570th Aerospace Medical Division (AFSC)
U.S. Air Force
Wright Patterson Air Force Base, Ohio
Attn: H.E. Vongierke

Radio Corporation of America
Defense Electronic Products
Data Systems Division
8500 Balboa Blvd
Van Nuys, California

Martin Company
Space Systems Division
Baltimore 3, Maryland
Attn: W.P. Sommers

Scientific and Technical Information Facility (2)
Attn: NASA Representative (S-AK/RKT)
P.O. Box 5700
Bethesda, Maryland

Grumman Aircraft Engineering Corp.
Apollo Space Program Office
Bethpage, Long Island, N. Y.
Attn: Jack Small (3)